Small Angle X-ray Scattering (SAXS) as a Complementary Structural Biology Technique: Perils, Pitfalls and Potential.

Edward H. Snell and many others

Hauptman Woodward Medical Research Institute, Buffalo, NY 14203, USA.

Pessimists, Optimists, and Crystallographers

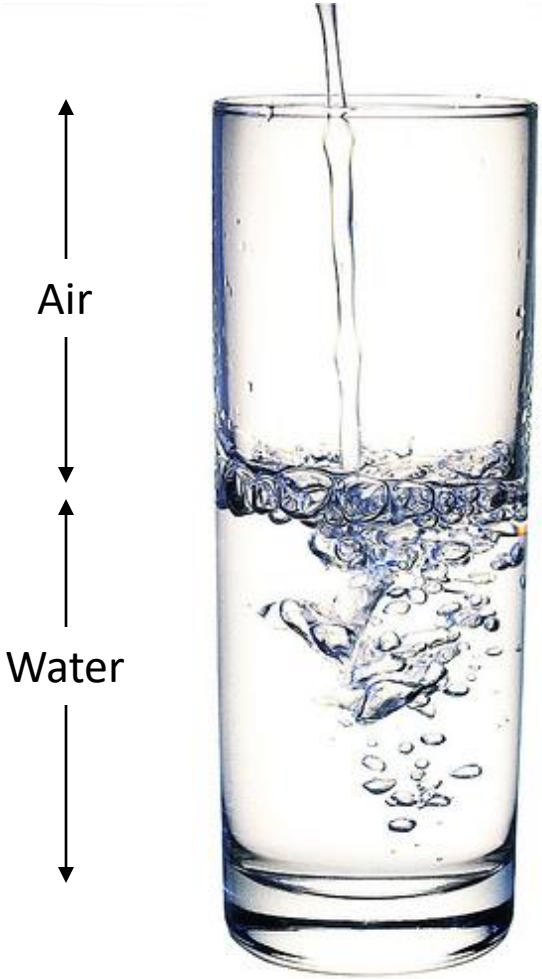

Consider a glass of water

Pessimist
(the glass is half empty)

Optimist
(the glass is half full)

Crystallographer
(the glass is completely full)

Fantasy

Acta Crystallographica Section F
Structural Biology and Crystallization Communications
ISSN 1744-3091

On the need for an international effort to capture, share and use crystallization screening data

Janet Newman,[a]* Evan E. Bolton,[b] Jochen Müller-Dieckmann,[c] Vincent J. Fazio,[a] Travis Gallagher,[d] David Lovell,[e] Joseph R. Luft,[f,g] Thomas S. Peat,[a] David Ratcliffe,[e] Roger A. Sayle,[h] Edward H. Snell,[f,g] Kerry Taylor,[e] Pascal Vallotton,[i] Sameer Velanker[j] and Frank von Delft[k]

[a]Materials Science and Engineering, CSIRO, 343 Royal Parade, Parkville, VIC 3052, Australia, [b]NCBI, NLM, NIH, Department of Health and Human Services, 8600 Rockville Pike, Bethesda, MD 20894, USA, [c]EMBL Hamburg Outstation c/o DESY, Notkestrasse 85, D-22603 Hamburg, Germany, [d]National Institute for Standards and

When crystallization screening is conducted many outcomes are observed but typically the only trial recorded in the literature is the condition that yielded the crystal(s) used for subsequent diffraction studies. The initial hit that was optimized and the results of all the other trials are lost. These missing results contain information that would be useful for an improved general understanding of crystallization. This paper provides a report of a crystallization data exchange (XDX) workshop organized by several international large-scale crystallization screening laboratories to discuss how this information may be captured and utilized. A group that administers a significant fraction of the world's crystallization screening results was convened, together with chemical and structural data informaticians and computational scientists who specialize in creating and analysing large disparate data sets. The development of a crystallization ontology for the crystallization community was proposed. This paper (by the attendees of the workshop) provides the thoughts and rationale leading to this conclusion. This is brought to the attention of the wider audience of crystallographers so that they are aware of these early efforts and can contribute to the process going forward.

Only approximately 11% of the proteins we target for crystallography yield a crystallographic structure.

At least 99.8% of crystallization experiments produce an outcome other than crystallization.

There exists a large quantity of soluble purified protein that remains structurally uncharacterized.

High Throughput Crystallization Screening

The Hauptman-Woodward Medical Research Institute Crystallization Screening Laboratory

Since February of 2000 the High Throughput Search (HTS) laboratory has been screening potential crystallization conditions for over 14,000 different proteins to date.

Over 1,000 different laboratories worldwide use the service with a total of 100-200 samples per month being screened at a nominal cost.

600 µl of protein is required at about 10 mg/ml concentration.

The microbatch-under-oil technique is used with each sample set up against 1,536 different chemical 'cocktails' which comprise an incomplete factorial sampling of chemical space and a large number of commercially available screens.

Each cocktail imaged at 1 day and weekly thereafter with the images immediately available to the individual investigator.

Google "crystallization" for full details.

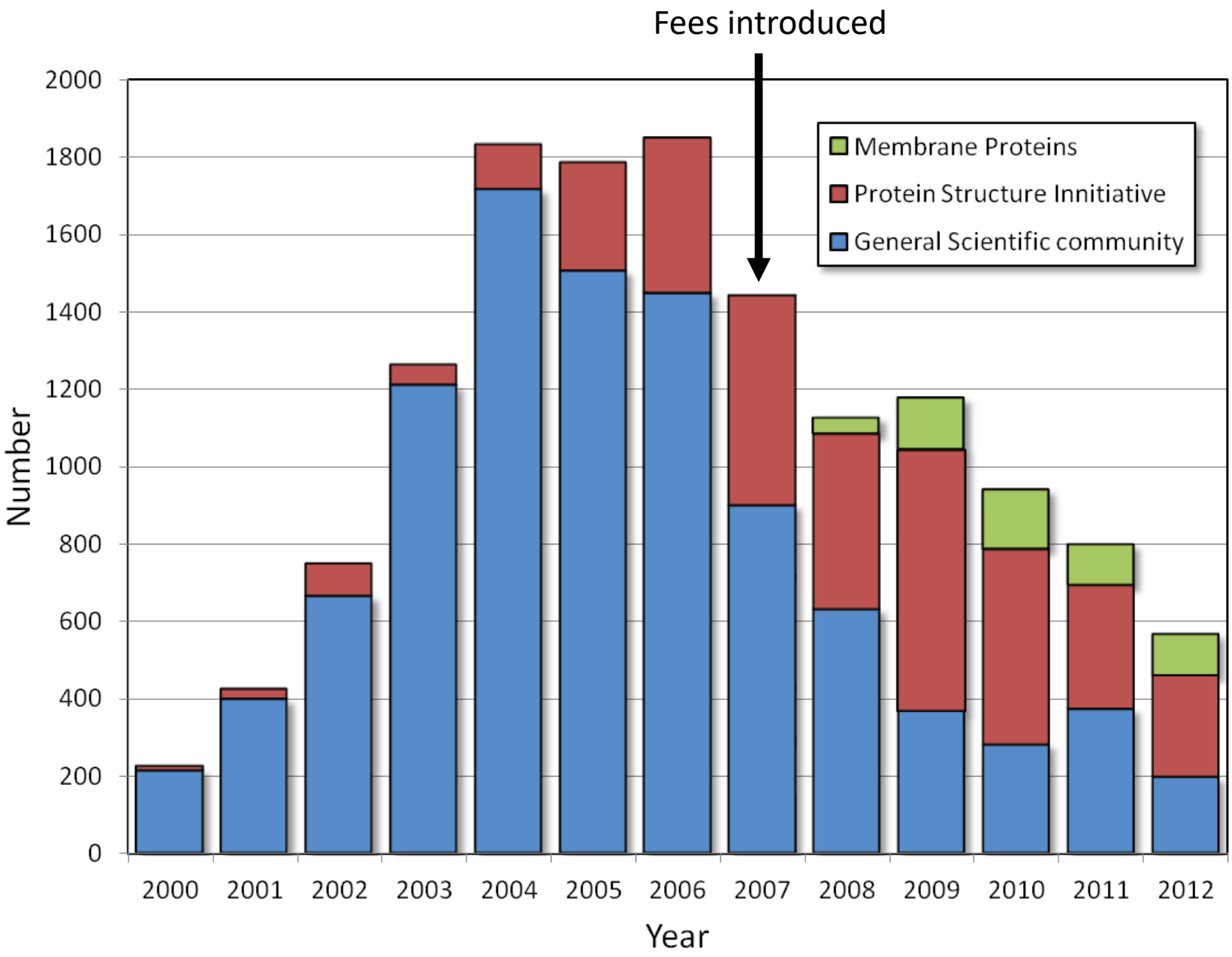
Fees introduced
Membrane Proteins
Protein Structure Innitiative
General Scientific community
Number
Year
0
200
400
600
800
1000
1200
1400
1600
1800
2000
2000
2001
2002
2003
2004
2005
2006
2007
2008
2009
2010
2011
2012

Born in Buffalo

Over 1,000 general biomedical laboratories world wide use the crystallization screening service with approximately 2,000 unique investigators.

Investigators are sent photographs of the results, analyze these images and perform their own optimization of any hits observed.

No information is released on targets. Progress is tracked by acknowledgements and citation searches. Currently no other metrics are used to measure success rates for the general biomedical community.

These images represent examples of structures from initial hits in the HTS laboratory.

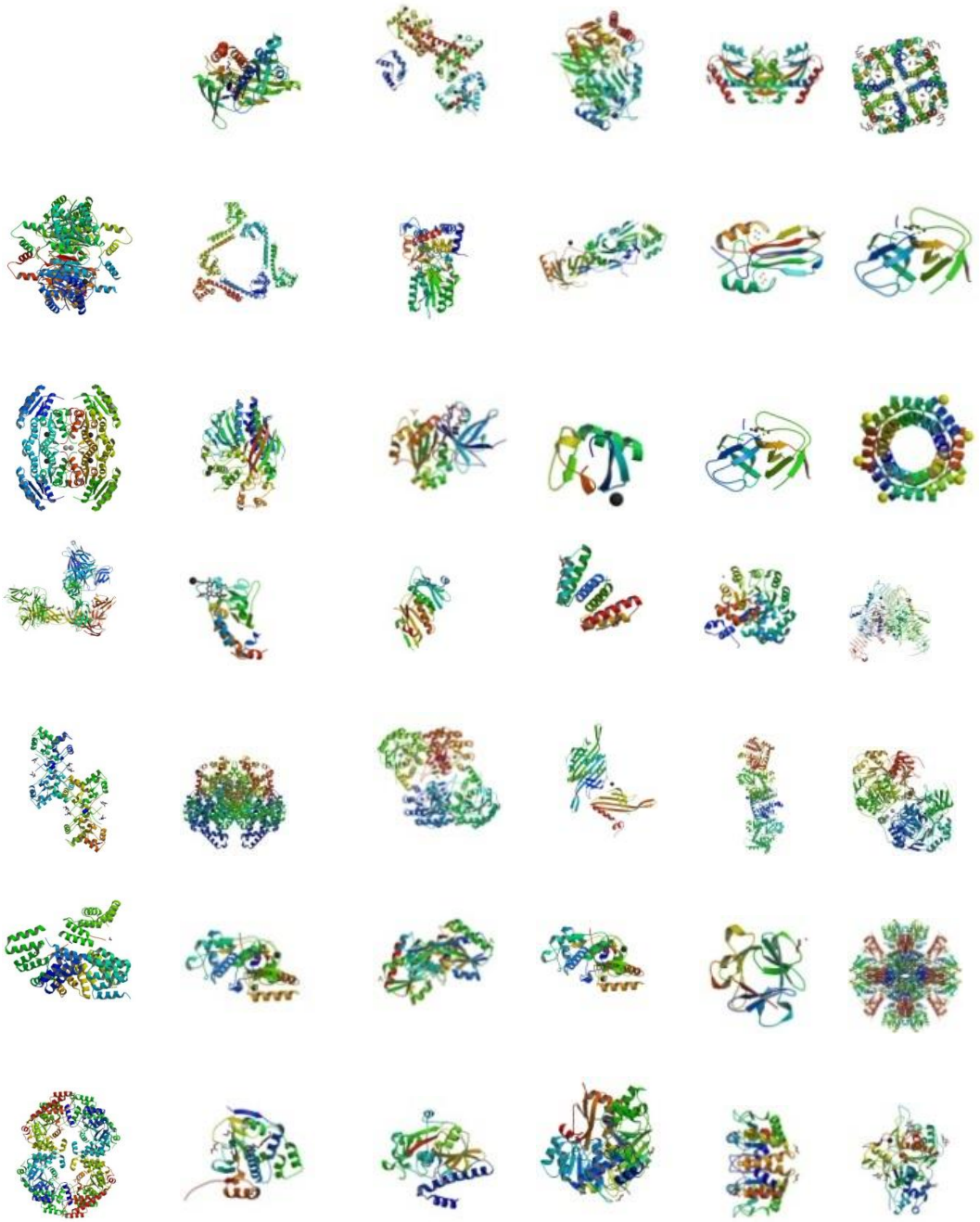

Where success is tracked.

For our Protein Structure Initiative partners both success and failure is tracked. In the case of NESG our initial screening hits enable on average 80 structures per year to be deposited to the PDB.

The graph demonstrates the ramp up of operations with maximum success reached from 2006 onward.

Our success rate from protein in the door to a crystallization hit leading to a PDB deposition is **22%**.

The NESG samples represent a special case in that they are well characterized beforehand – size exclusion chromatography, mass spec analysis and dynamic light scattering studies.

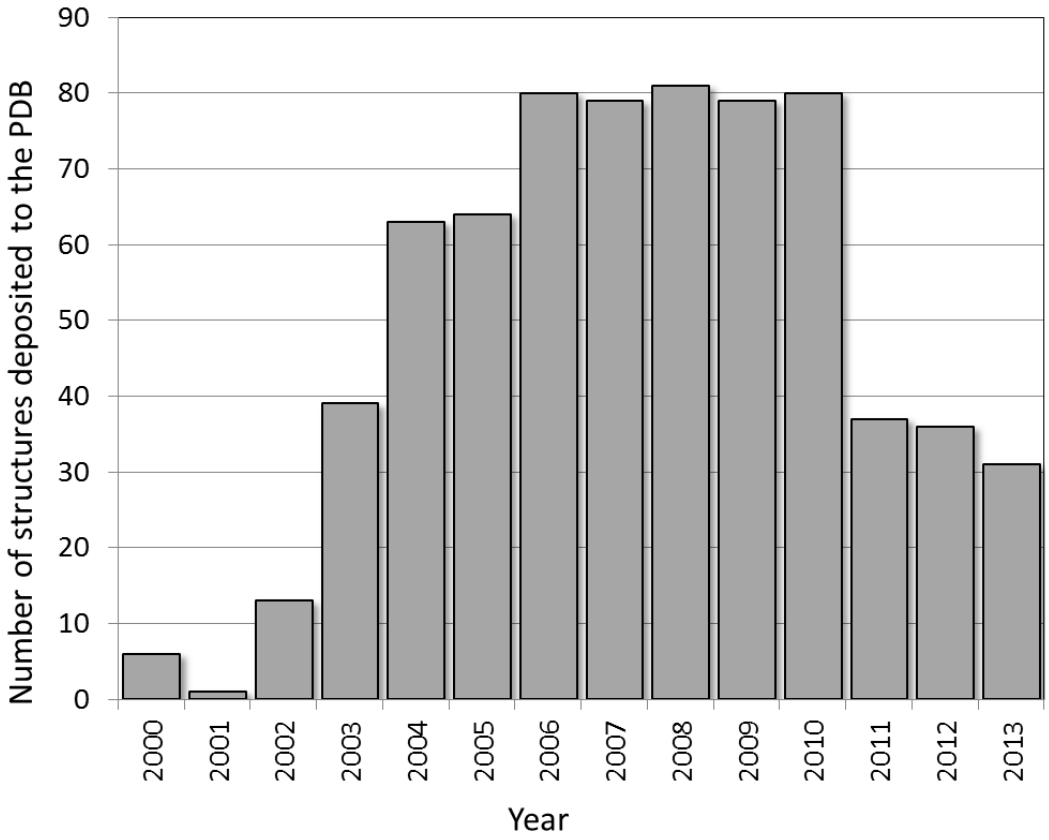

In 2011 we switched to PSI Biology – More difficult targets with 36 and 37 structures in 2011 and 2012 and 31 to date. Note the we do not solve the structures, only provide the initial crystallization hit.

- For high-throughput crystallization screening ~600 µl of protein in total is placed in a 12 well plate.
- Each well has ~ 5 µl of protein that can be retrieved after the crystallization screening sample has been setup (dead volume)
- 12 wells x 5 µl = 60 µl that we have leftover.
- Each sample is frozen at NESG, thawed at HWI for crystallization screening, retrieved from the source plate and then frozen at -80 °C.
- We have been using all the samples from one group, NESG, for SAXS experiments taking the 60 µl left over from some 4,000 different proteins.

Why Small Angle X-ray Scattering (SAXS)?

Crystallization is hard

Making the protein is easier

And we already have it …

History of SAXS

- In 1939 André Guinier found that X-ray scattering at the smallest angles was only present for heterogeneous solutions.
- He that the X-ray intensity was strongest at these angles for fine grains 10 to 100 nm in size and determined a method, to calculate the sizes of the particles from the scattering.
- SAXS began being used on biological macromolecules in the 1960s as a method to gain low-resolution structural information in the absence of crystals .
- The introduction of high-flux neutron sources enabled contrast variation studies using small angle neutron scattering (SANS) of perdeuterated solutions .
- Until the 1990s, only parameters about shape and size could be extracted from SAXS data including radius of gyration and particle volume,.
- Information about the 3D structure of a particle was limited to modeling estimations using simple geometrical bodies such as ellipsoids.

Developments in the last decade that have revolutionized SAXS

- Modern third-generation sources offer brilliance, i.e. flux on the sample and a highly parallel beam.
- Rapid readout noiseless detectors provide high-signal to noise (the SAXS signal is weak and has a high dynamic range)
- Computational algorithms have advanced (spherical harmonic approaches and more recently, molecular dynamics coupling to bead modeling).
- Computational power – thank the video gamers!

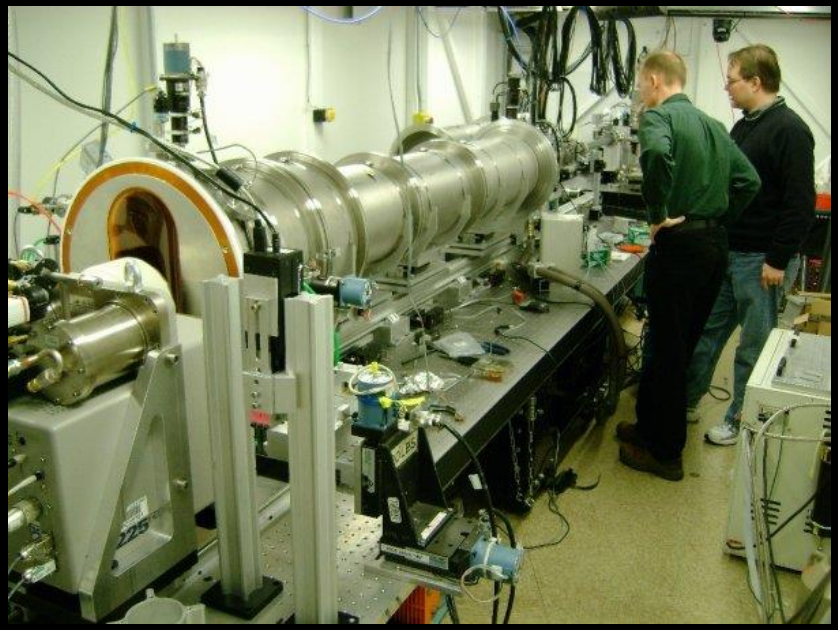

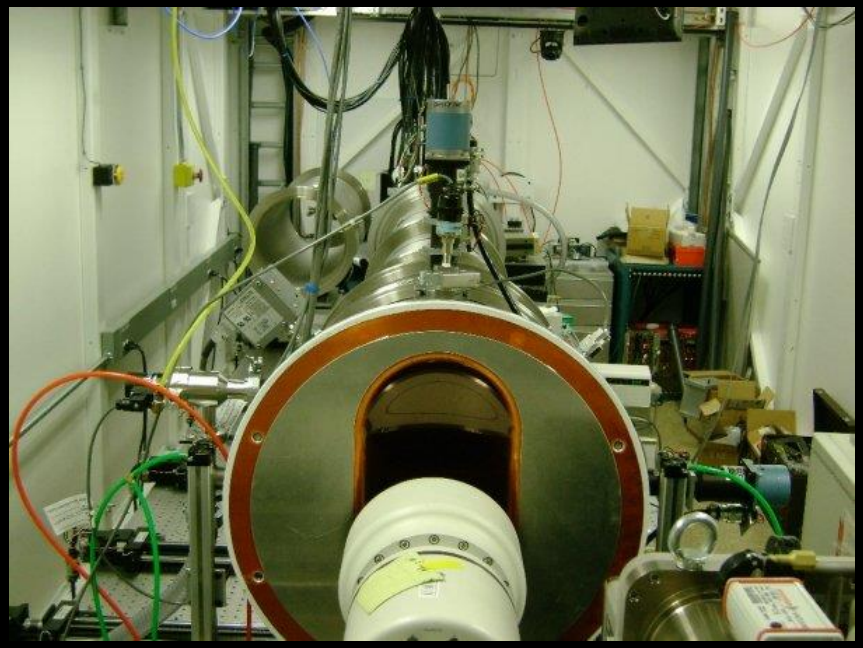

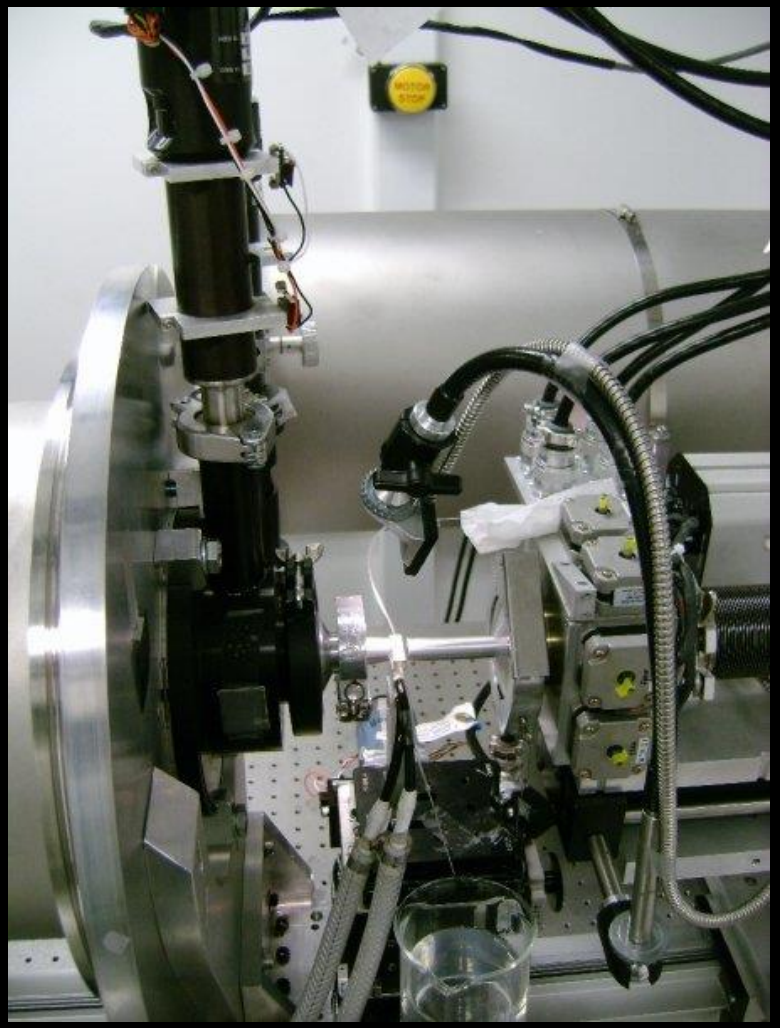

Beamline 4-2 SSRL

High throughput protocol

Up to 12 different PCR strips.

3-7 different concentrations per sample.

For high-throughput studies, 2 samples per strip, 24 samples in total

Start with buffer then lowest concentration first. End with buffer

8 exposures, 1-2s each dependent on sample molecular weight, buffer and concentration.

Oscillate sample to minimize radiation damage

Repeat the buffer.

Load next sample

Time per concentration series – approximately 10 to 15 minutes. In high-throughput mode 24 samples in 3 to 4 hours.

Enables two important things – eat and sleep!

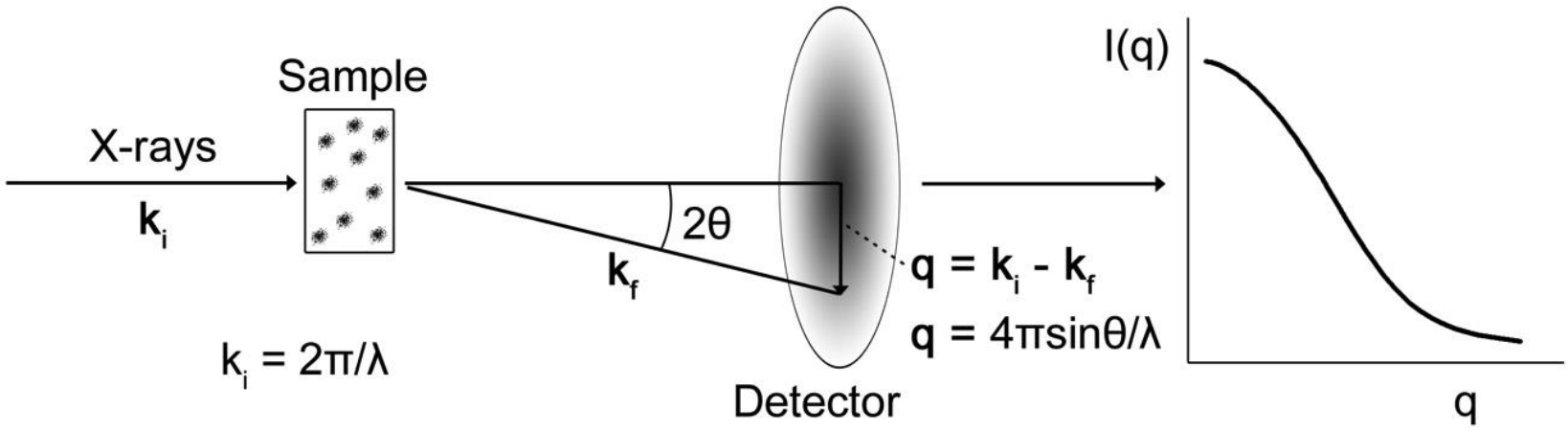

$$I(q) = \int 4\pi r^2 \cdot \bar{\rho}^2(r) \cdot \frac{\sin qr}{qr}\, dr$$

Data

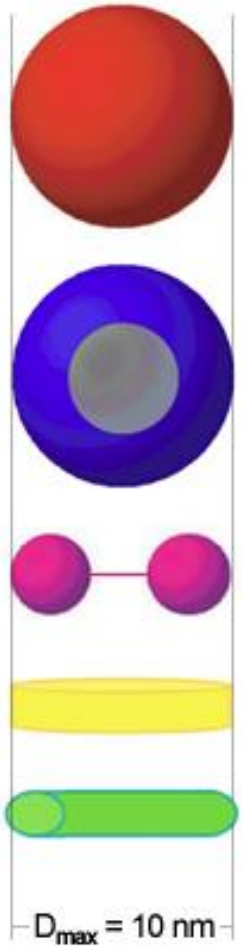

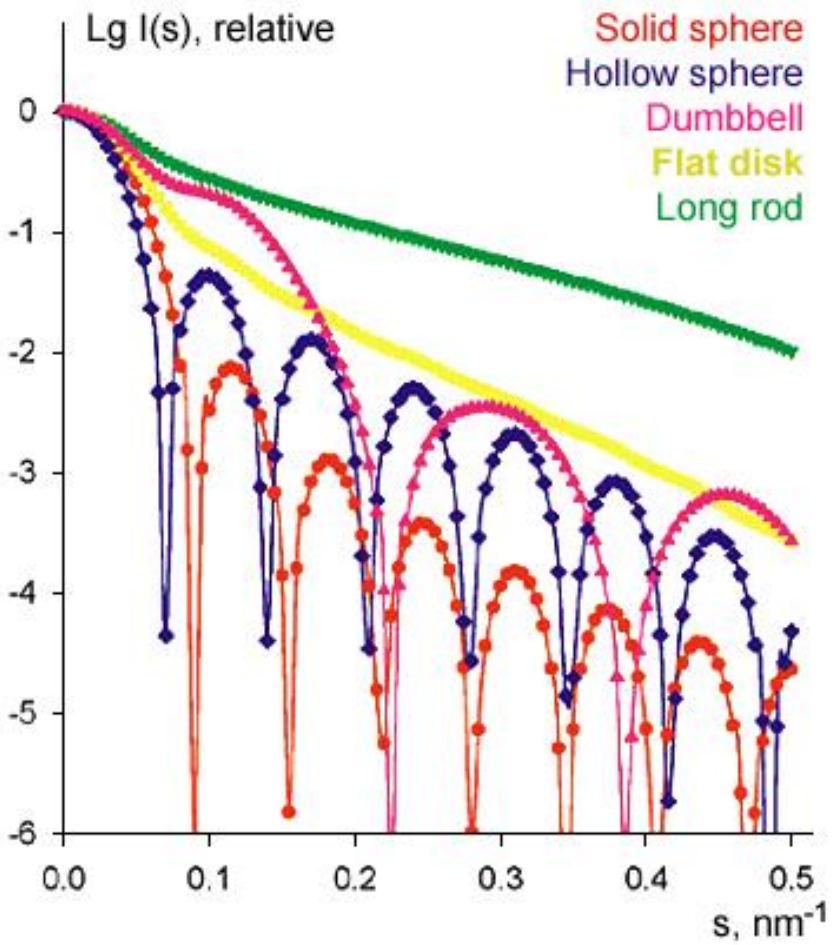

From: Small-angle scattering studies of biological macromolecules in solution, Svergun and Koch, Rep. Prog. Phys., 1735-1782 (2003)

Pair distribution function

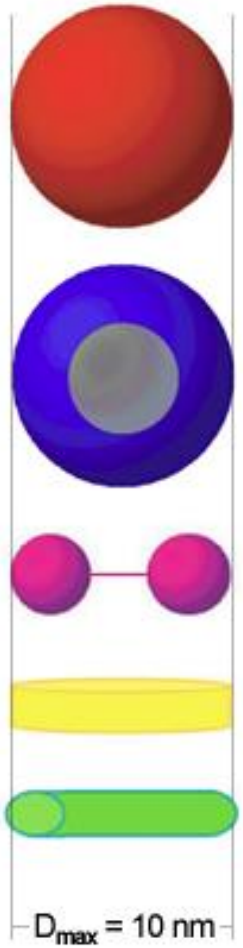

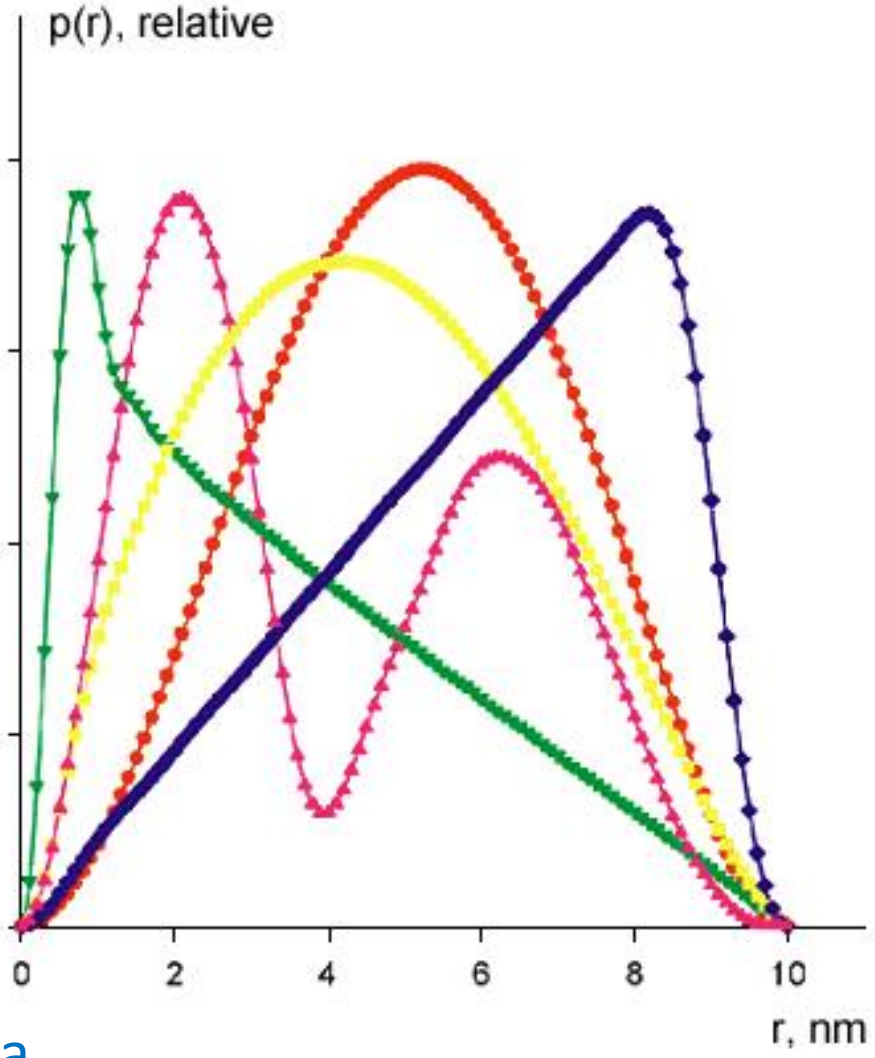

Fourier transform of data.

From: Small-angle scattering studies of biological macromolecules in solution, Svergun and Koch, Rep. Prog. Phys., 1735-1782 (2003)

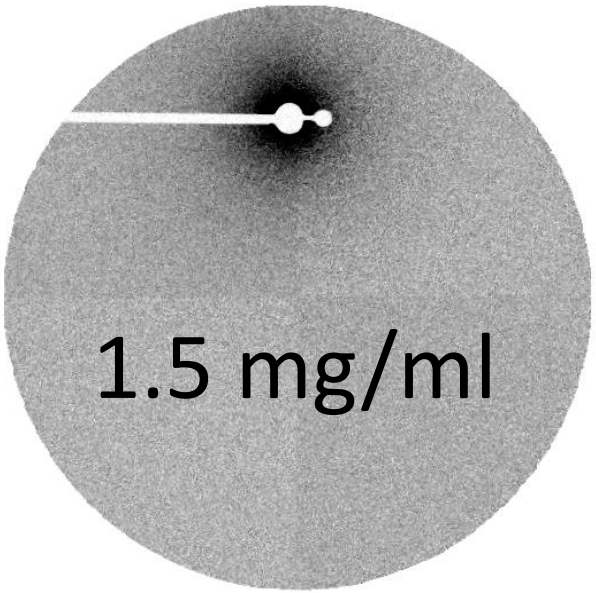
1.5 mg/ml

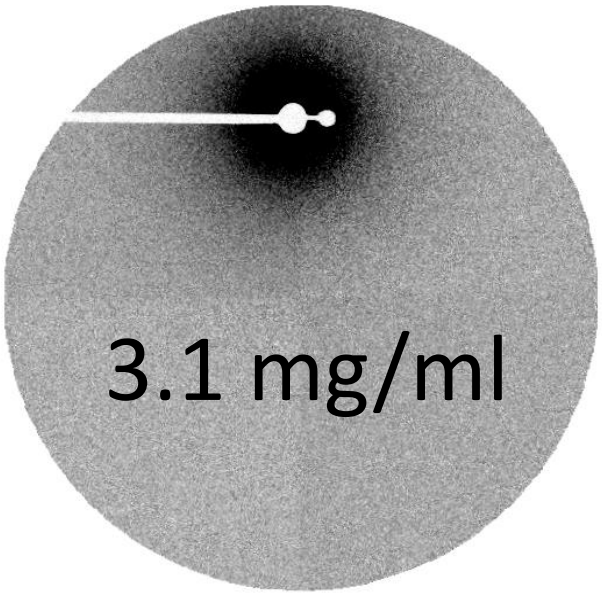
3.1 mg/ml

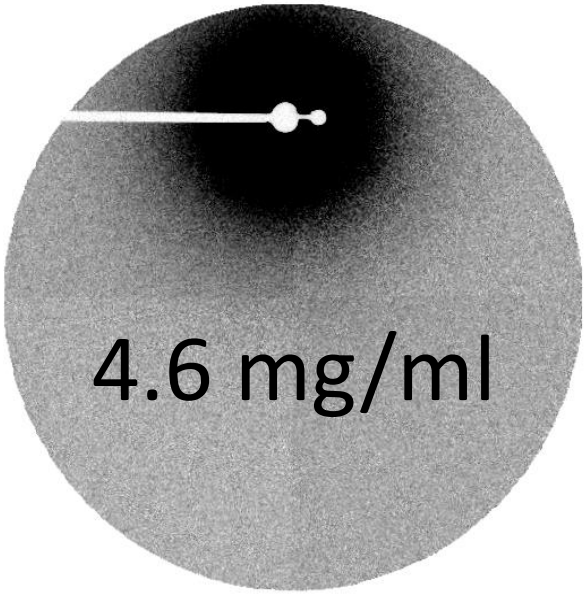
4.6 mg/ml

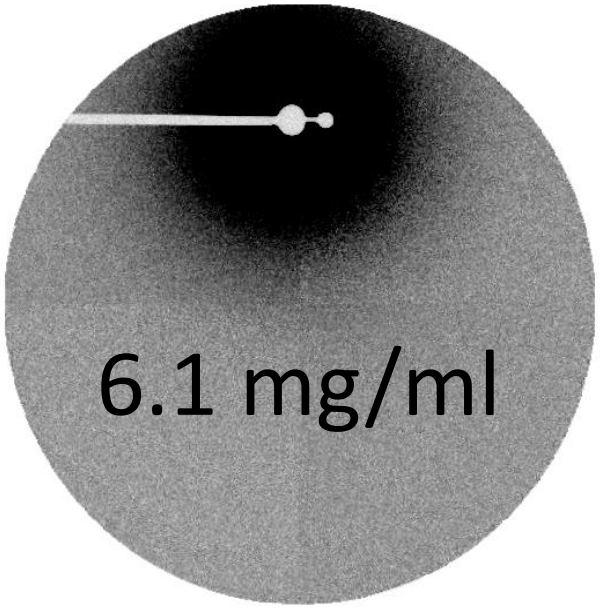
6.1 mg/ml

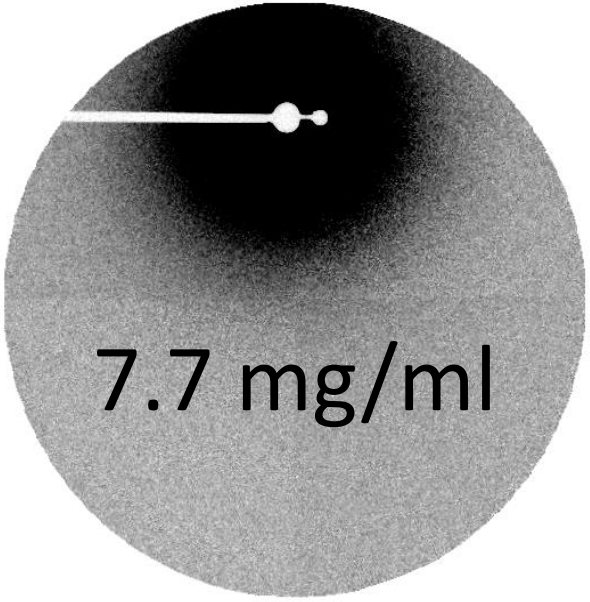
7.7 mg/ml

SAXS can determine *ab initio* molecular envelopes

Ab intio envelopes

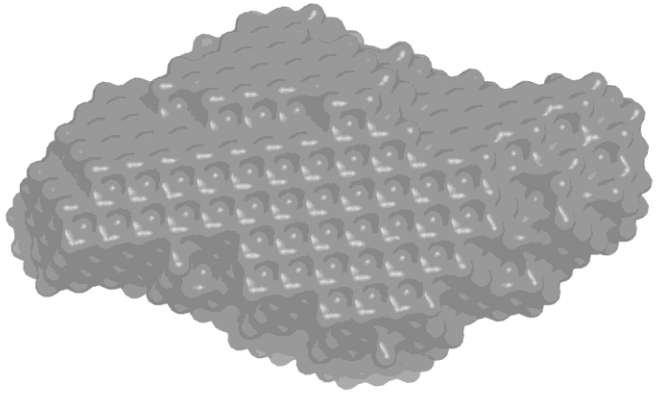

1). alr0221 protein from Nostoc (18.6 kDa)

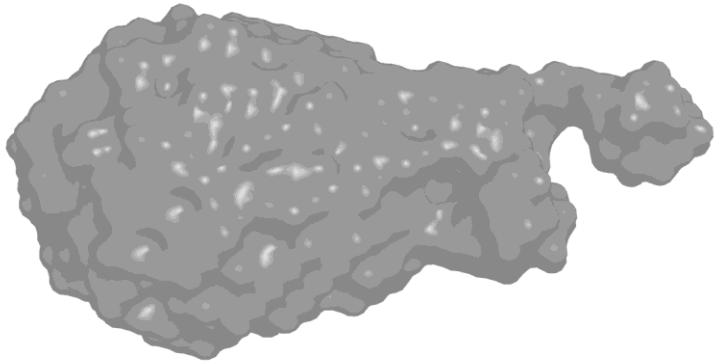

2). C-terminal domain of a chitobiase (17.9 kDa)

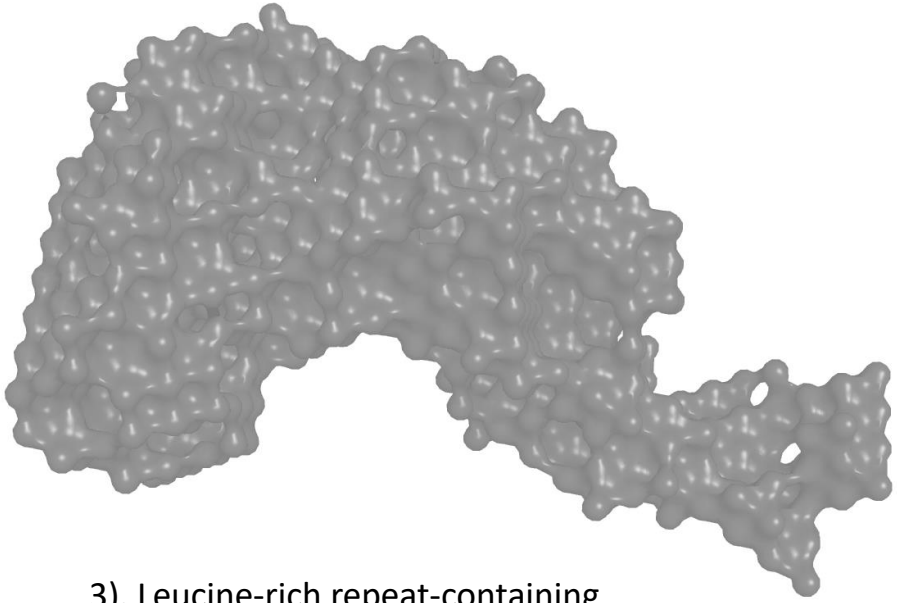

3). Leucine-rich repeat-containing protein LegL7 (39 kDa)

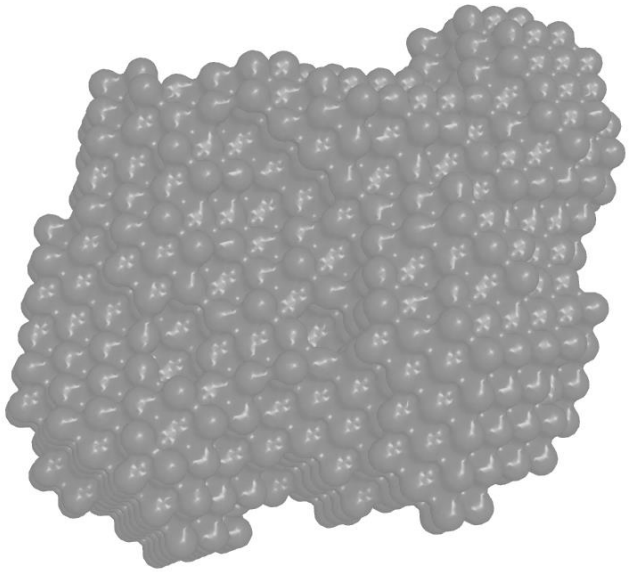

4). *E. Coli.* Cystine desulfurase activator complex (170 kDa)

These are compatible with structural data

Overlaid with subsequent X-ray structures

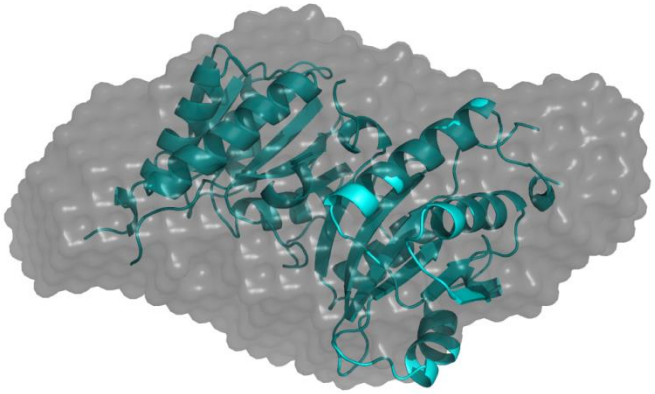

1). alr0221 protein from Nostoc (18.6 kDa)

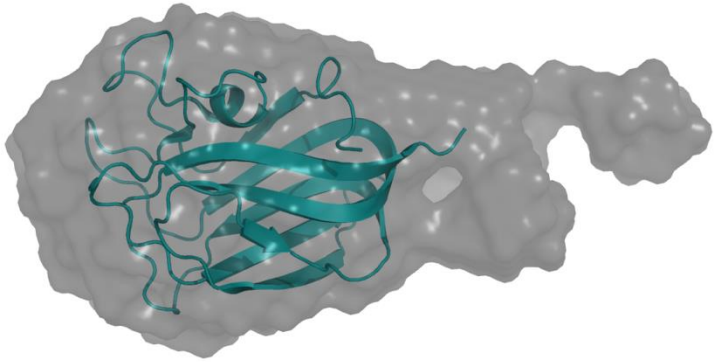

2). C-terminal domain of a chitobiase (17.9 kDa)

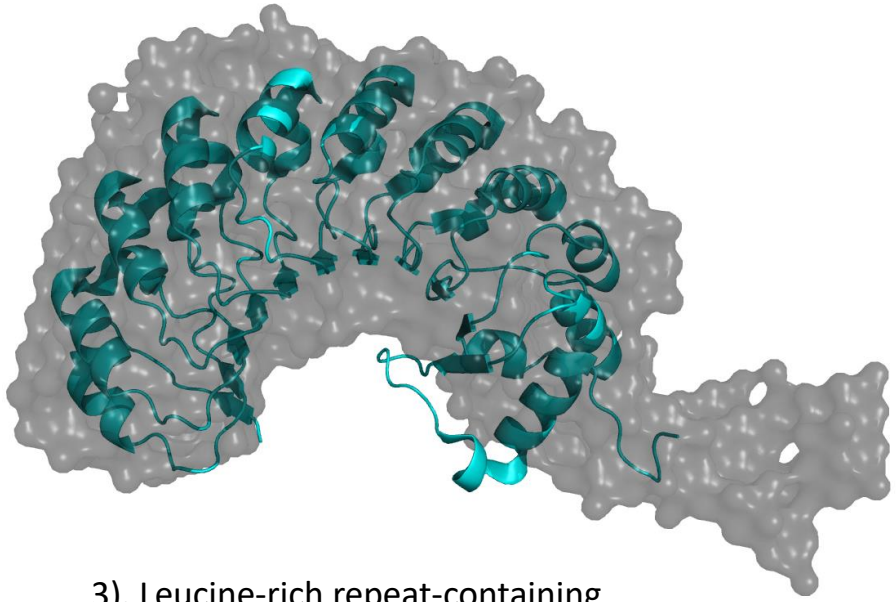

3). Leucine-rich repeat-containing protein LegL7 (39 kDa)

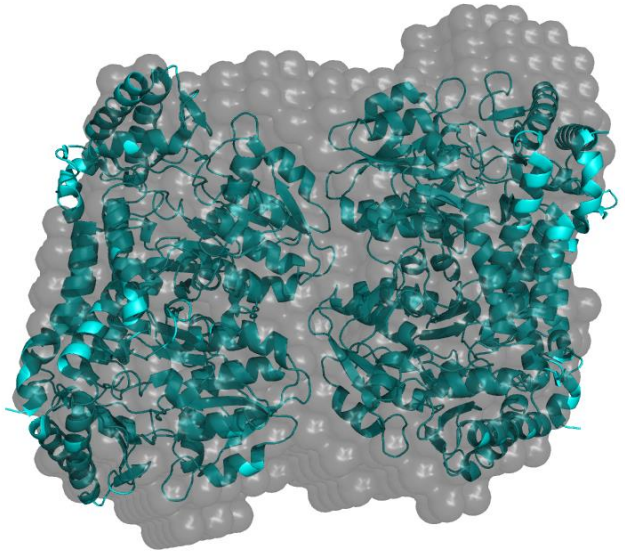

4). *E. Coli.* Cystine desulfurase activator complex (170 kDa)

And provide extra information on residues present in the construct but structurally undefined

And data on what was missing …

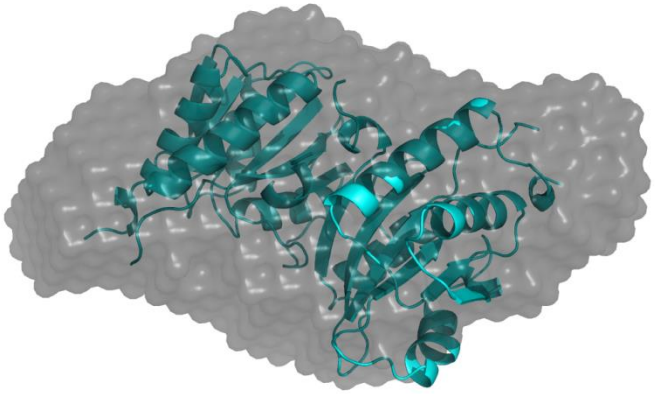

1). alr0221 protein from Nostoc (18.6 kDa)

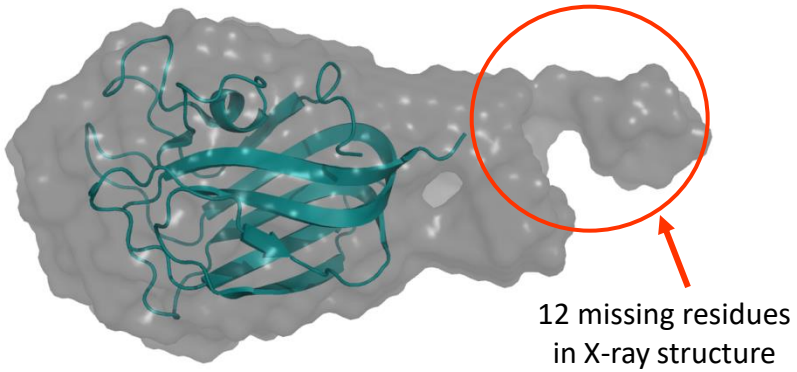

2). C-terminal domain of a chitobiase (17.9 kDa)

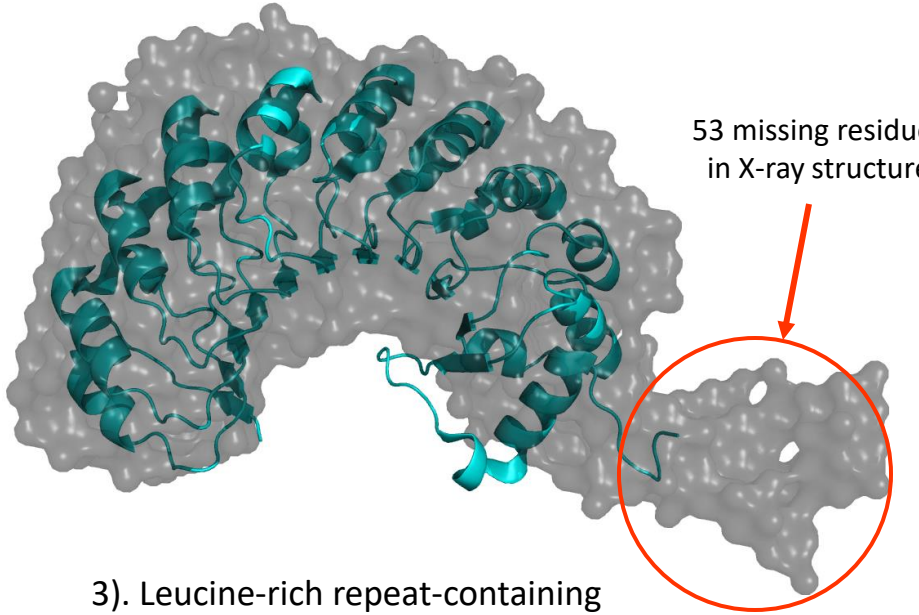

3). Leucine-rich repeat-containing protein LegL7 (39 kDa)

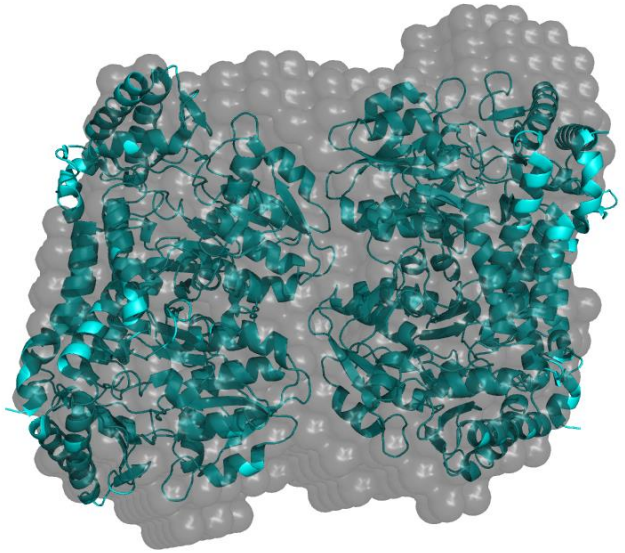

4). *E. Coli.* Cystine desulfurase activator complex (170 kDa)

SAXS Envelopes

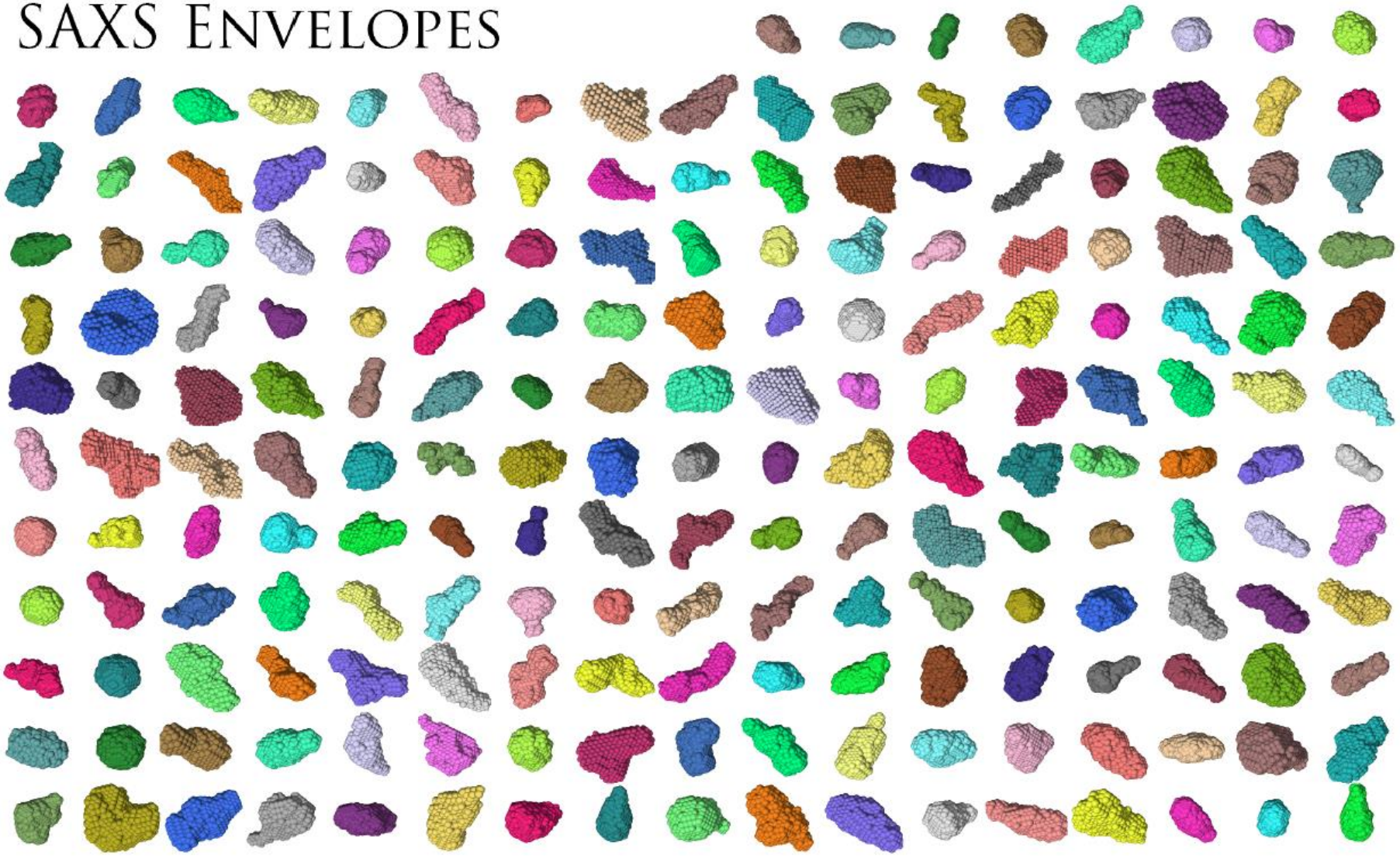

Comparing X-ray structures

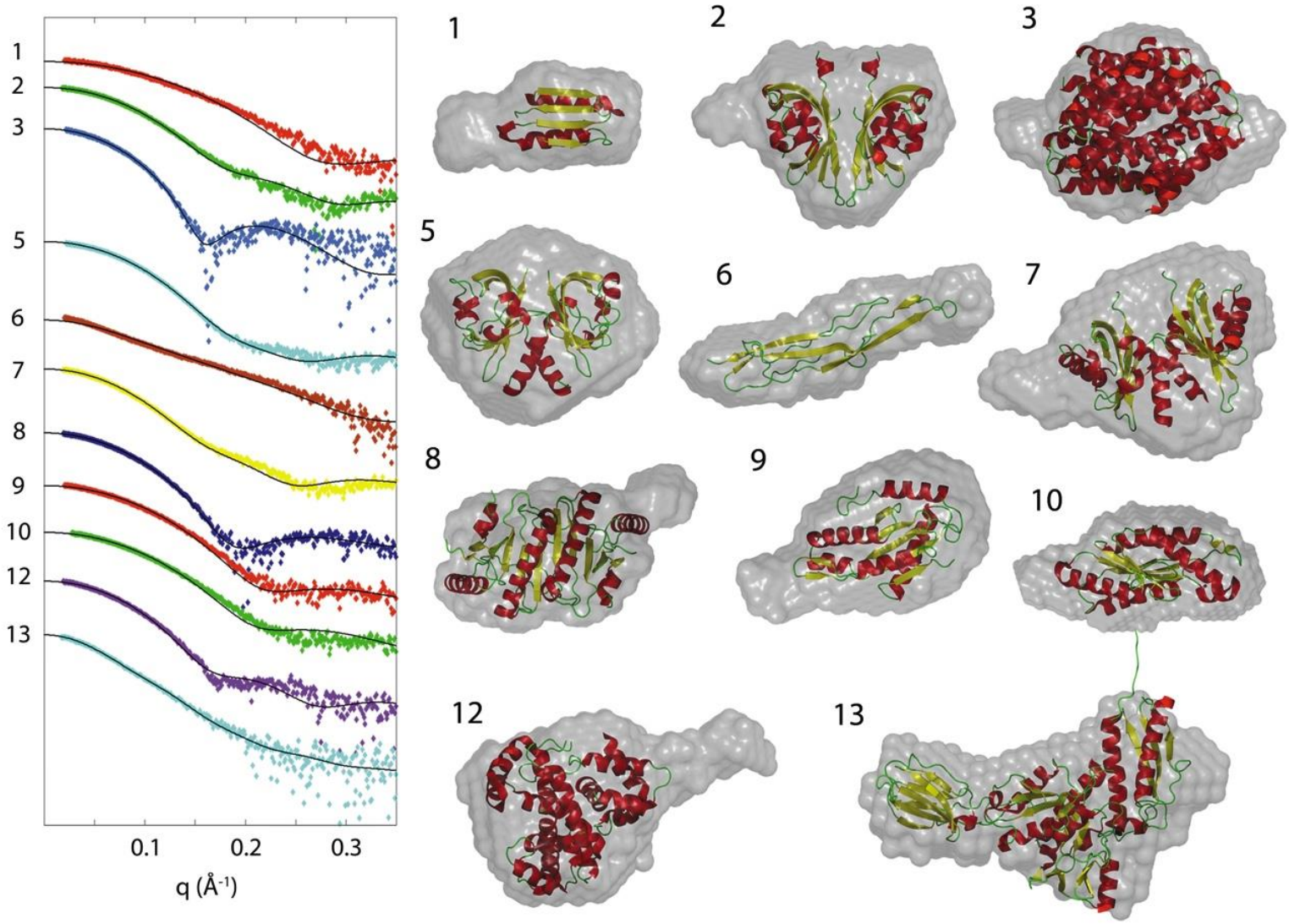

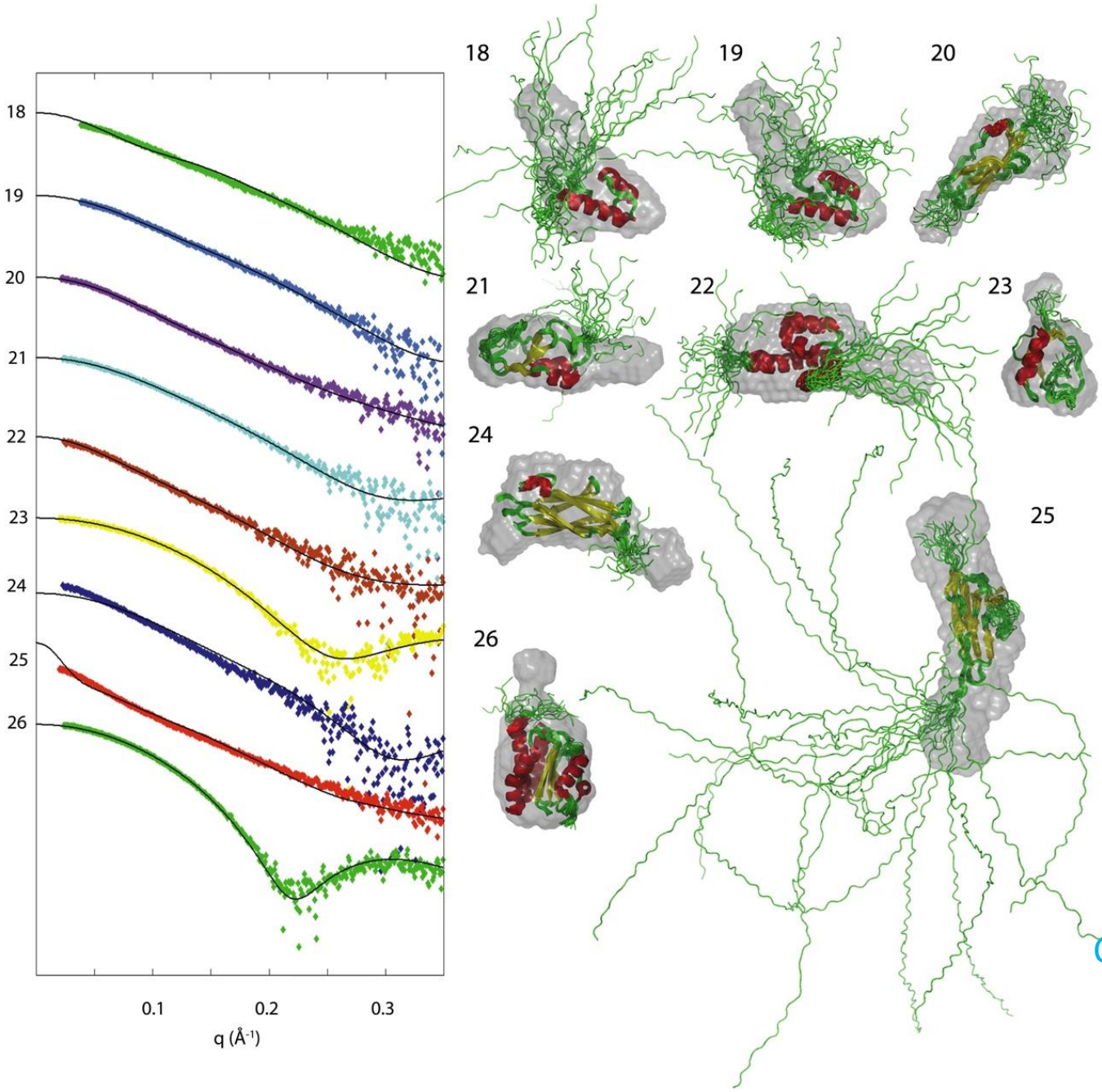

Comparing NMR structures

#	Name	NESG ID	PDB	Ref	State	Conc	MW	Res
Samples where crystallographic structures were available								
1	Domain of unknown function	DhR2A	3HZ7	16	M	6.9	9523	87
2	Diguanylate cyclase with PAS/PAC sensor	MqR66C	3H9W	17	D	8.2	13,611	210
3	Nmul_A1745 protein from *Nitrosospira multiformis*	NmR72	3LMF	18	T	6.9	14,069	484
4	Domain of unknown function	DhR85C	3MJQ	19	D	10.7	14,609	252
5	Sensory box/GGDEF family protein	SoR288B	3MFX	20	D	9.1	14,779	258
6	MucBP domain of the adhesion protein PEPE_0118	PtR41A	3LYY	21	M	9.5	14,300	131
7	Sensory box/GGDEF domain protein	CsR222B	3LYX	22	D	12.7	15,341	248
8	HIT family hydrolase	VfR176	3I24	23	D	11.0	17,089	298
9	EAL/GGDEF domain protein	McR174C	3ICL	24	M	5.0	18,738	171
10	Diguanylate cyclase	MqR89A	3IGN	25	M	7.5	20,256	177
11	Putative NADPH-quinone reductase	PtR24A	3HA2	26	D	9.5	20,509	354
12	MmoQ (response regulator)	McR175G	3LJX	27	M	8.8	32,032	288
13	Putative uncharacterized protein	DhR18	3HXL	28	M	9.6	48,519	446
Samples where multiple constructs and crystallographic structures were available								
14	Putative hydrogenase	PfR246A (78–226)	3LRX	29	D	11.4	17,701	316
15		PfR246A (83–218)	3LYU	30	D	8.4	16,321	284
16	Alr3790 protein	NsR437I	3HIX	31	M	5.3	11,760	105
17		NsR437H	3HIX	31	M	6.5	15,700	141
Samples where NMR structures were available								
18	MKL/myocardinlike protein 1	HR4547E	2KW9 (NMR)	32	D	10.4	8276	75
19	MKL/myocardinlike protein 1	HR4547E	2KVU (NMR)	33	D	10.4	8276	75
20	Putative peptidoglycan bound protein (LPXTG motif)	LmR64B	2KVZ (NMR)	34	M	5.0	9712	85
21	E3 ubiquitin-protein ligase Praja1	HR4710B	2L0B (NMR)	35	M/D	5.6	10,297	91
22	Transcription factor NF-E2 45 kDa subunit	HR4653B	2KZ5 (NMR)	36	M	10.0	10,623	91
23	YlbL protein	GtR34C	2KL1 (NMR)	37	M	11.0	10,661	94
24	Cell surface protein	MvR254A	2L0D (NMR)	38	Tri	5.9	12,385	114
25	Domain of unknown function	MaR143A	2KZW (NMR)	39	M	6.6	16,312	145
26	N-terminal domain of protein PG_0361 from *P. gingivalis*	PgR37A	2KW7 (NMR)	40	M	12.9	17,485	157
Samples where both crystallographic and NMR structures were available								
27	GTP pyrophosphokinase	CtR148A	2KO1 (NMR)	41	D	8.0	10,042	176
			3IBW	42	T	8.0	10,042	176
28	Lin0431 protein	LkR112	2KPP (NMR)	43	M/Hep	6.3	12,747	114
			3LD7	44	M	6.3	12,747	100

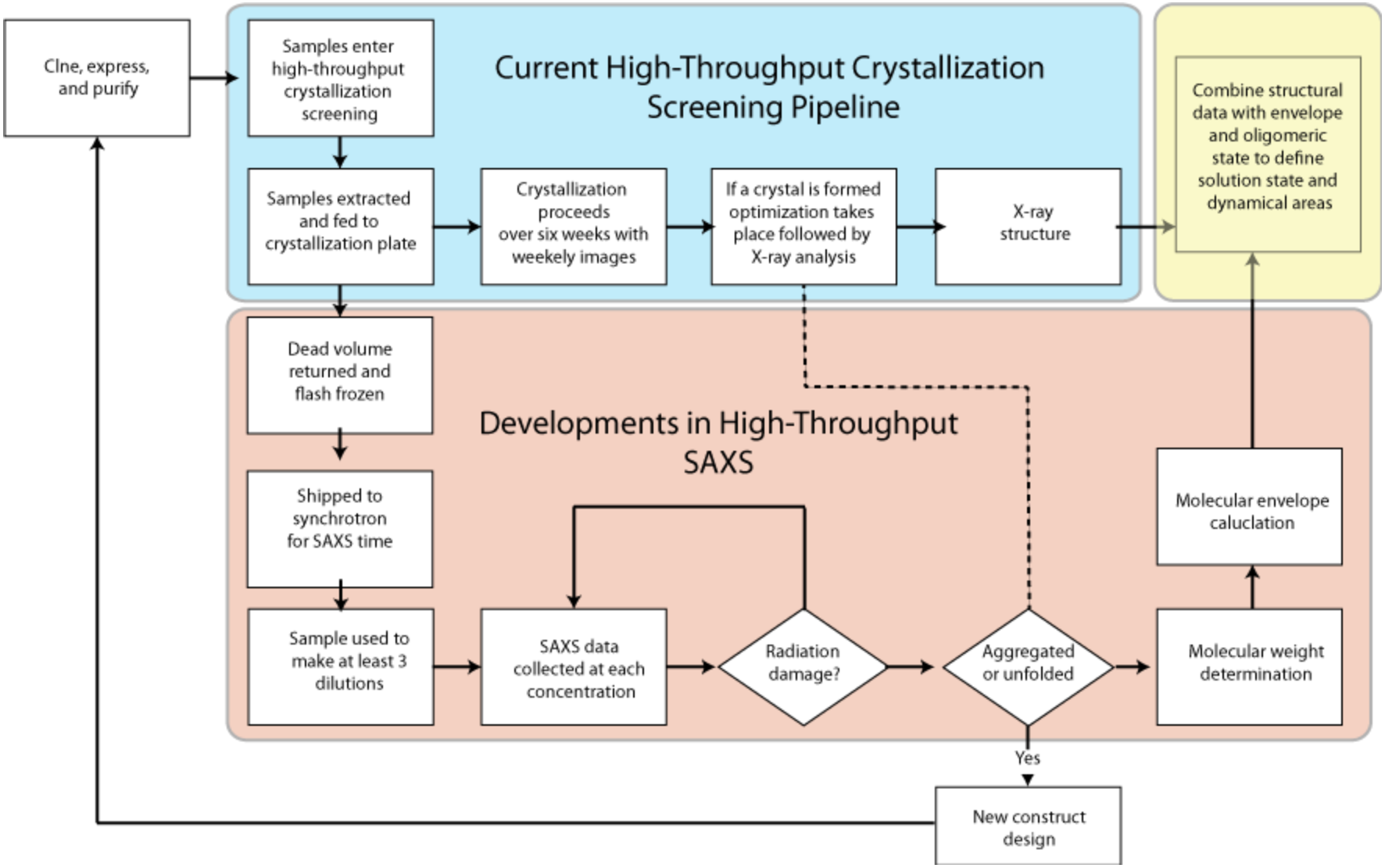
Clne, express, and purify
Samples enter high-throughput crystallization screening
Current High-Throughput Crystallization Screening Pipeline
Samples extracted and fed to crystallization plate
Crystallization proceeds over six weeks with weekely images
If a crystal is formed optimization takes place followed by X-ray analysis
X-ray structure
Combine structural data with envelope and oligomeric state to define solution state and dynamical areas
Dead volume returned and flash frozen
Developments in High-Throughput SAXS
Shipped to synchrotron for SAXS time
Molecular envelope caluclation
Sample used to make at least 3 dilutions
SAXS data collected at each concentration
Radiation damage?
Aggregated or unfolded
Molecular weight determination
Yes
New construct design

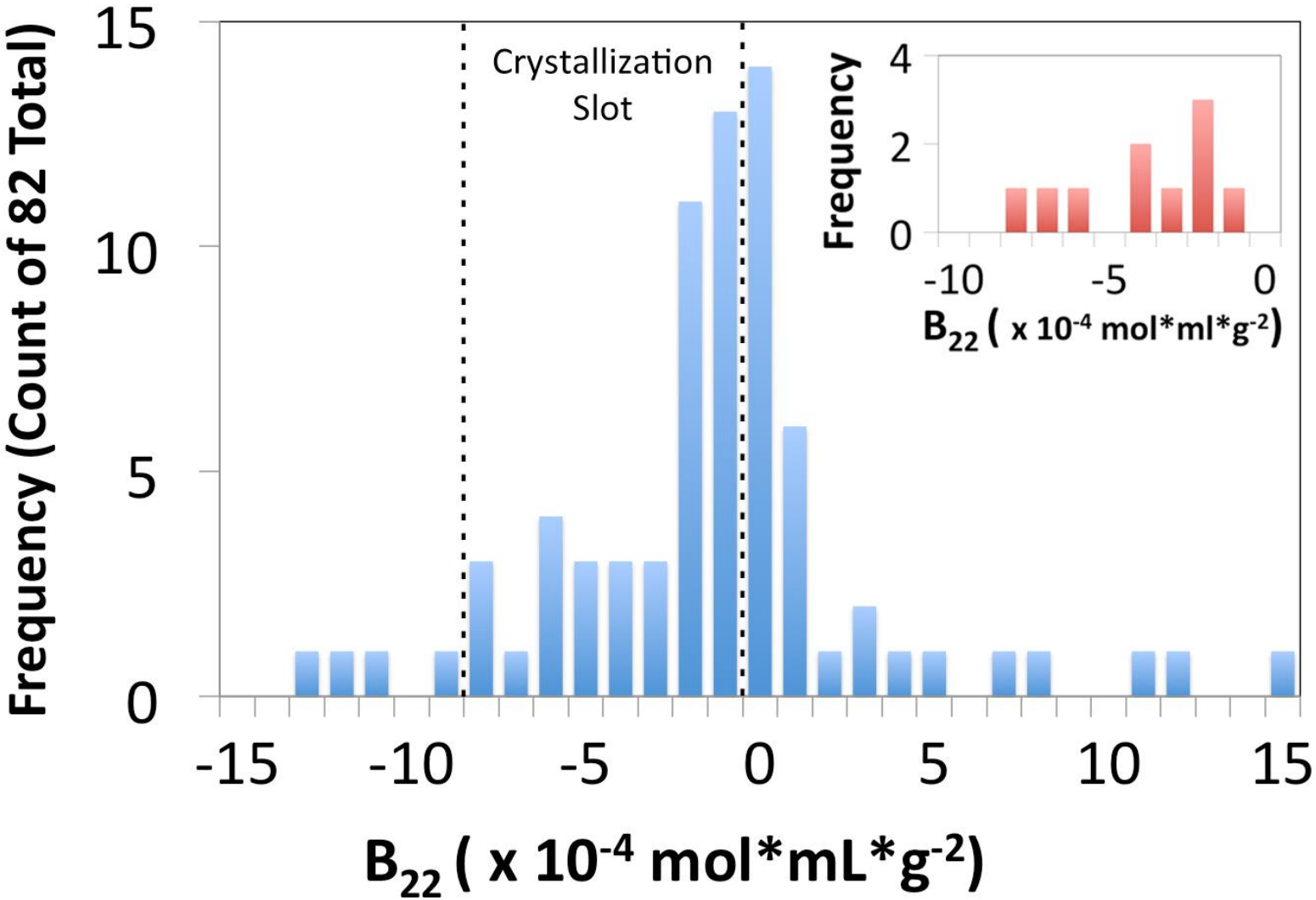
Frequency (Count of 82 Total)
15
10
5
0
Crystallization
Slot
-15
-10
-5
0
5
10
15
B22 (x 10-4 mol*mL*g-2)
Frequency
4
2
0
-10
-5
0
B22 (x 10-4 mol*ml*g-2)

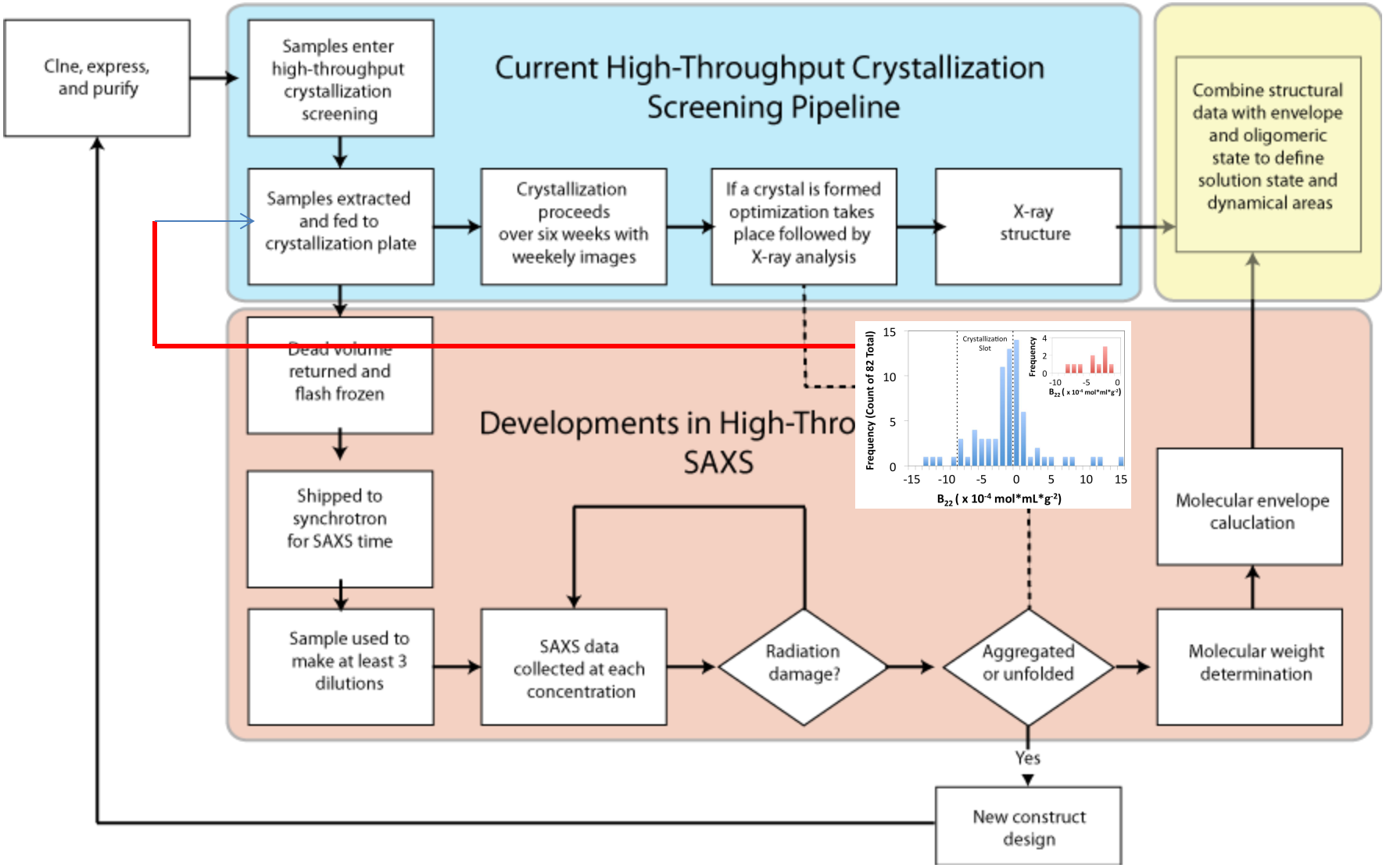
Clne, express, and purify
Samples enter high-throughput crystallization screening
Current High-Throughput Crystallization Screening Pipeline
Samples extracted and fed to crystallization plate
Crystallization proceeds over six weeks with weekely images
If a crystal is formed optimization takes place followed by X-ray analysis
X-ray structure
Combine structural data with envelope and oligomeric state to define solution state and dynamical areas
Dead volume returned and flash frozen
Developments in High-Thro
SAXS
Frequency (Count of 82 Total)
Crystallization Slot
Frequency
B22 (x 10-4 mol*mL*g-2)
Shipped to synchrotron for SAXS time
Molecular envelope caluclation
Sample used to make at least 3 dilutions
SAXS data collected at each concentration
Radiation damage?
Aggregated or unfolded
Molecular weight determination
Yes
New construct design

A Biological Puzzle

PHYSICS FOR BIOLOGISTS

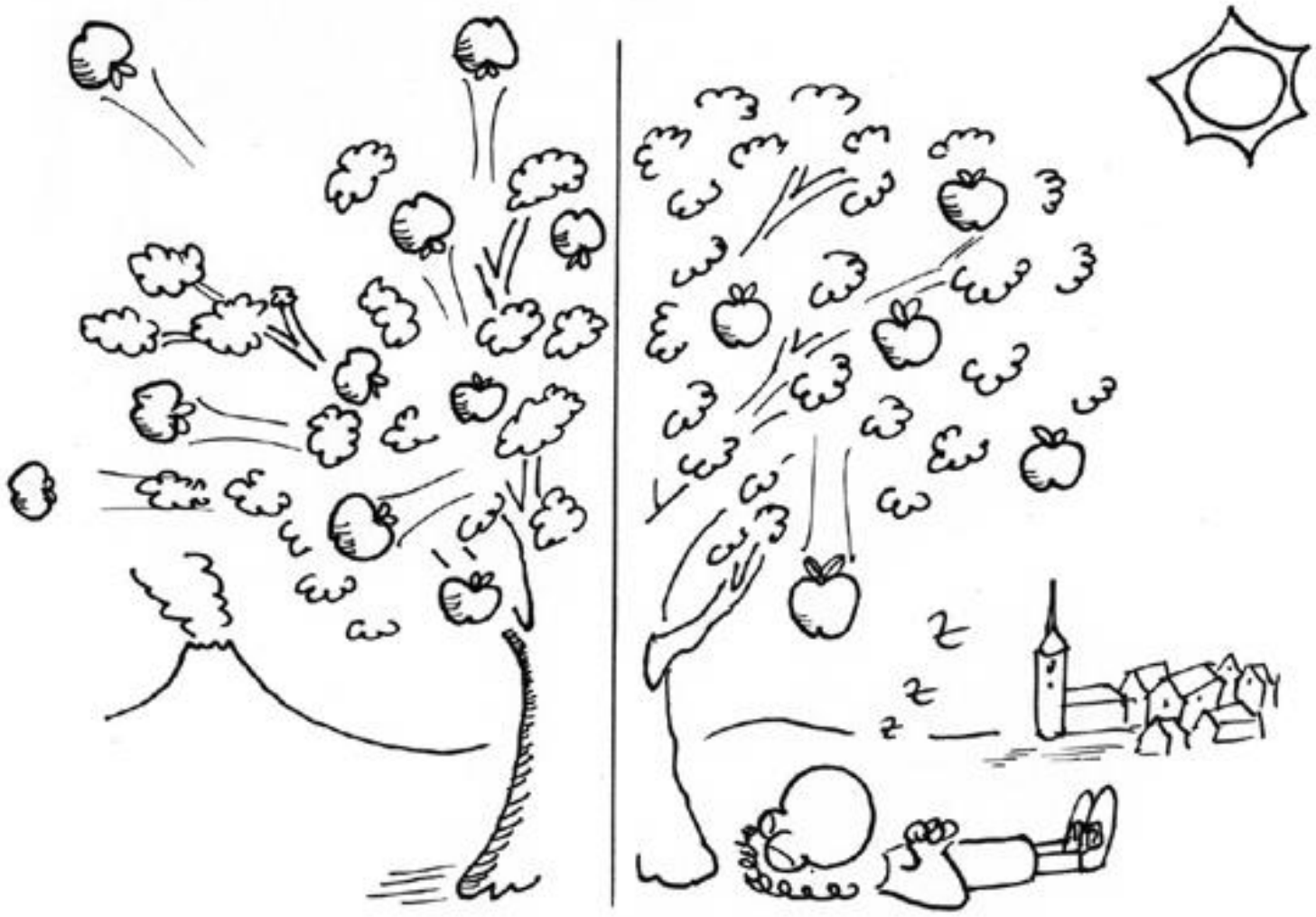

A long time ago the apple trees used to shoot the apples in all directions. Only those that did it downward got reproduced. Then, after millions years of natural selection and evolution, gravity was finally discovered.

tRNA Synthetases

- Amino acids are attached to tRNA molecules which are then transferred to the ribosome for use in protein synthesis
- tRNA synthetases act as the “codebook” in the central dogma
- In most cases, one tRNA synthetase exists for each amino acid

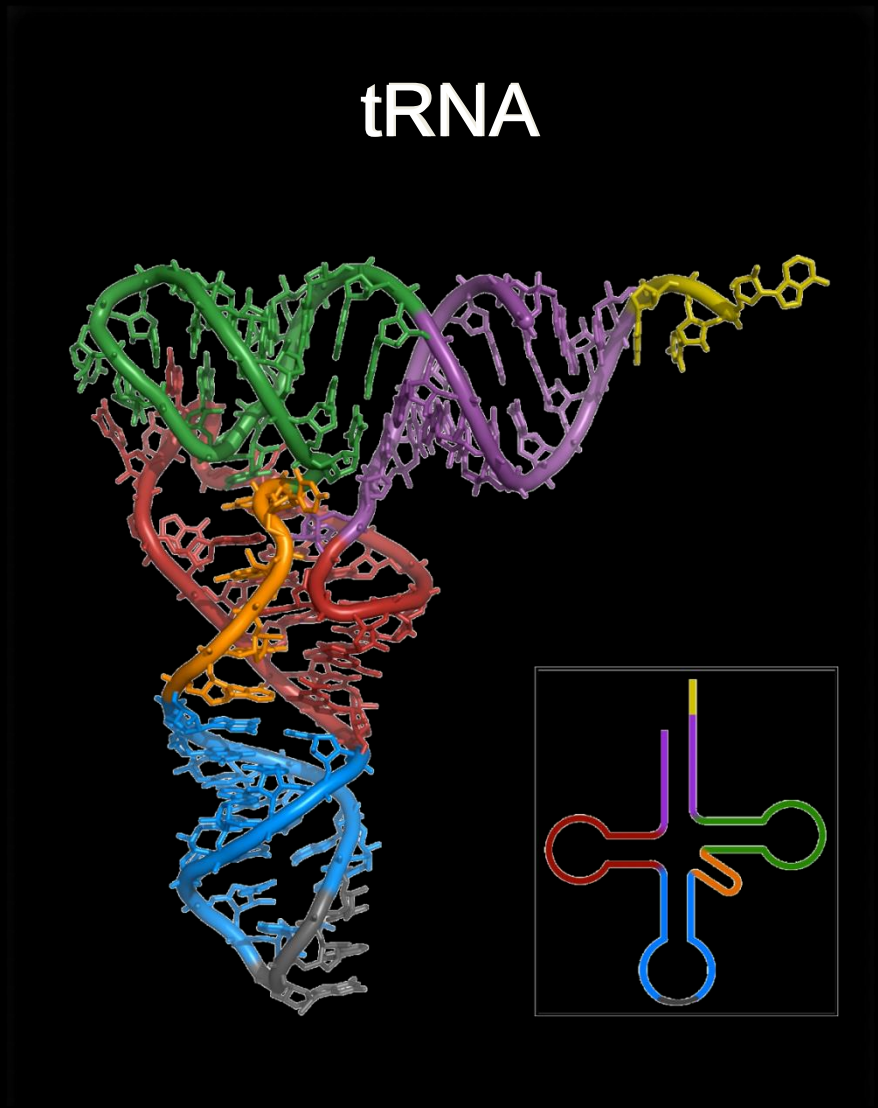

Two routes of gln-tRNA^{GLN} Formation

Direct Route: Eukaryotes and few bacteria

Two routes of gln-tRNA^{GLN} Formation

Indirect Route: Archaea and Most Bacteria

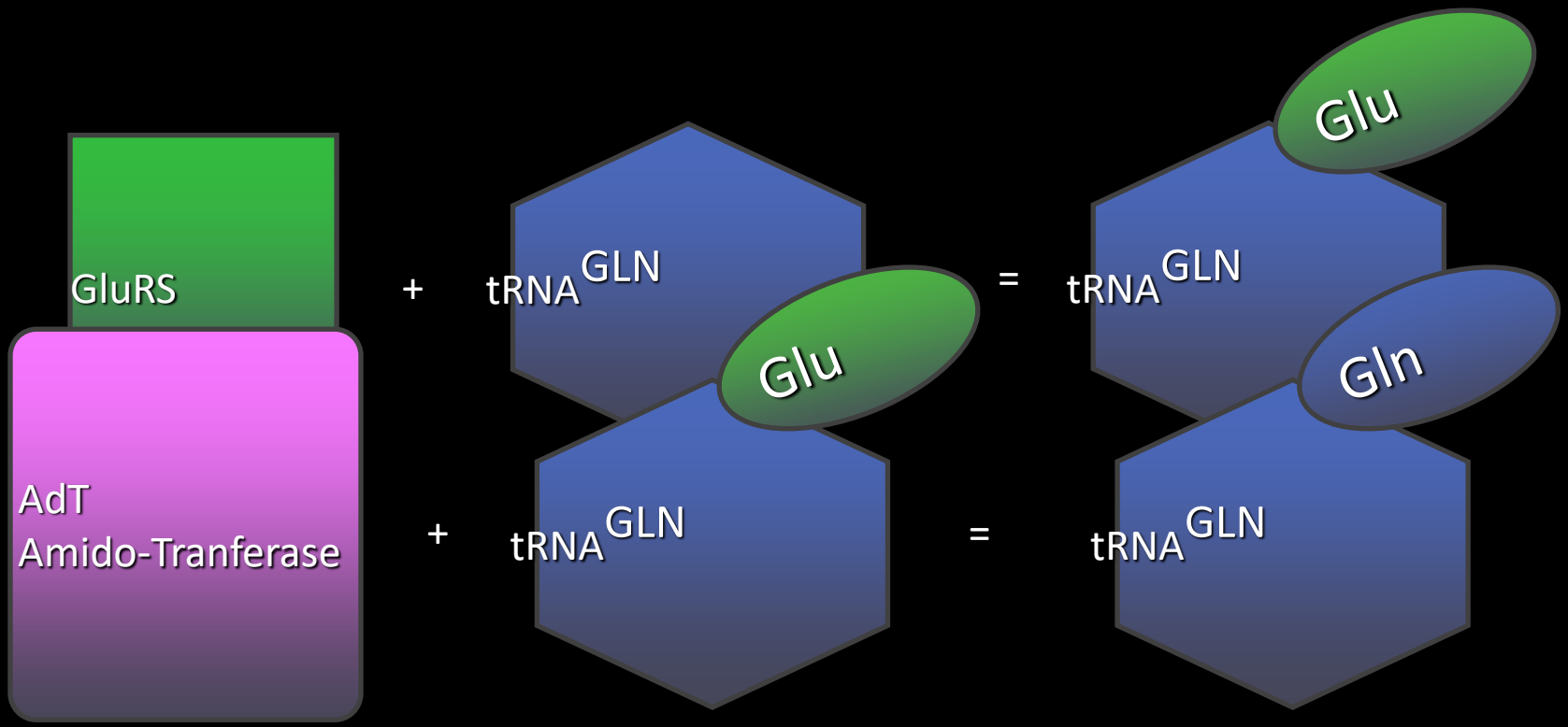

tRNA synthetase of Eukaryotes and Prokaryotes

- Most of our structural knowledge of tRNA synthetases comes from prokaryotes

Appended Domains

- Eukaryotic tRNA synthetases often carry appended domains not present in prokaryotic homologs
- These domains are known to bind RNA non-specifically
- Little is known about their function or structure

The N-terminal domain (NTD)

- Eukaryotic tRNA synthetases are distinctly more complex than their prokaryotic homologs because they have progressively acquired and retained additional domains throughout evolution
- Like other eukaryotic GlnRS species, *Saccharomyces cerevisiae* Gln4 contains both a highly conserved C-terminal domain (CTD) with all of the known features of class I synthetases, as well as a less conserved appended N-terminal domain (NTD) with no obvious sequence homology to any known protein domain.
- While some appended domains are shared among synthetase families and are similar to domains in other proteins implicated in either nucleic acid binding or protein-protein interactions at least eight domains are uniquely associated with a single synthetase family, and neither their structures nor their roles are generally understood.
- The origin and function of the NTD in GlnRS are of particular interest.

Glutamine tRNA Synthetase

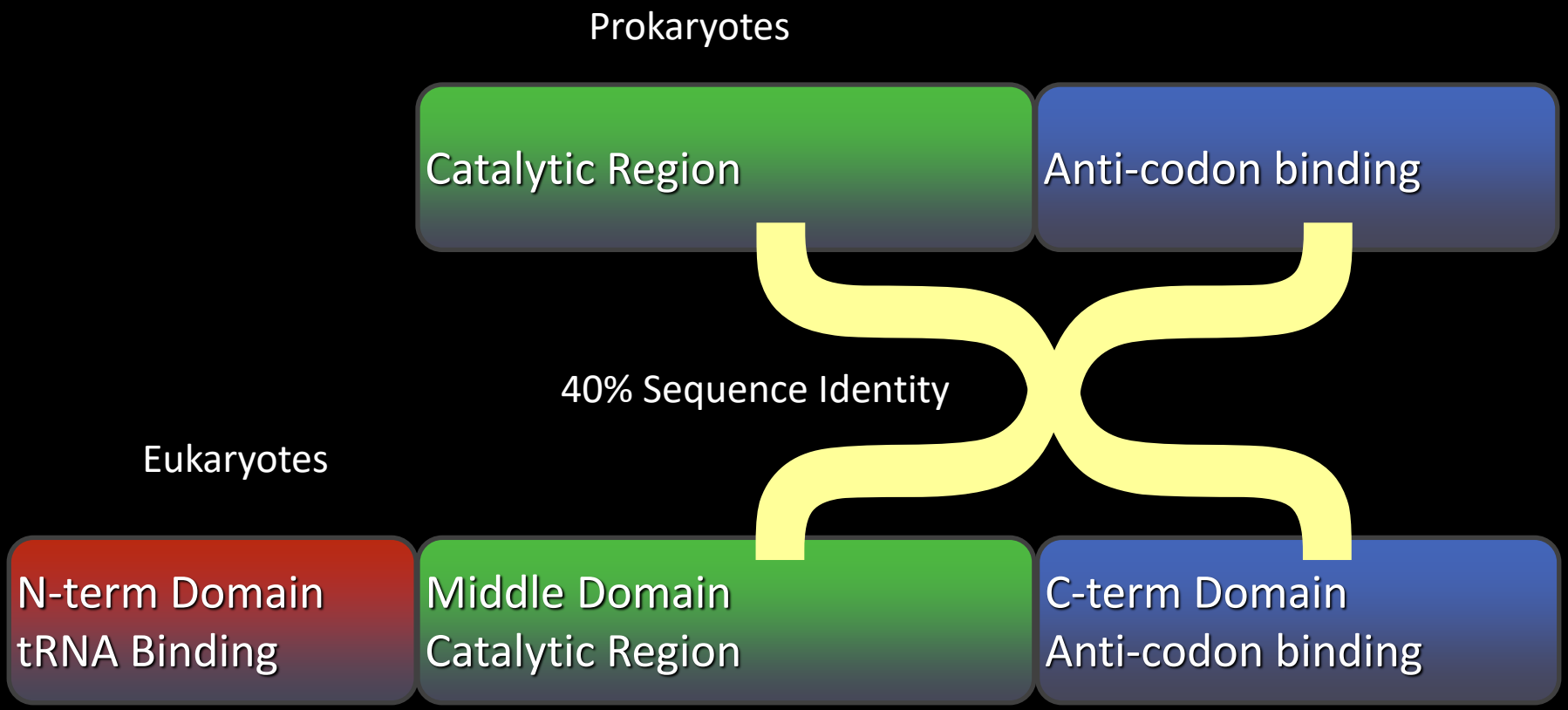

Target

- Our target is Glutaminyl tRNA synthetase (Gln4) from yeast *Saccharomyces cerevisiae*

- Yeast *Saccharomyces cerevisiae is* a well-established model system for understanding fundamental cellular processes of higher eukaryotic organisms.

- Many eukaryotic tRNA synthetases like Gln4 differ from their prokaryotic homologs by the attachment of an additional domain appended to their N or C-terminus, but it is unknown how these domains contribute to tRNA synthetase function, and why they are not found in prokaryotes

- The 228 amino acid N-terminal domain of Gln4 is among the best studied of these domains, but is structurally uncharacterized.

- The N-terminal domain appears to have non specific RNA binding.

- The role of a nonspecific RNA binding domain in the function of a highly specific RNA binding enzyme is baffling, but clearly crucial given its prevalence among tRNA

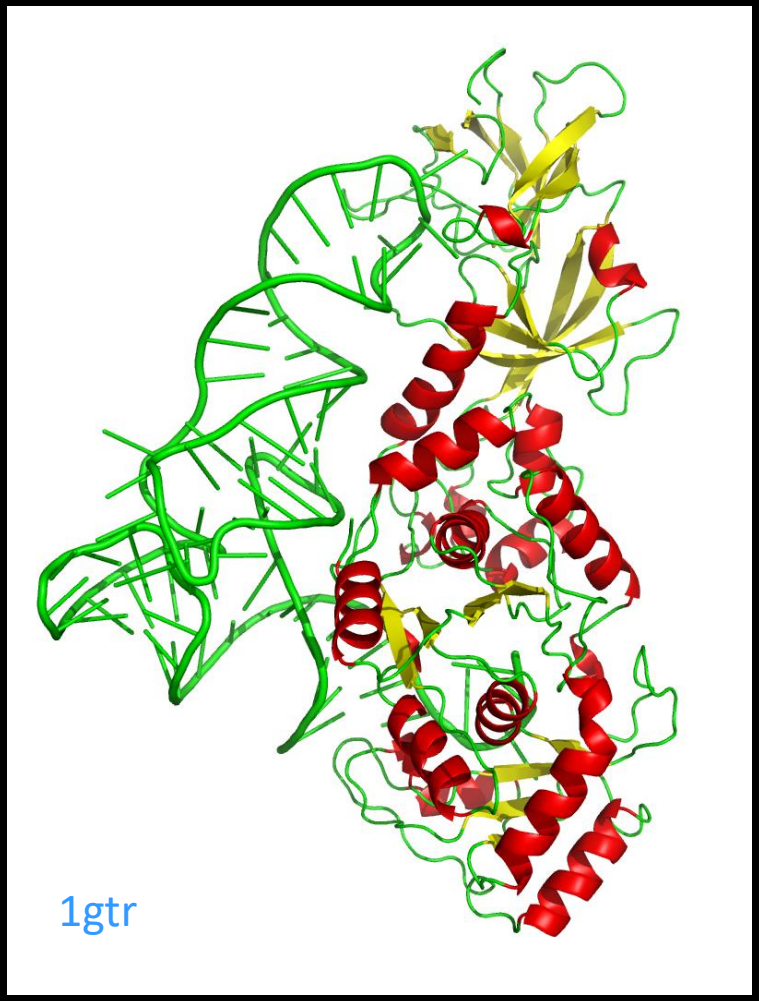

Structural model of *E. coli* glutaminyl-tRNA synthetase

These enzymes are not gentle with tRNA molecules. The enzyme firmly grips the anticodon, spreading the three bases widely apart for better recognition. At the other end, the enzyme unpairs one base at the beginning of the chain, seen curving upward here, and kinks the long acceptor end of the chain into a tight hairpin, seen here curving downward. This places the 2' hydroxyl on the last nucleotide in the active site, where ATP and the amino acid (not present in this structure) are bound.

Structural basis of anticodon loop recognition by glutaminyl-tRNA synthetase. Rould, Perona, and Steitz **Journal:** (1991) Nature**352:** 213-218

Structures only known from *E.coli* and *D. radiodurans*

Model of *D. radiodurans* GlnRStRNA^{Gln} complex

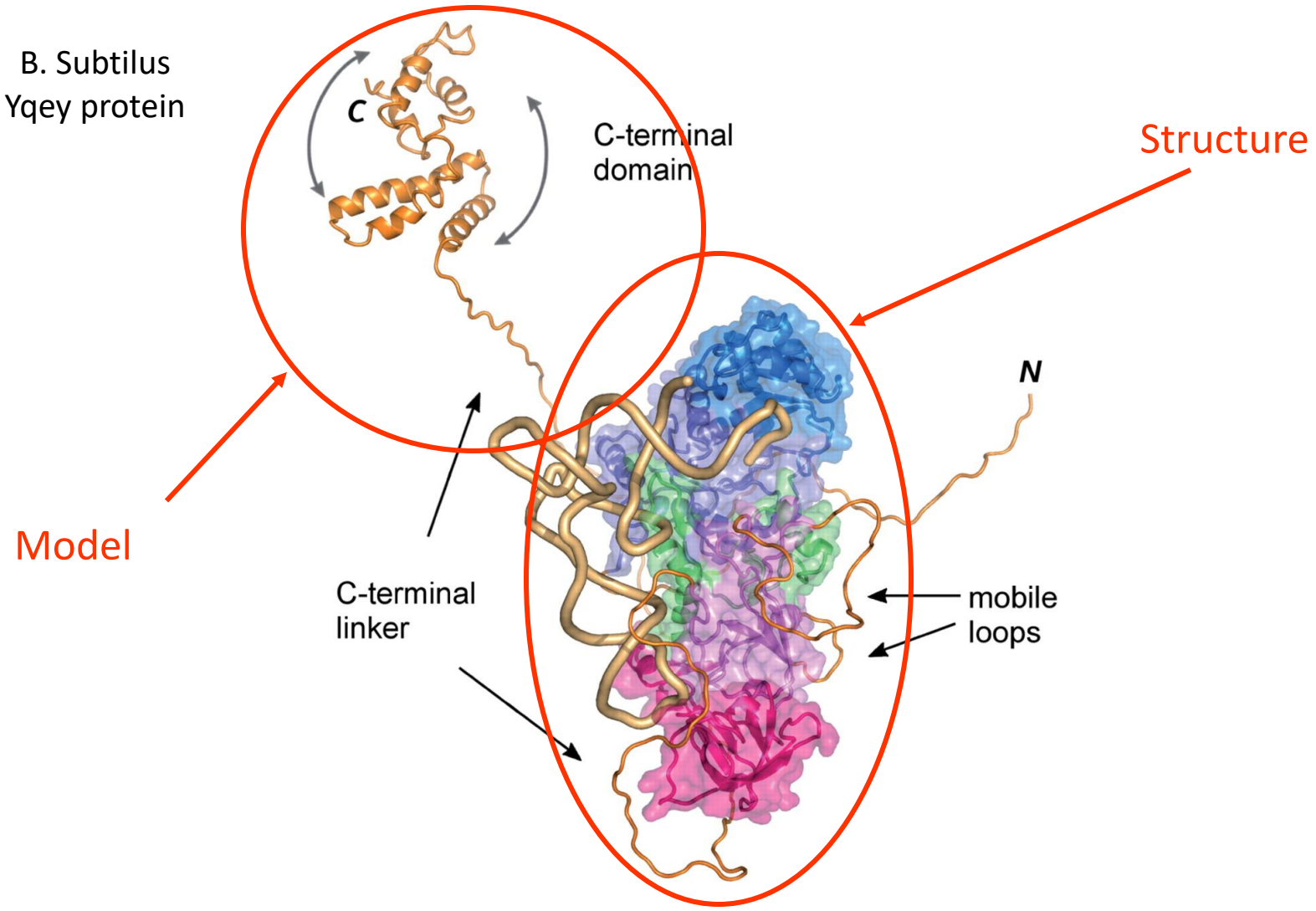

Crystallography

Crystallization/Data collection

- Gln4 Screened against 1536 different biochemical conditions, ~1000 forming an incomplete factorial of chemical space and ~500 representing commercially available screens.
- Crystal leads seen, several were chosen based on ease of cryoprotection of the native hit.
- Crystals were optimized with a Drop Volume Ratio versus Temperature (DVR/T) technique. Cryoprotected and shipped to SSRL by FedEx.

- Only 2 structures for related glutaminyl tRNA synthetases are available (~40% sequence homology), we had 228 extra residues (almost 40% more residues) therefore we expected problems in molecular replacement and didn't have a SeMet example.
- EXAFS data indicate Zinc present in the E. coli. Case (not seen in the X-ray structure). The zinc acts to stabilize the structure in a pseudo zinc finger motif.
- We collected data remotely with an excitation scan to determine if Zinc was present

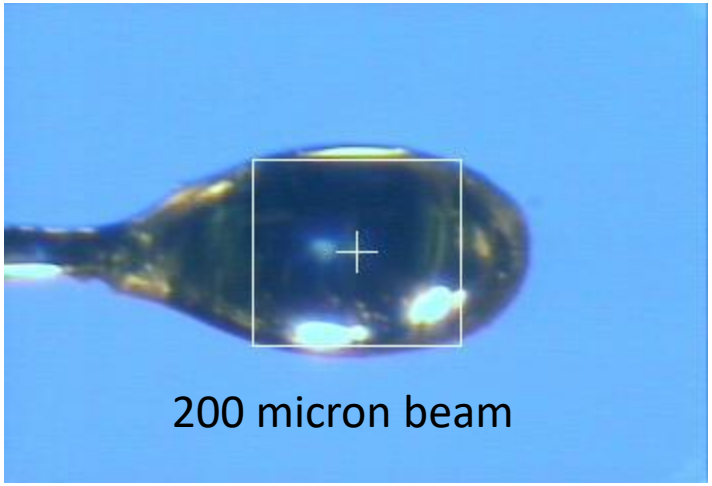

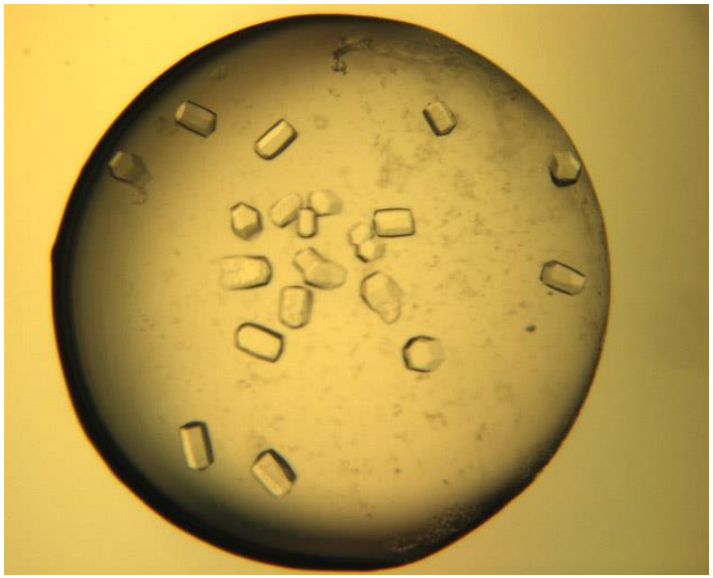

80% PEG 400 in the
crystallization cocktail

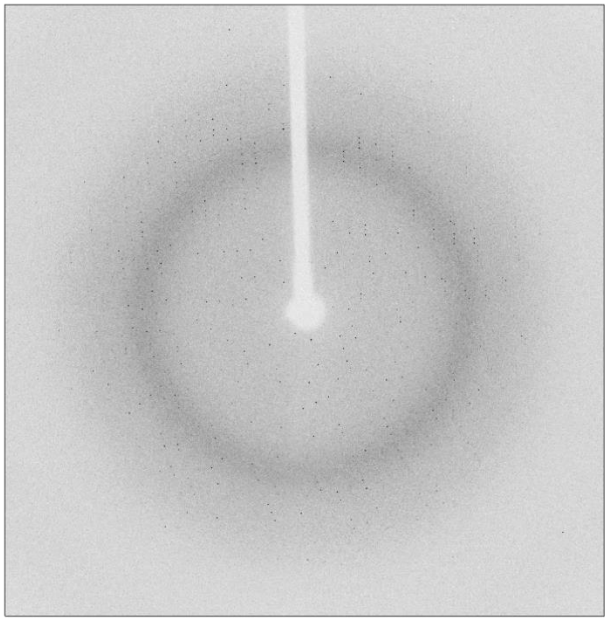

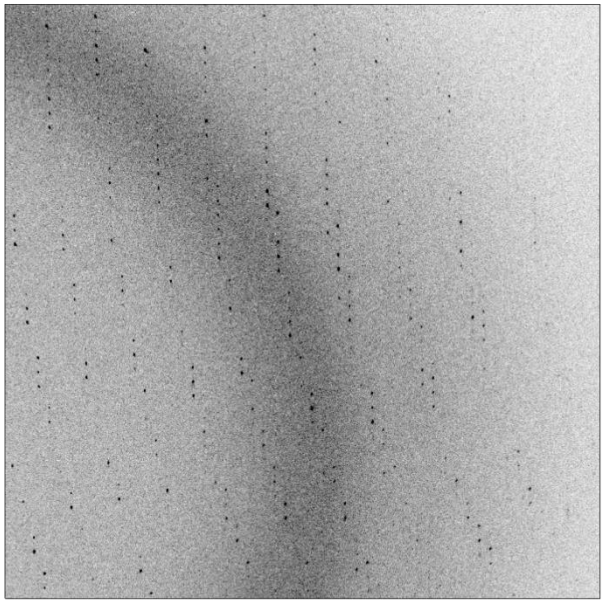

	*Sc*GlnRS
Data collection	
Beamline	SSRL BL 11-1
Wavelength (Å)	1.169
Space group	P 3_1 2 1
Cell dimensions	
a, *b*, *c* (Å)	176.611, 176.611, 72.1884
α, β, γ (°)	90, 90, 120
Resolution (Å) *	52.49 – 2.15 (2.23 – 2.15)
R_{sym} or R_{merge} *	0.068 (0.348)
Completeness (%) *	99.86 (99.84)
$I/\sigma I$ *	23.26 (2.98)
Unique reflections *	70276 (6963)
Redundancy *	11.2 (4.5)
Wilson B-factor (Å^2)	33.55
Refinement	
Resolution (Å)	52.49 – 2.15
R_{work}/ R_{free} *	0.1633/0.1826 (0.2232/0.2514)
No. atoms	10537
Protein	5043
Ligand/ion	75
Water	449
B-factors (Å^2)	
Protein	40.40
Ligand/ion	34.47
Water	44.90
R.m.s deviations	
Bond lengths (Å)	0.005
Bond angles (º)	0.90
Ramachandran favored (%)	98.0
Ramachandran outliers (%)	0.17
Clashscore	6.55

Structure solved (with help of the zinc signal) and refined with Phenix.

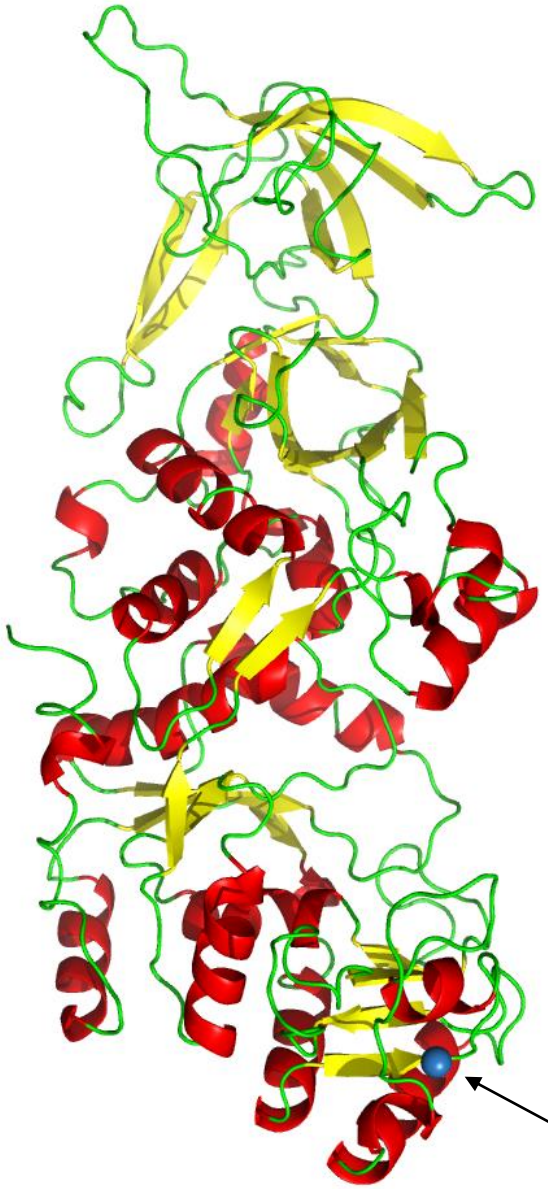

Zinc

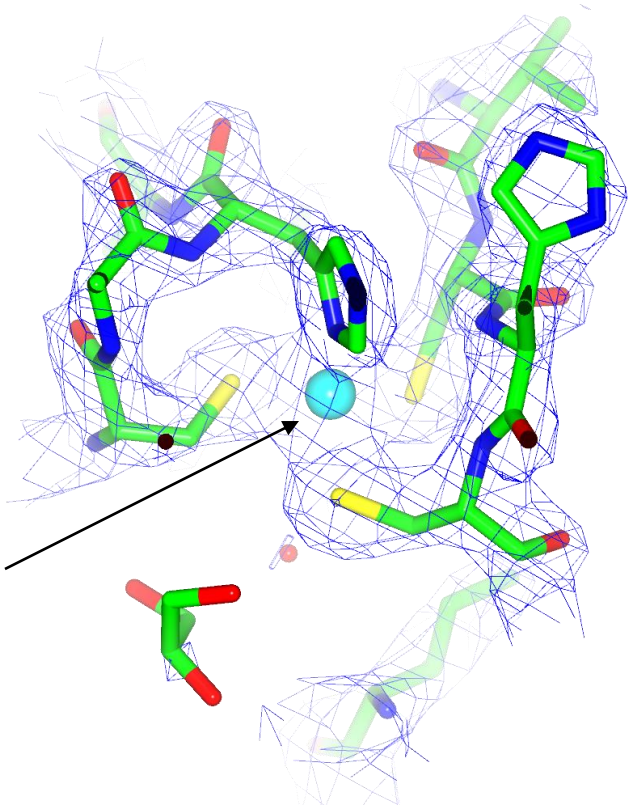

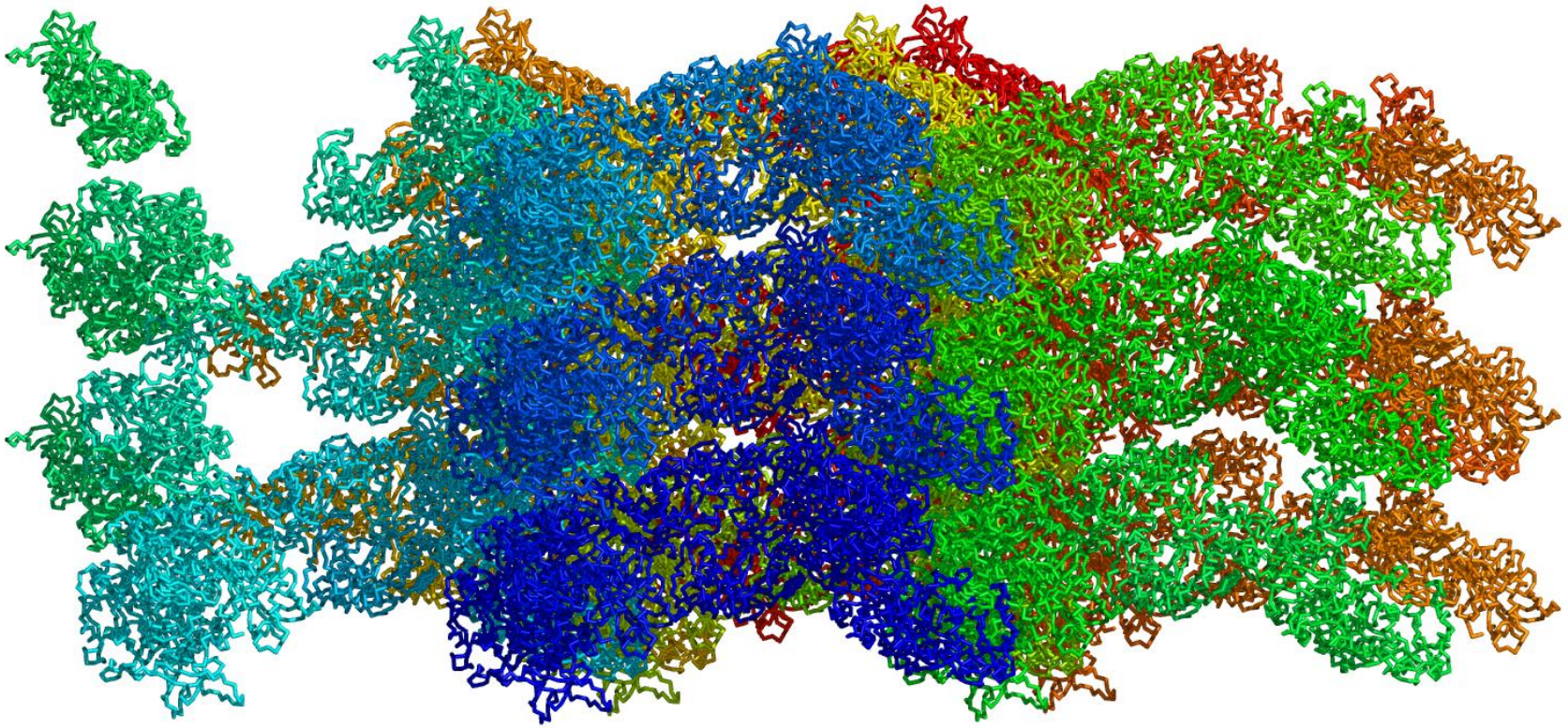

Tight packing in z and y

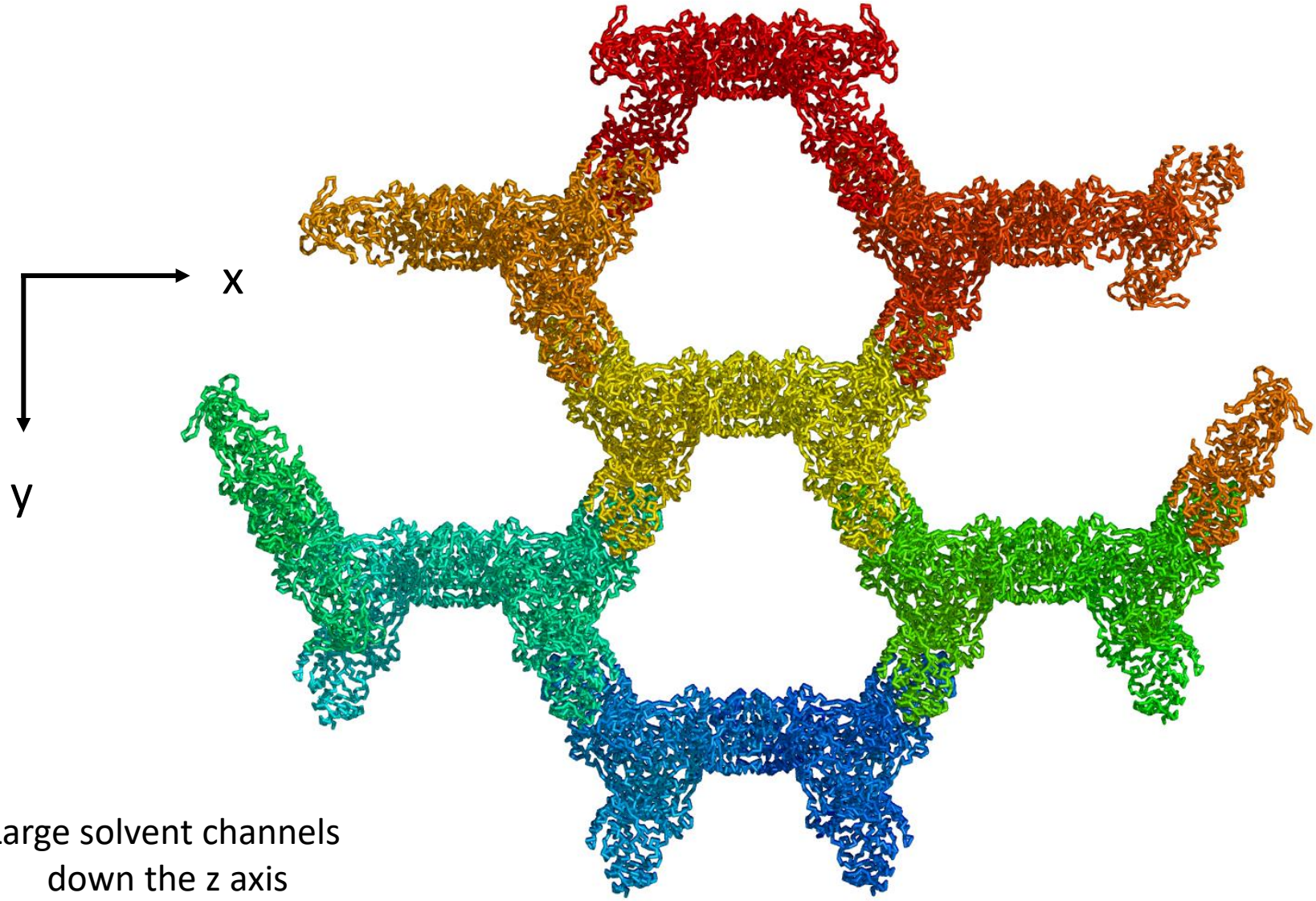

Large solvent channels
down the z axis

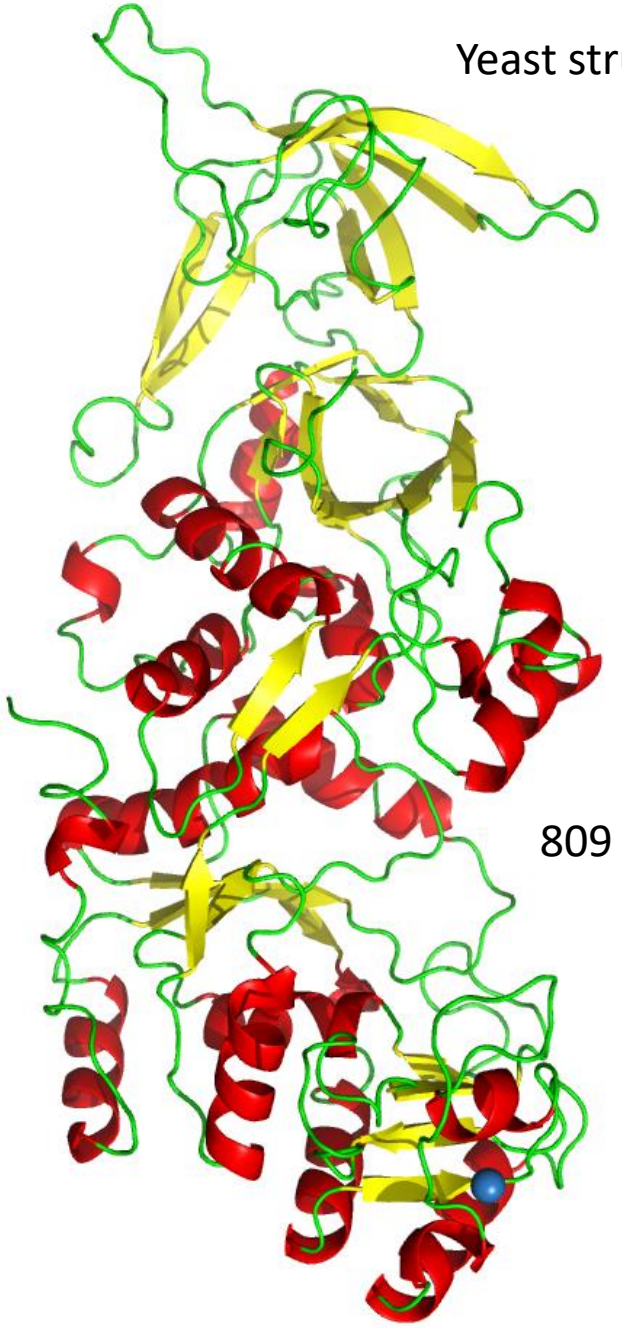

Yeast structure

?

809 residues

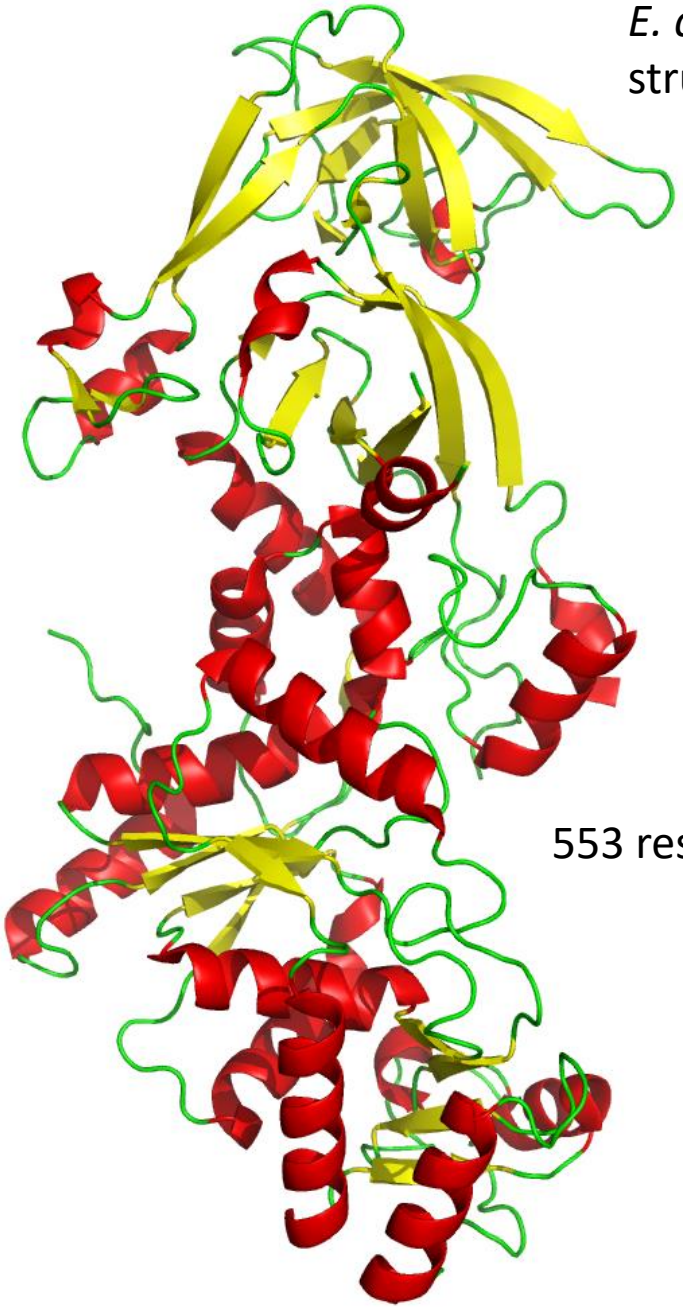

E. coli. structure

553 residues

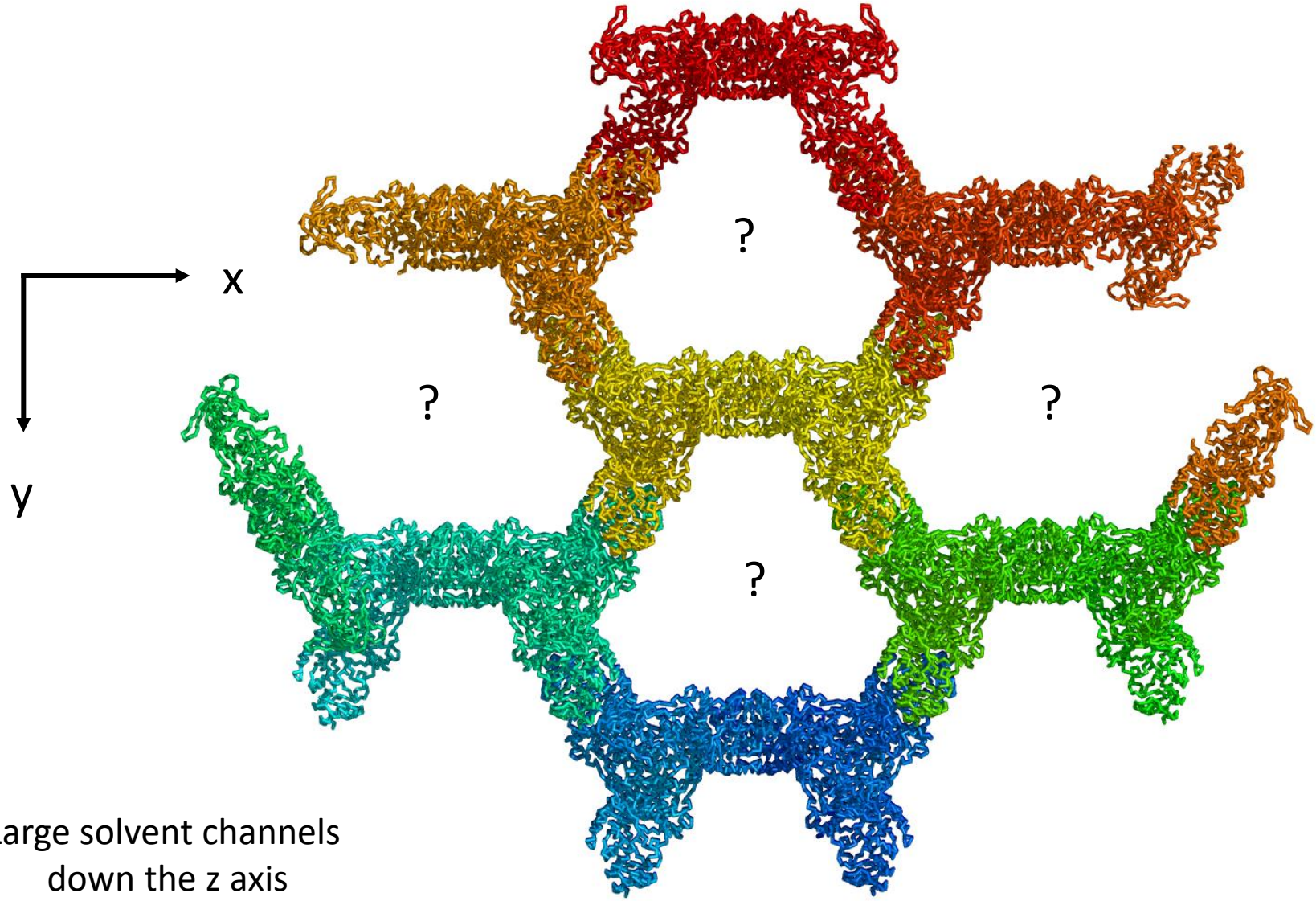

Large solvent channels
down the z axis

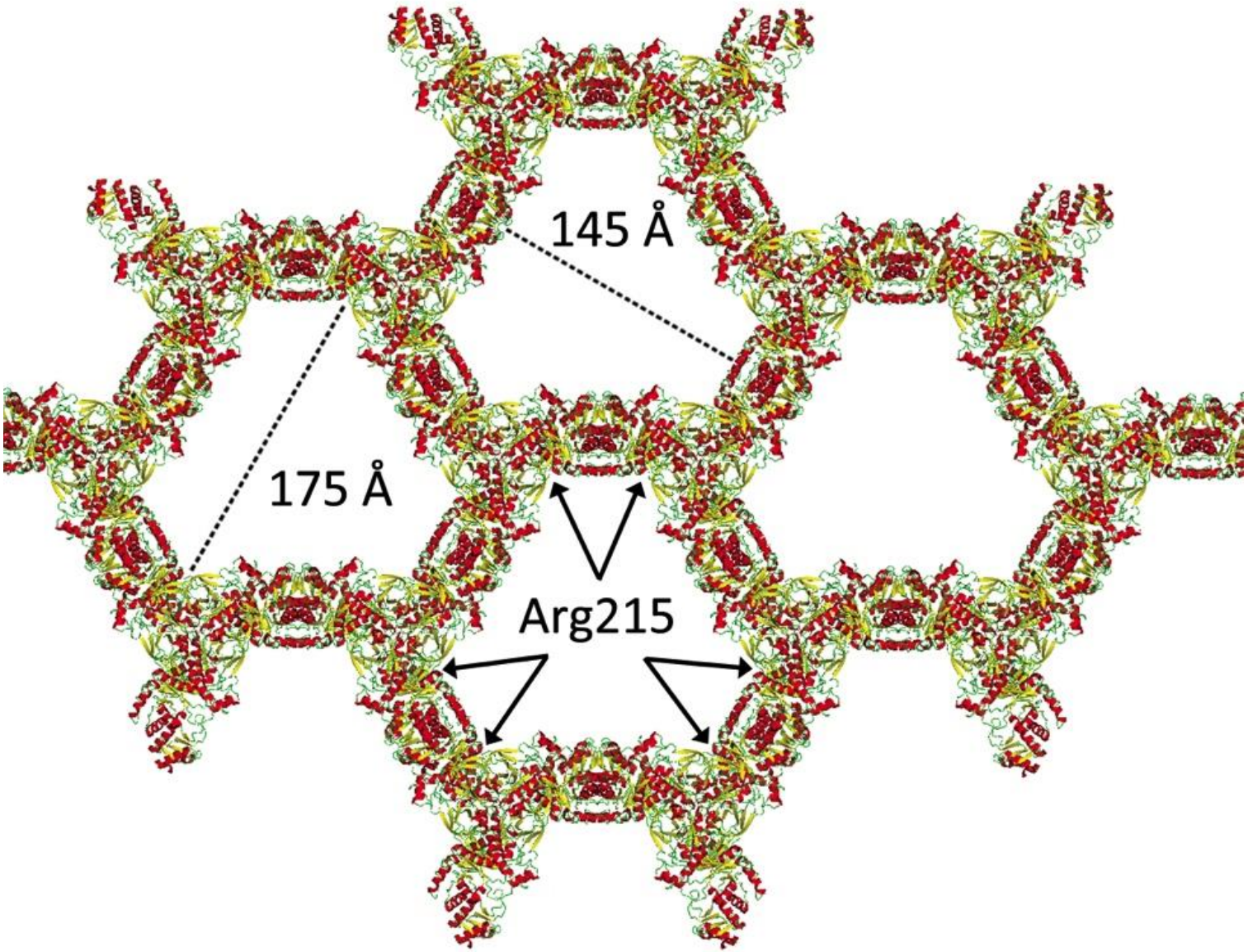
145 Å
175 Å
Arg215

Missing residues

- There were 216 missing residues from the structure, 95% of the N-terminal domain.
- Where they in the mix to start with?
- SDS PAGE gel on the remaining crystals indicated that the full length protein was present.
- For a more concrete answer the protein was re-expressed with a His tag attached to the N-terminal domain.
  - It was purified with a nickel affinity column.
  - It was crystallized and the structure solved, again with missing residues.
  - A western blot on the dissolved crystals confirmed the presence of the N-terminal domain His tag.
  - No protein degradation had taken place during crystallization.
- For the re-expressed protein the full N-terminal domain was present in the protein but not seen in the crystallographic structure.

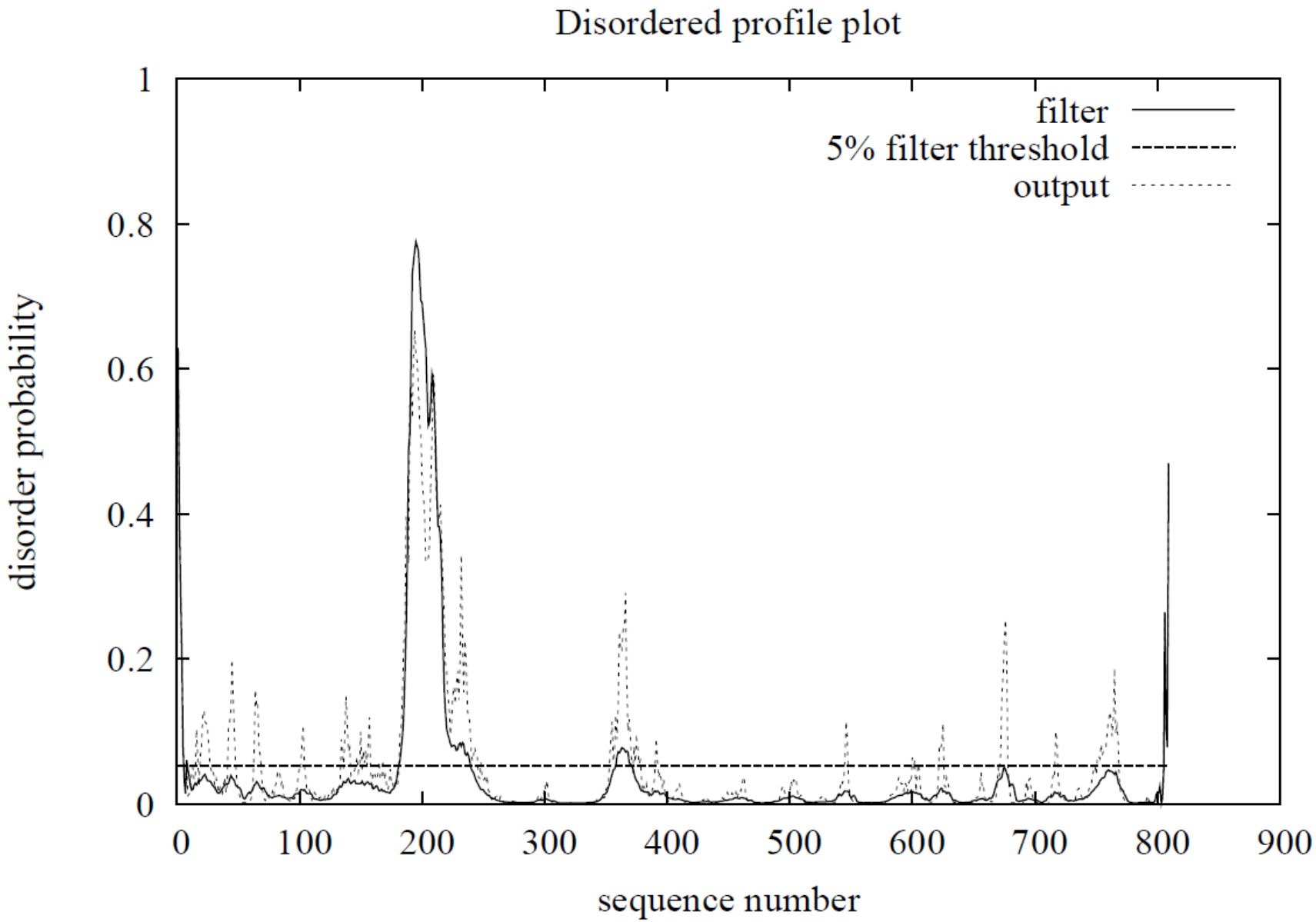
Disordered profile plot
filter
5% filter threshold
output
disorder probability
sequence number
0
0.2
0.4
0.6
0.8
1
0
100
200
300
400
500
600
700
800
900

Back to SAXS

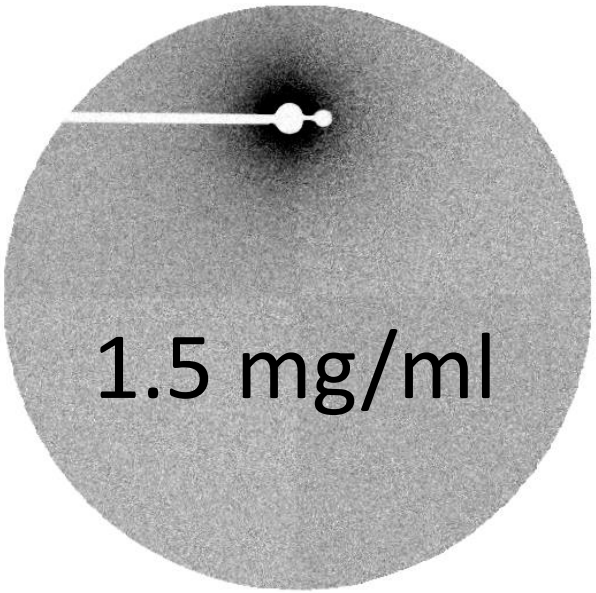
1.5 mg/ml

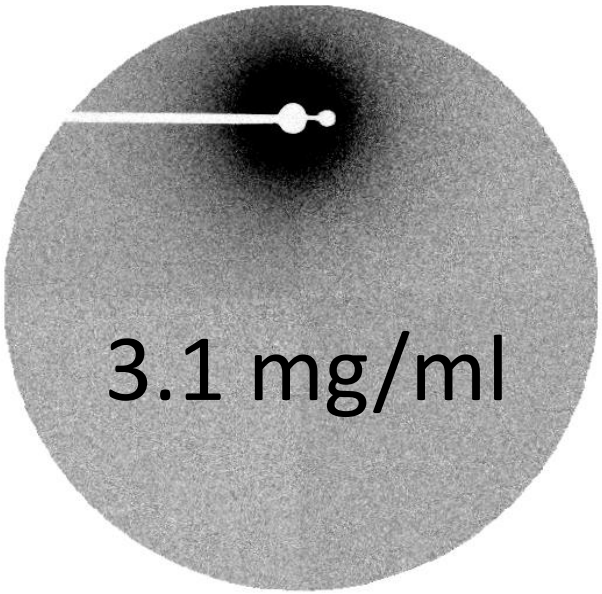
3.1 mg/ml

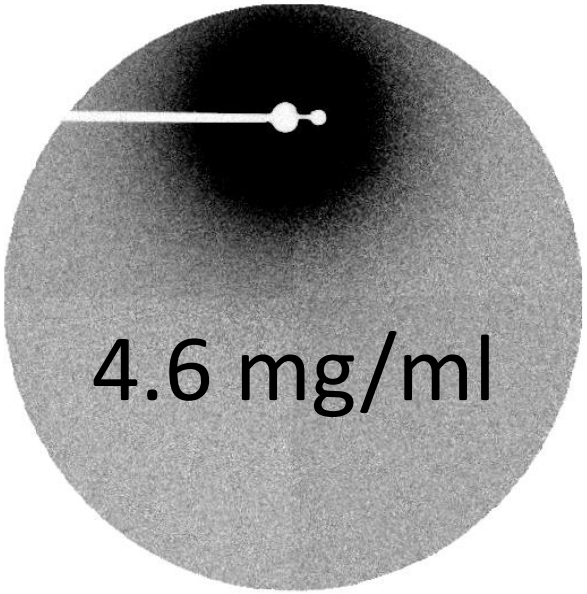
4.6 mg/ml

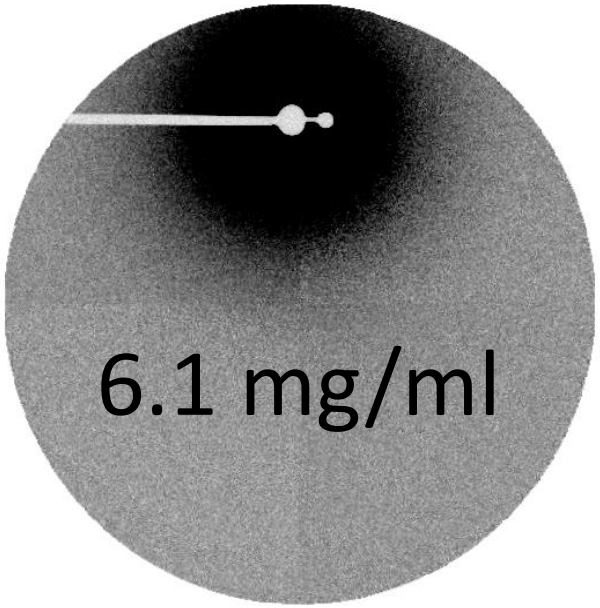
6.1 mg/ml

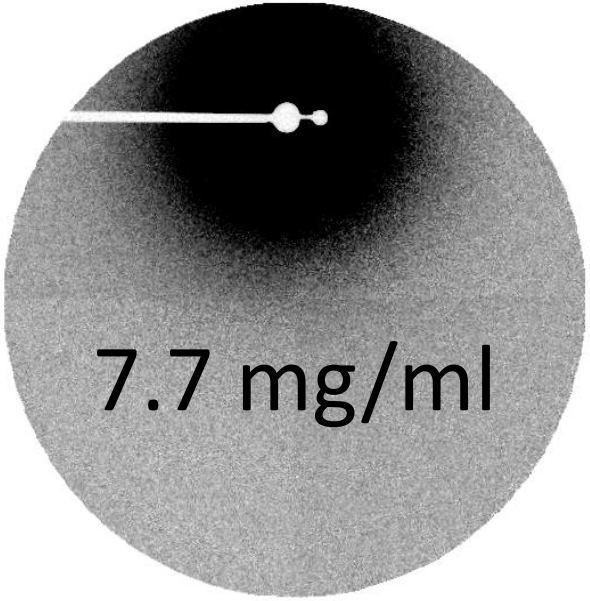
7.7 mg/ml

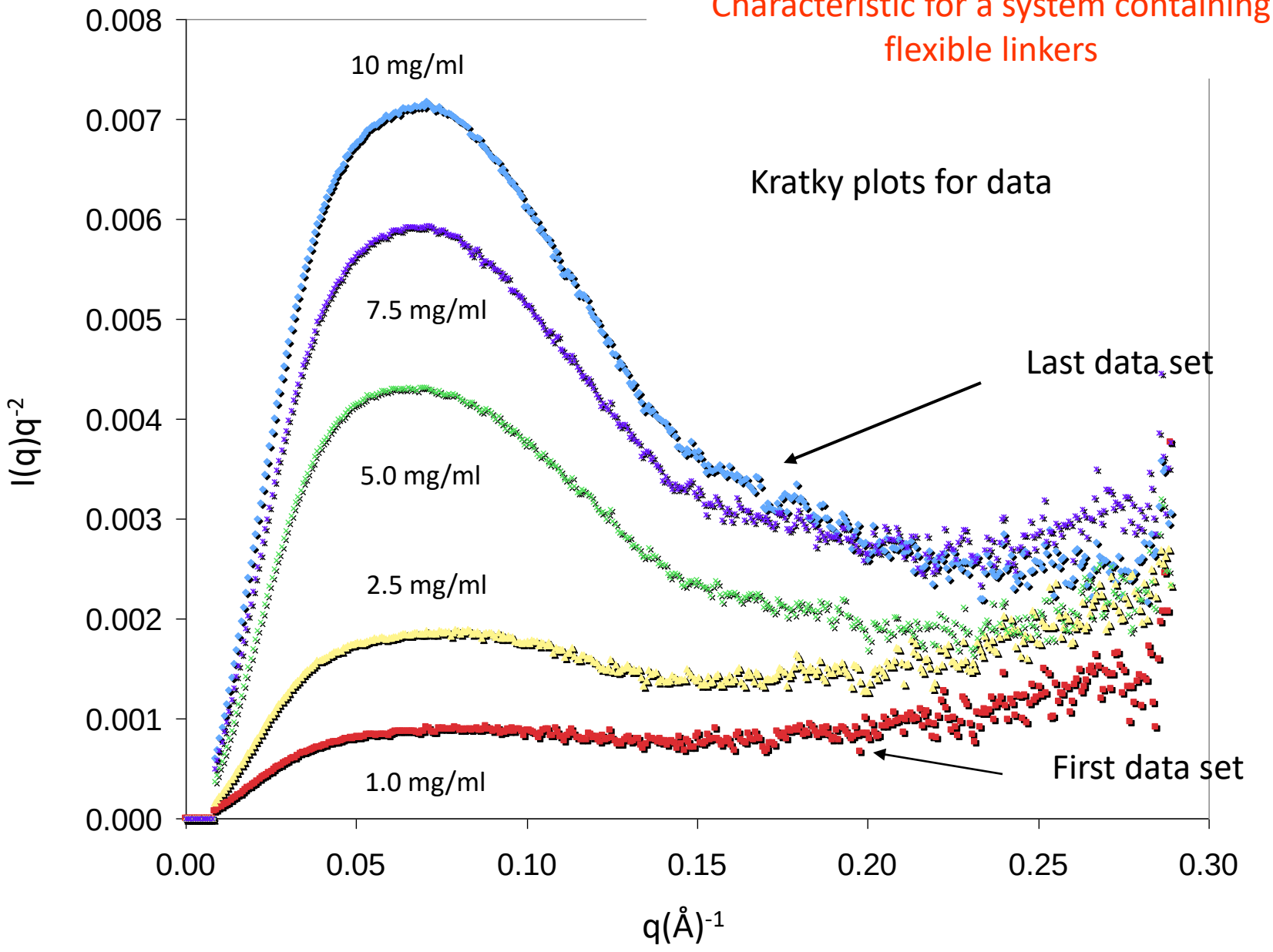
Characteristic for a system containing flexible linkers
Kratky plots for data
10 mg/ml
7.5 mg/ml
5.0 mg/ml
2.5 mg/ml
1.0 mg/ml
Last data set
First data set
I(q)q-2
q(Å)-1
0.000
0.001
0.002
0.003
0.004
0.005
0.006
0.007
0.008
0.00
0.05
0.10
0.15
0.20
0.25
0.30

Envelope reconstruction using the crystallographic structure

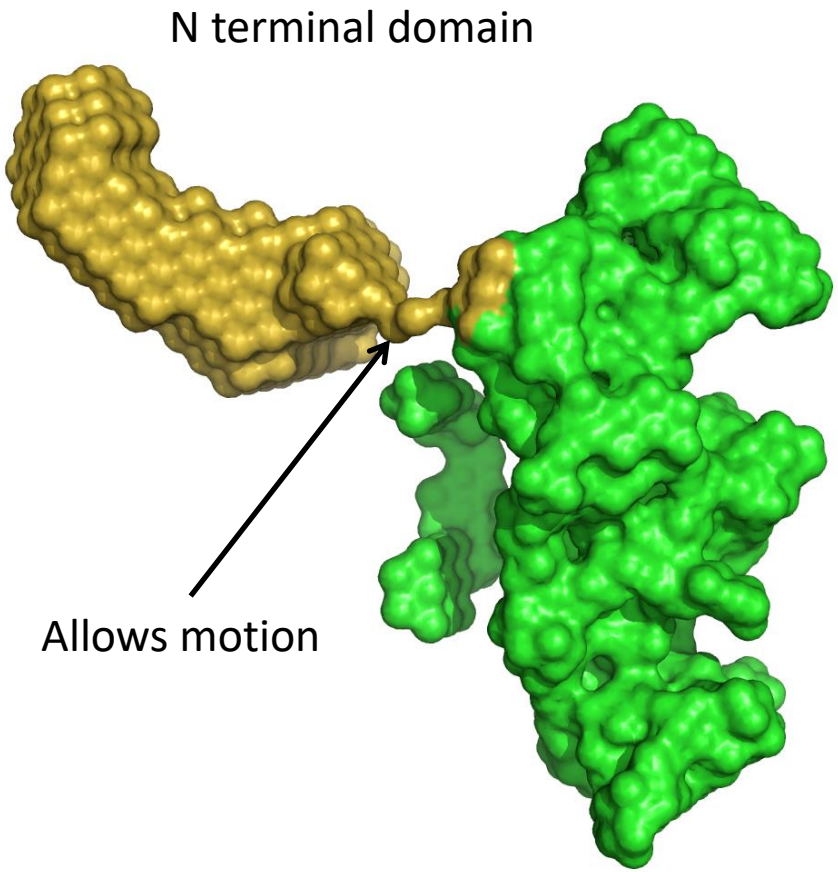

C terminal domain

The crystal structure (which shows only the C-domain)

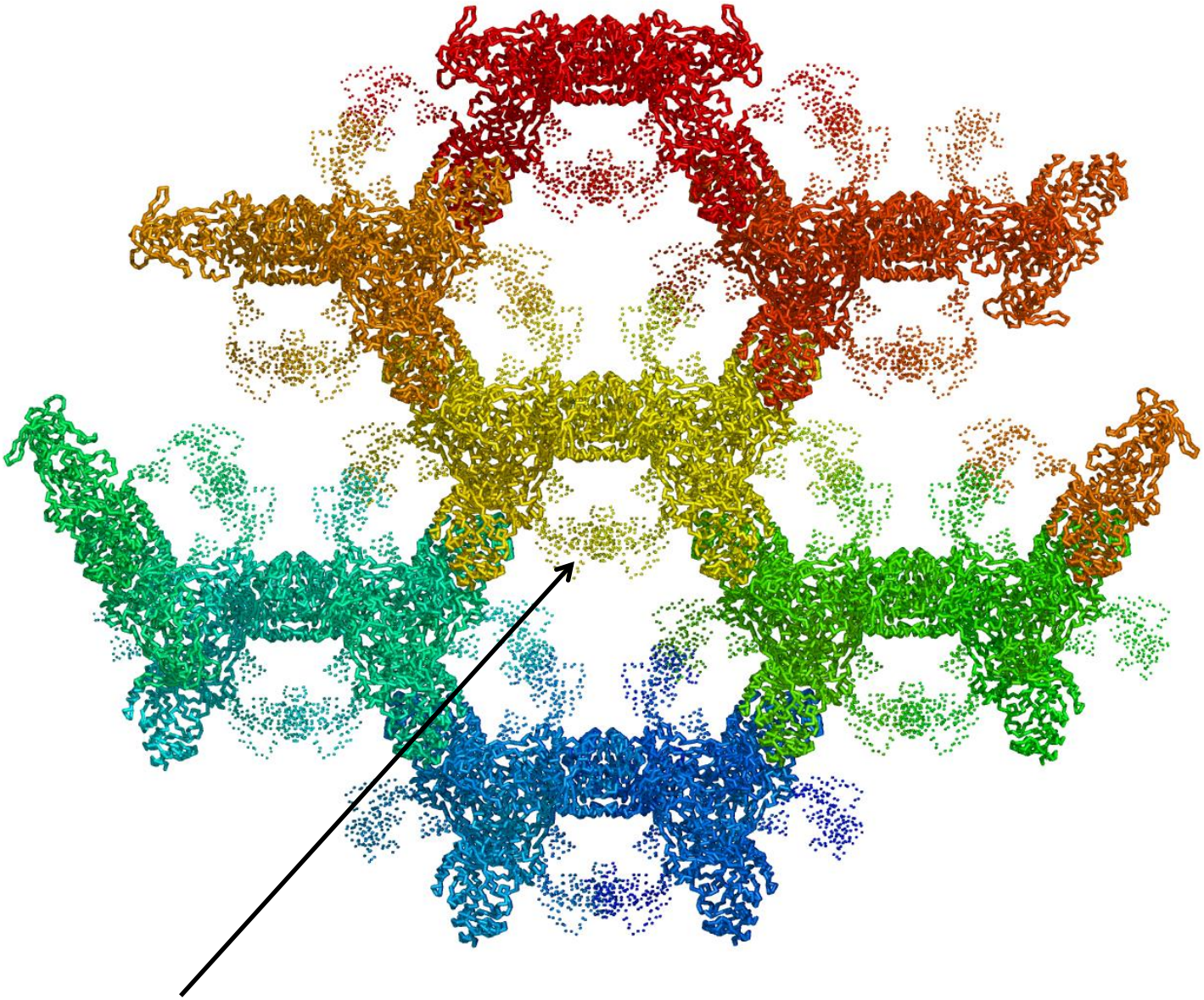

The N-terminal ‘arm’ is completely compatible with the crystal structure

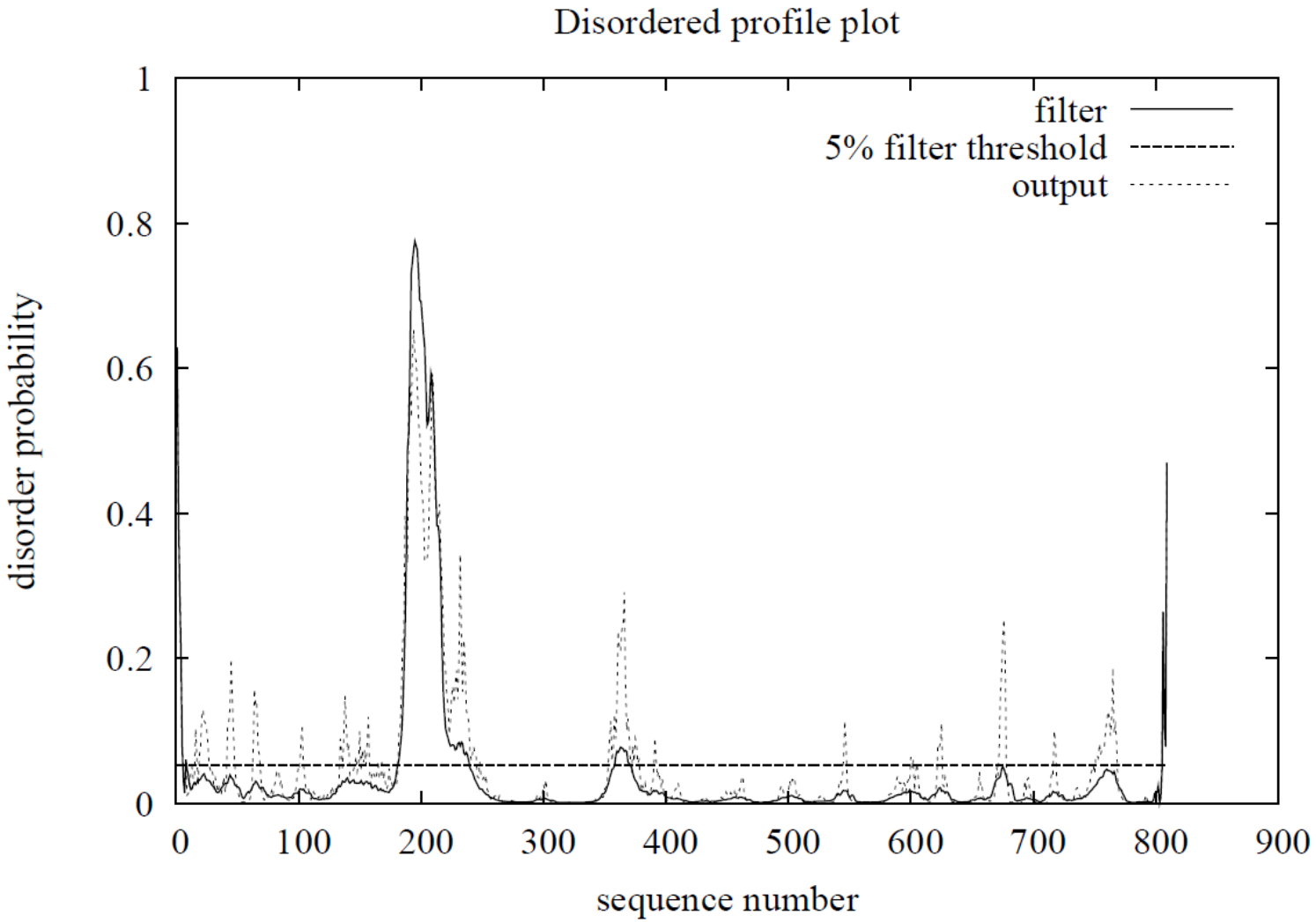

Disorder Prediction Analysis of the Primary Sequence of ScGlnRS. The probability of disorder is shown on the y-axis and the residue number is shown on the x-axis. The linker connecting the N-terminal and C-terminal domains extends from residue 188 to 214. Disorder probability was calculated using DISOPRED2.

Express and purify multiple Constructs

- Full length protein, residues 1 to 809
- N-terminal domain, residues 1 to 189
- C-terminal domain, residues 216 to 809

Envelope reconstruction of the N-terminal domain

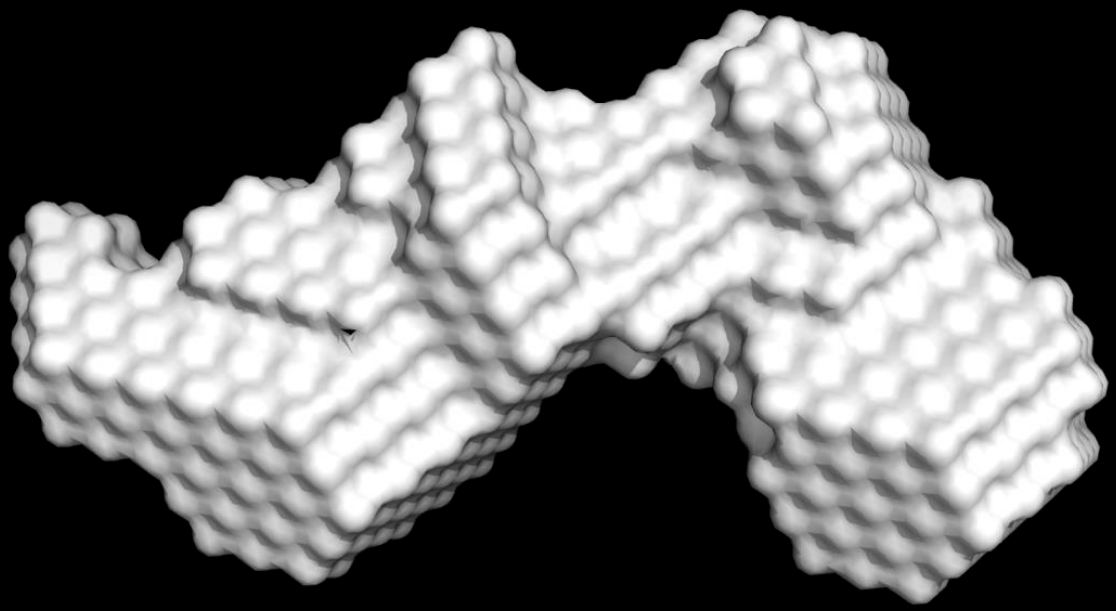

Express N-terminal domain, C-terminal domain, tRNA, SAXS studies on all

Check the crystallography again

Protein with N-terminal arm cleaved

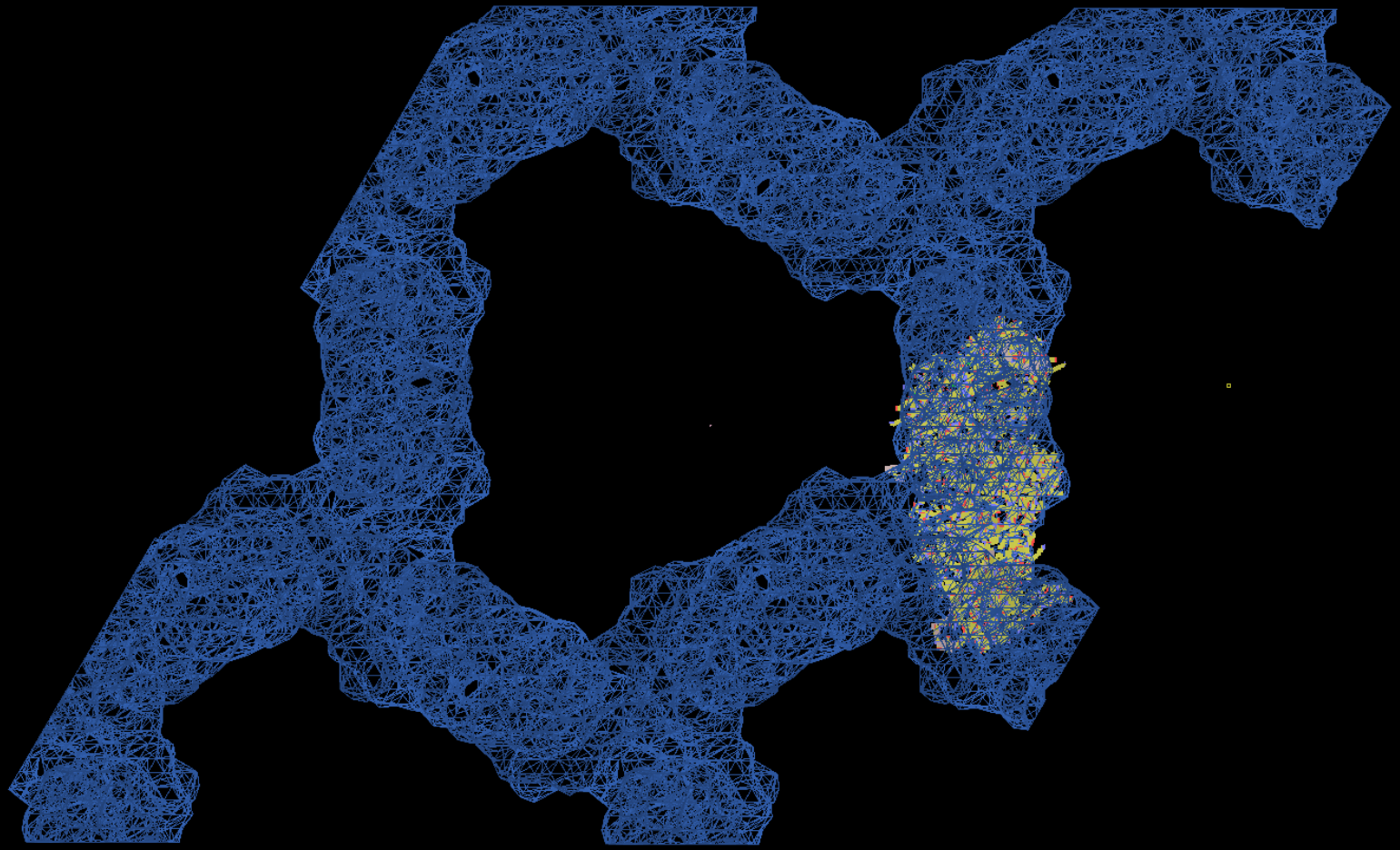

Crystallized, data truncated to 20A (data to 78A still plenty of reflections due to geometry and wavelength used purposely used for data collection)

Low resolution electron density map of full length protein in red

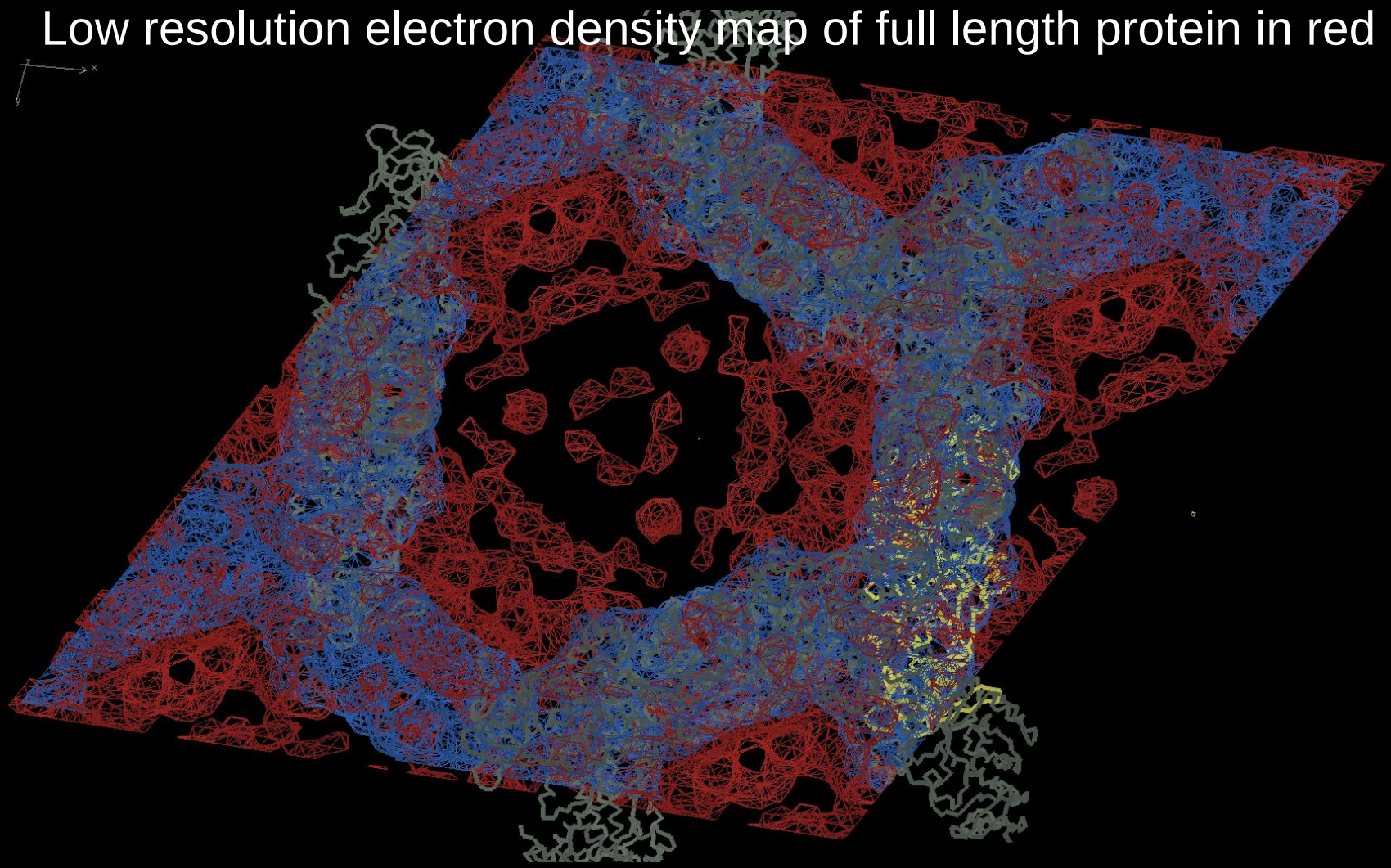

Data truncated to 20A (data to 78A still plenty of reflections due to geometry and wavelength used purposely used for data collection)

Crystallization trials of the N-terminal domain

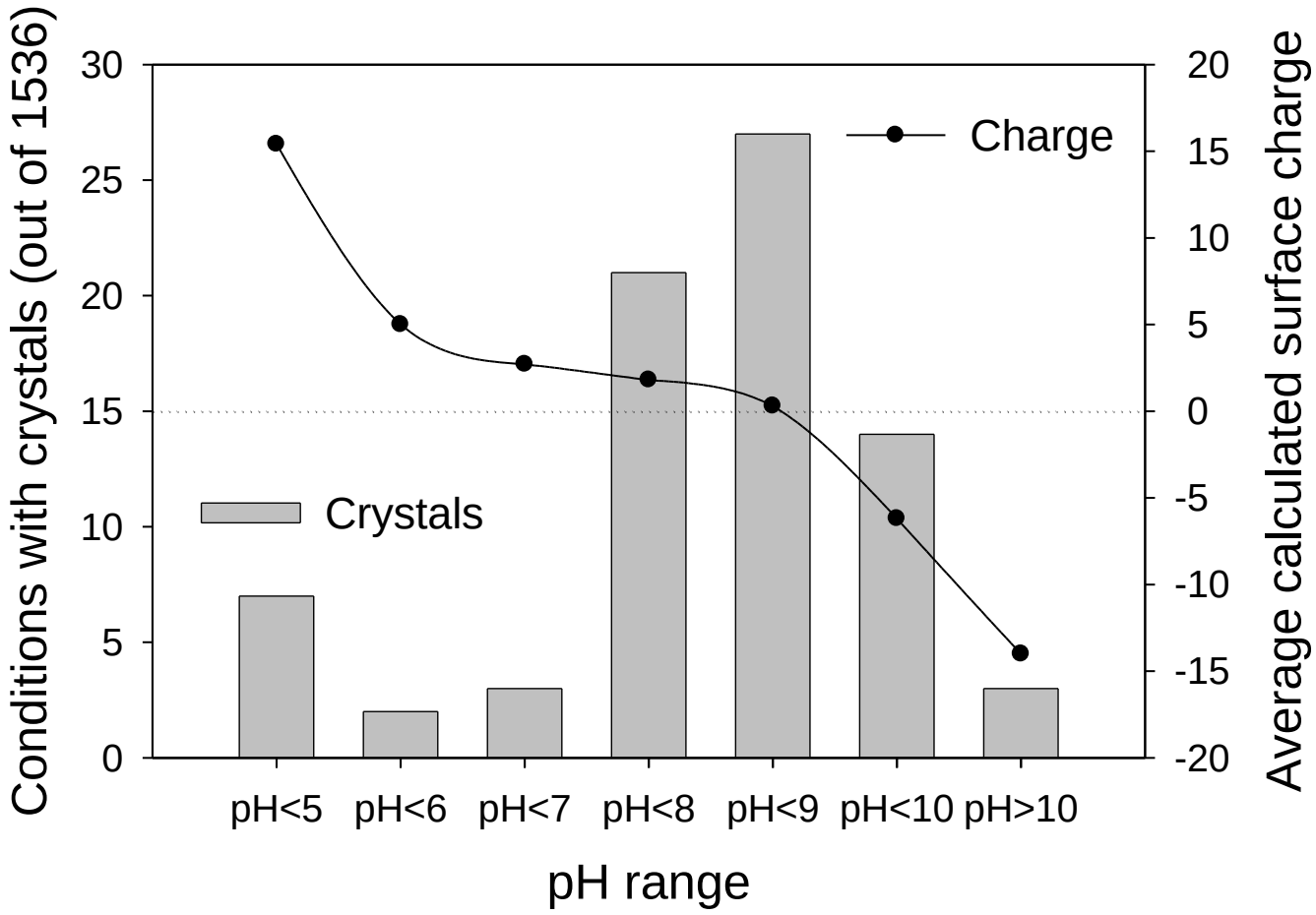

Does it diffract? Screening before the synchrotron

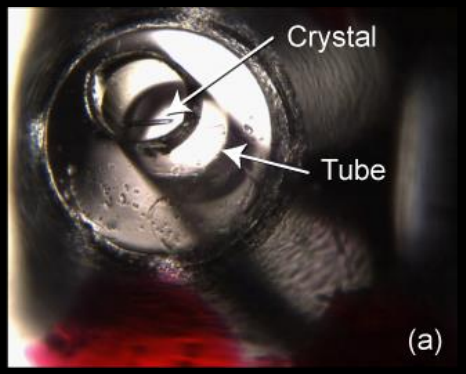

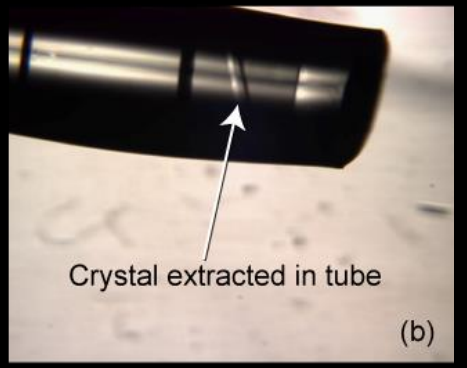

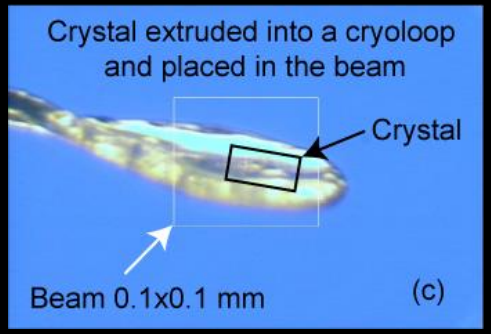

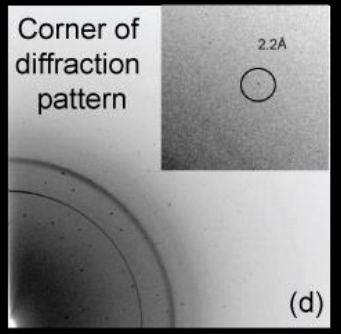

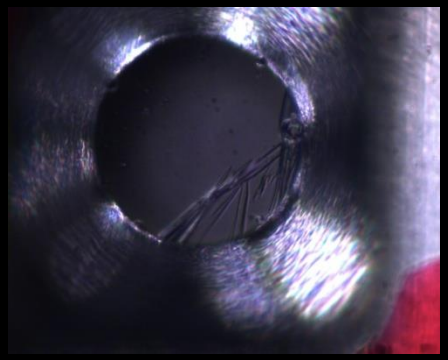

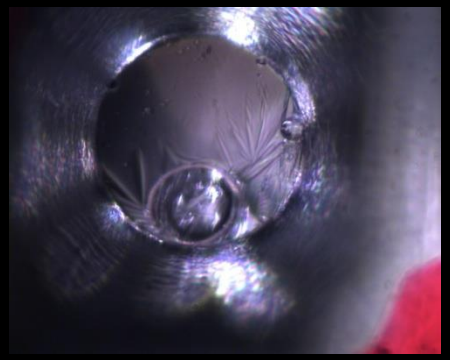

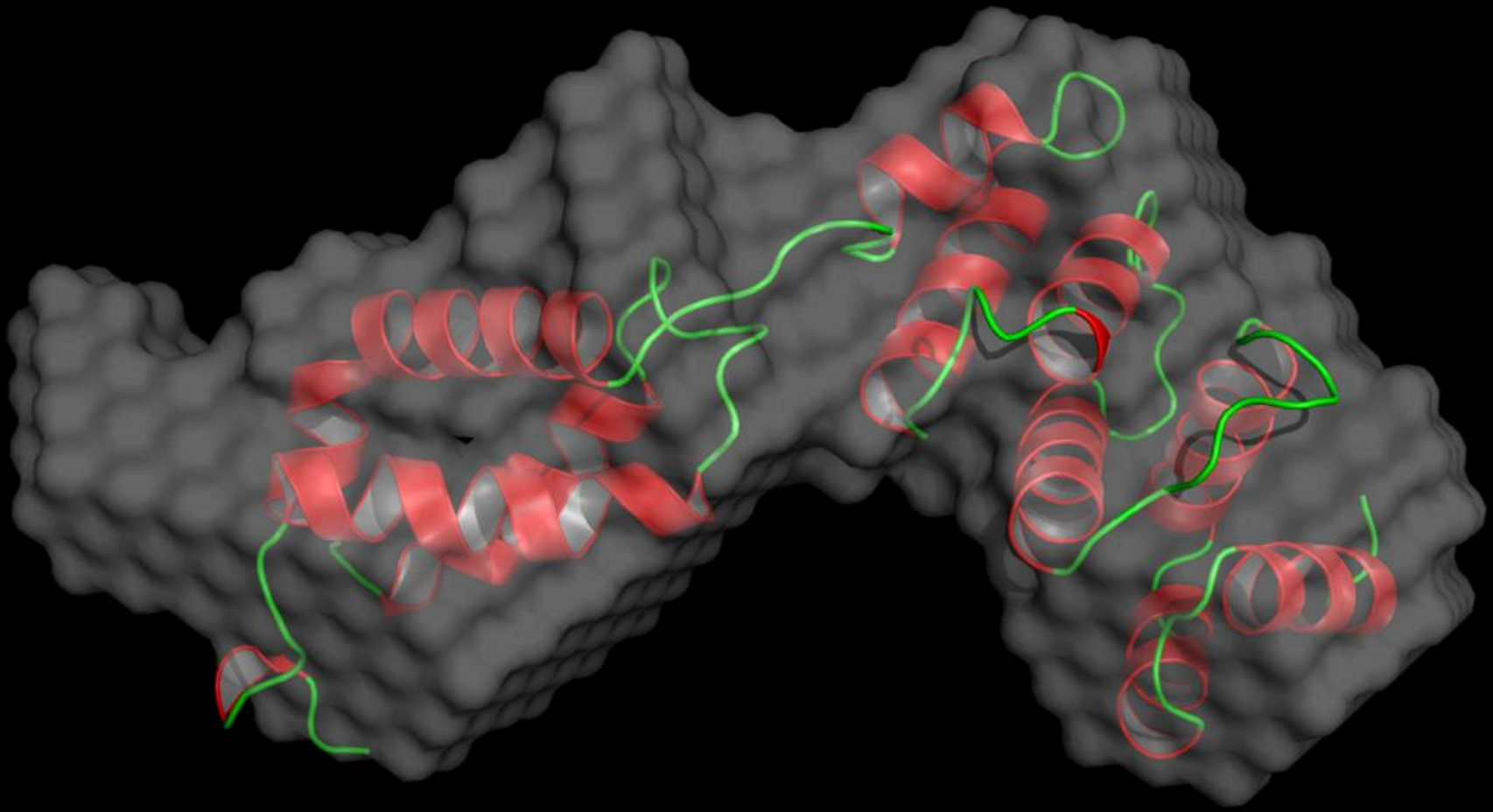

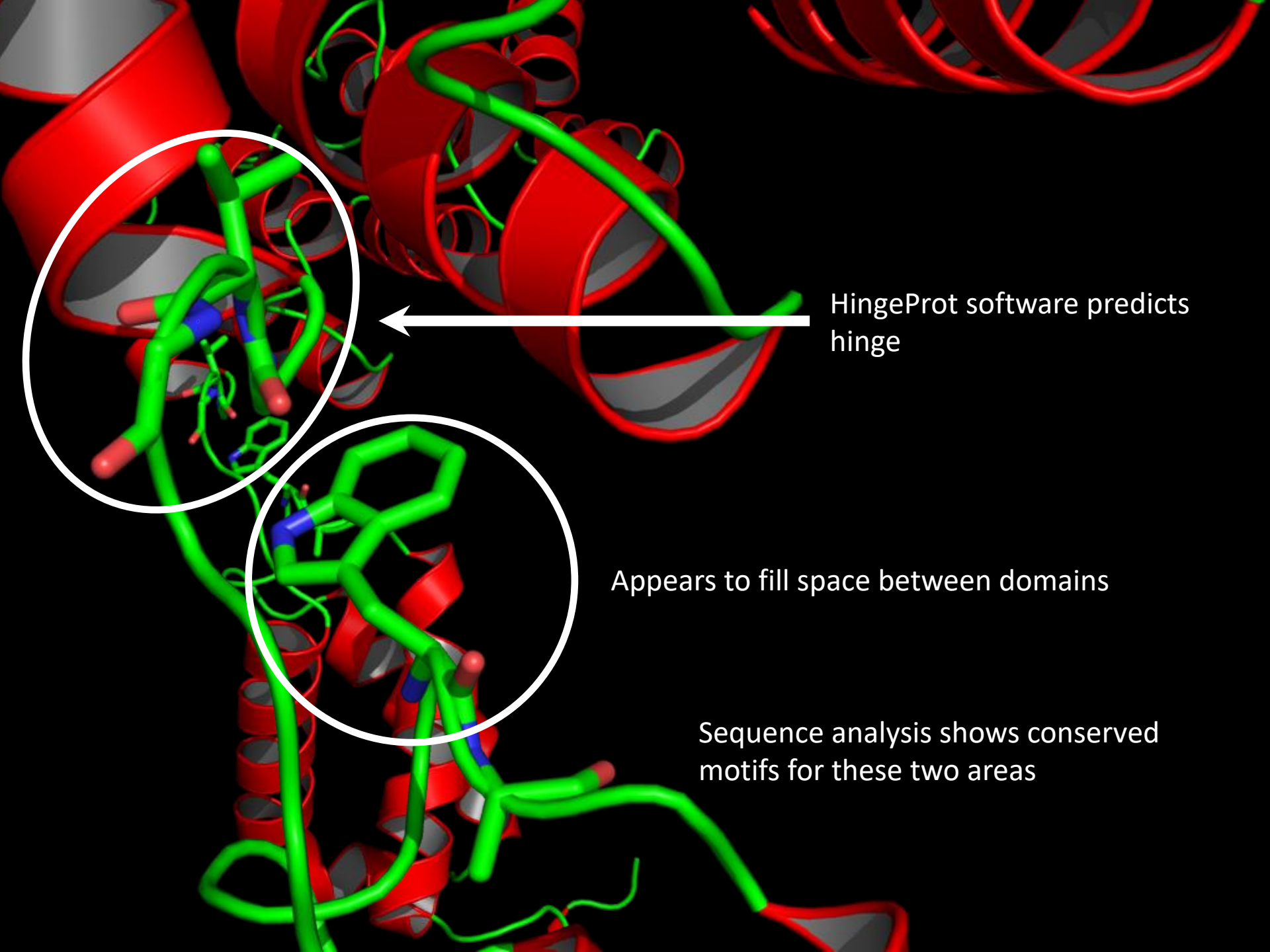
HingeProt software predicts hinge
Appears to fill space between domains
Sequence analysis shows conserved motifs for these two areas

Structural Homologs

- DALI search resulted in two hits of structurally similar molecules
- Combined with the SAXS this allowed us to position the N-terminal
- Due to the nature of the homologs we have a ‘big clue’ to the function of the N-terminal appended domain.
- SAXS studies of other species show a similar domain.
- Allowed us to better understand the evolutionary tree.

A blast search did not reveal structural homologs – having the structure of the N-terminal arm was critical.

Structure of Gln4(1–187) with comparisons to domains in S. aureus GatB (PDB ID: 3IP4).

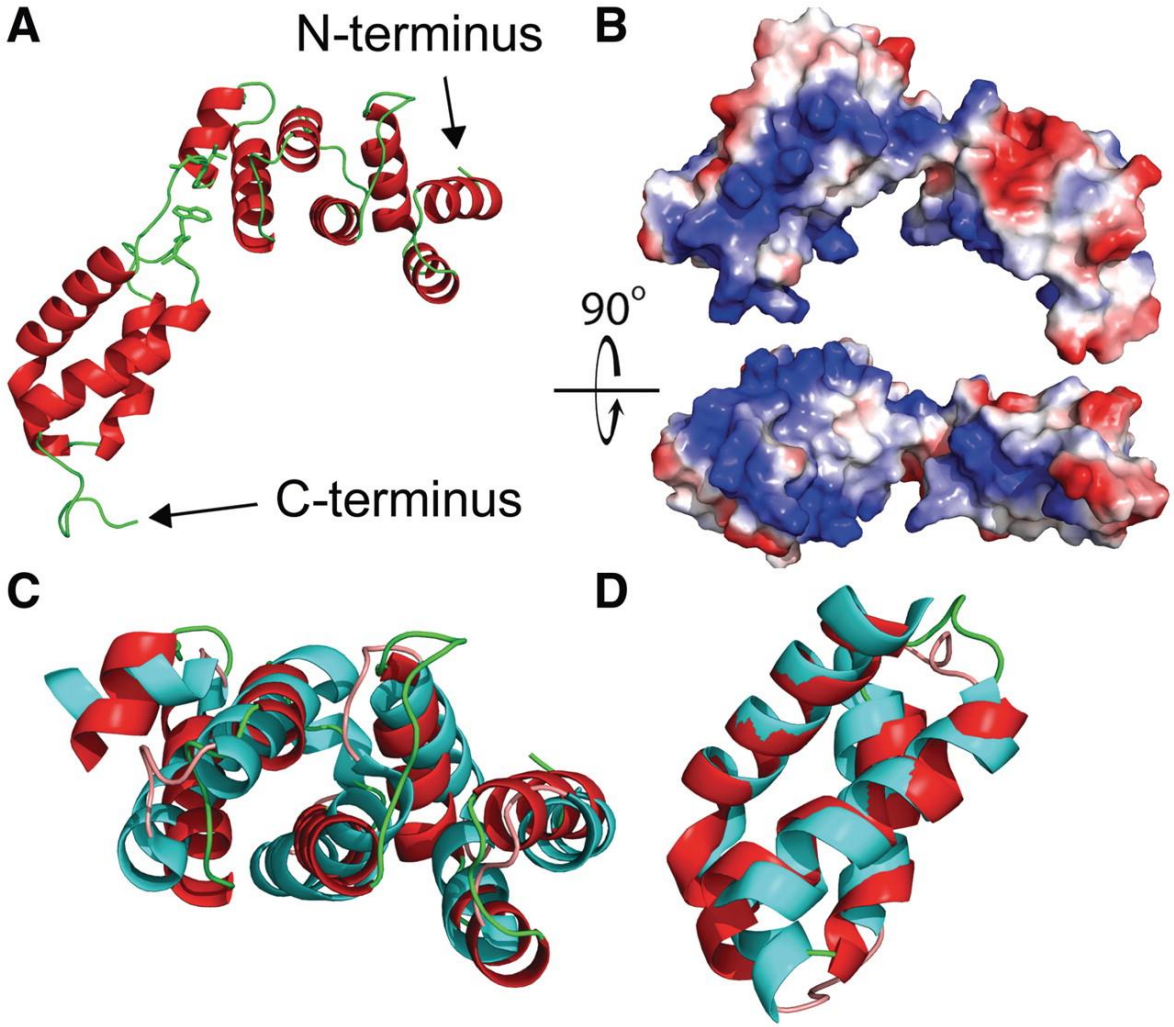

Grant T D et al. Nucl. Acids Res. 2011;nar.gkr1223

Nucleic Acids Research

The linker between the two domains in Gln4(1–187) likely behaves as a hinge, is highly conserved and is important for tRNA binding.

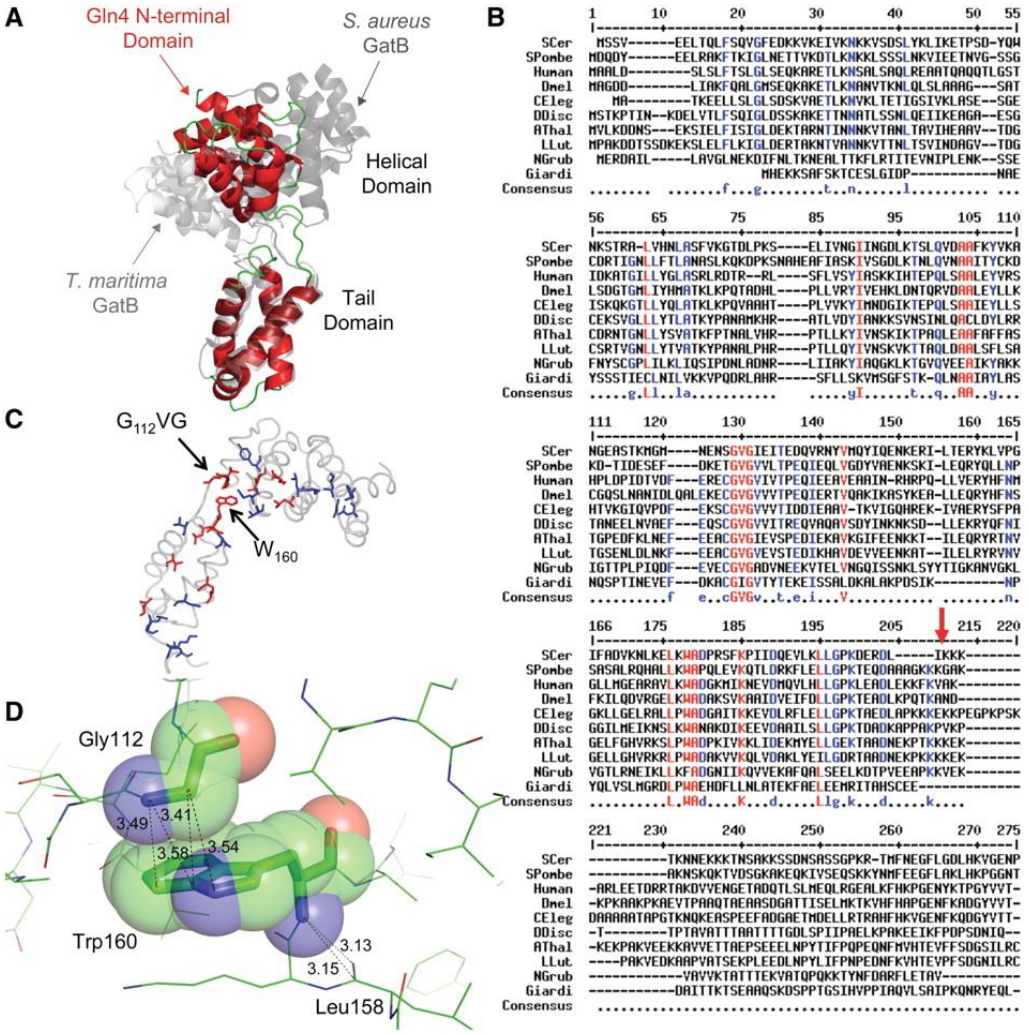

Grant T D et al. Nucl. Acids Res. 2011;nar.gkr1223

Nucleic Acids Research

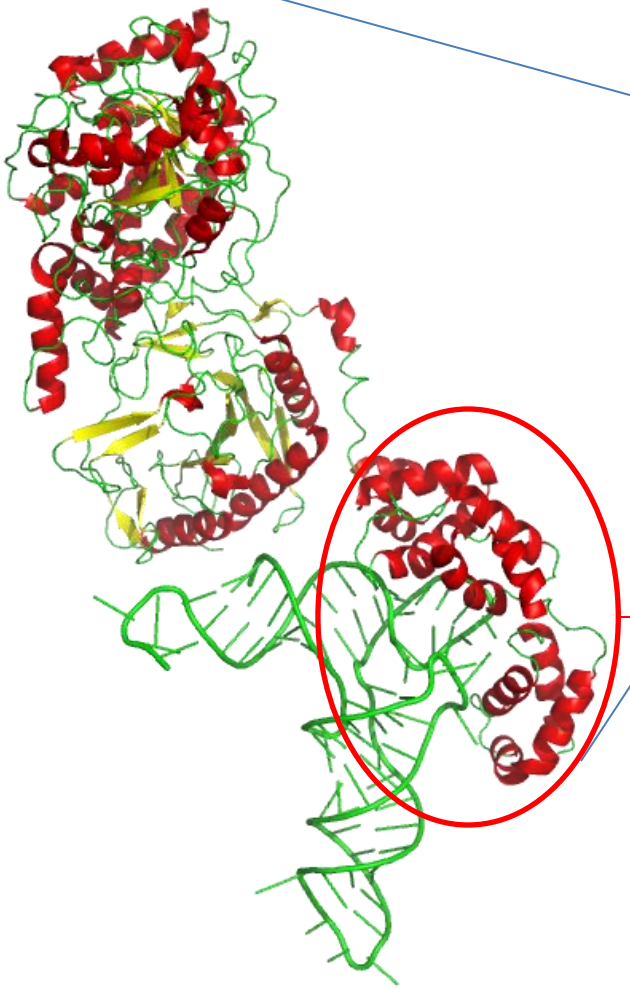

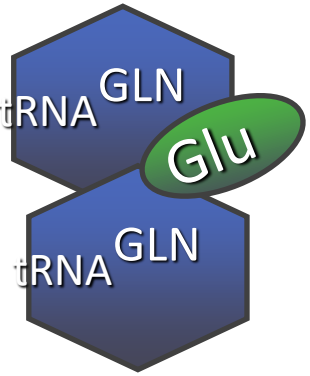

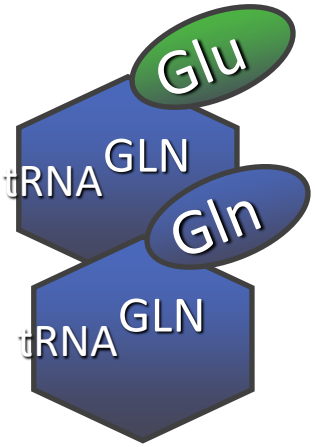

Remarkably similar to the N-terminal domain of Eukaryotic GlnRS

Combine the SAXS and Crystallography

Gln4 a Eukaryotic
Glutaminyl-tRNA Synthetase

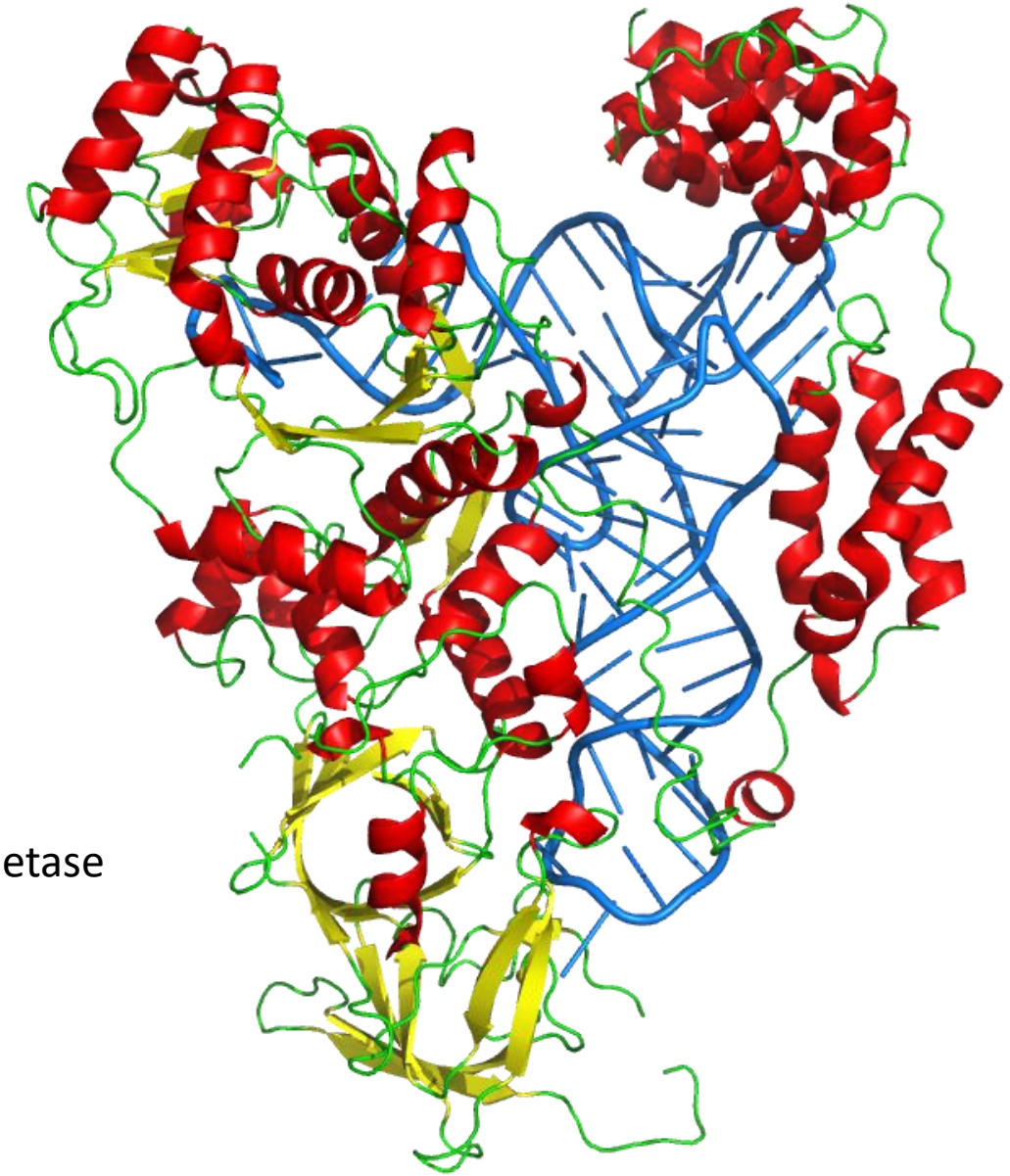

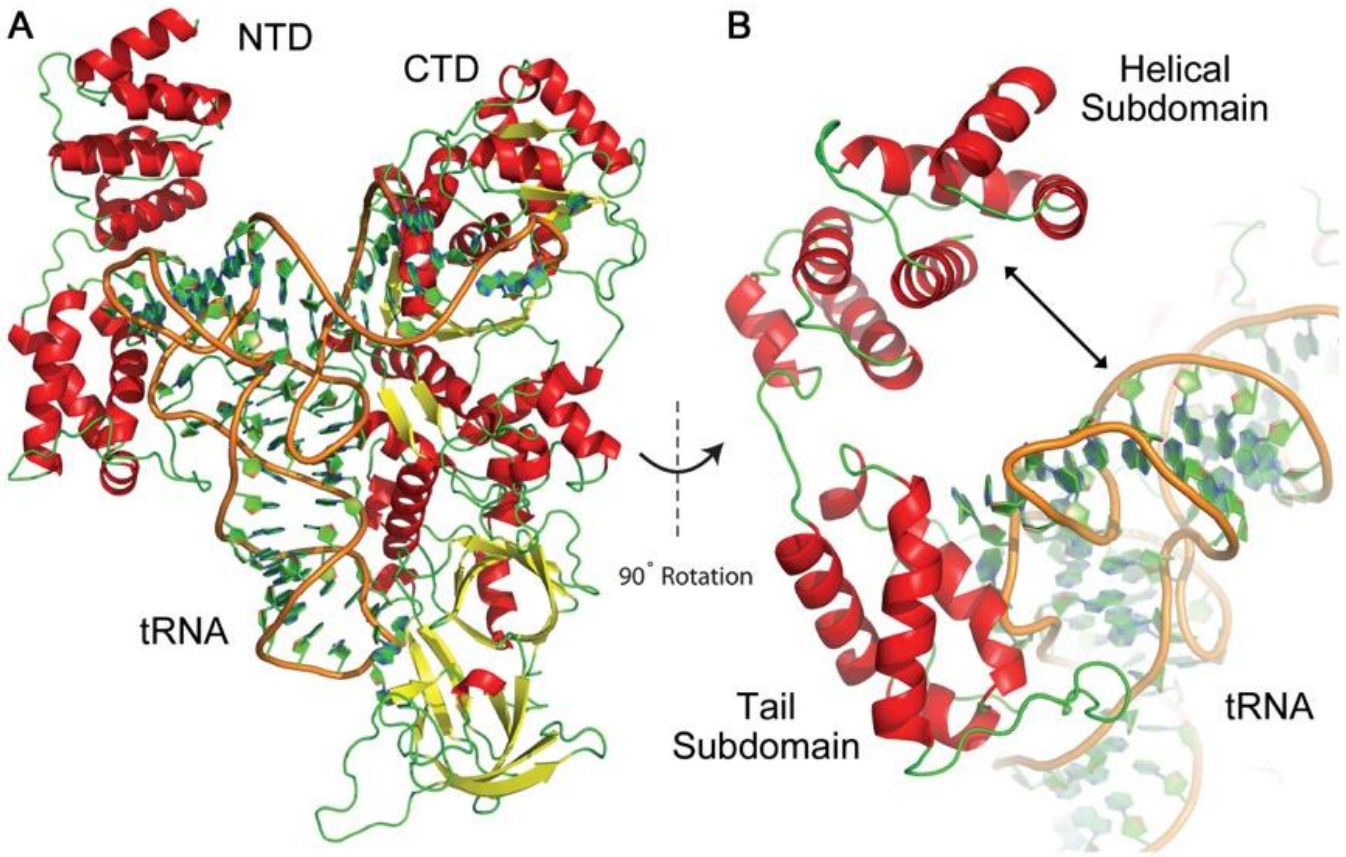

Homology Model of Full-length *Sc*GlnRS Bound to $tRNA^{gln}$. A. Full-length *Sc*GlnRS shown bound to $tRNA^{gln}$. B. Enlarged and rotated model showing gap between NTD helical subdomain and tRNA molecule.

Molecular Dynamics Simulations

- Performed in GROMACS with the AMBER99SB force field.
- The initial model was solvated using a cubic SPC/E water model and neutralized with ions prior to minimization via steepest descents.
- Distance restraints were added to keep the zinc ion in place.
- The model was then equilibrated under an isothermal-isochoric ensemble for 100 picoseconds at 300K followed by equilibration under an isothermal-isobaric ensemble for 100 picoseconds.
- Simulations were then performed at the Center for Computational Resources (CCR) in Buffalo on 512 processors. Total simulation time was 70 ns.

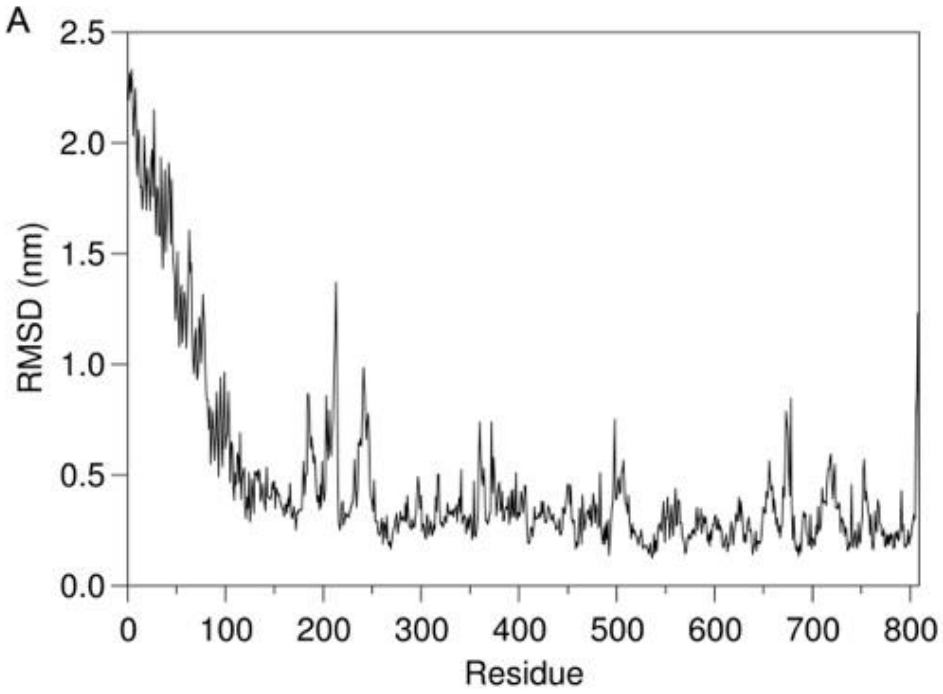

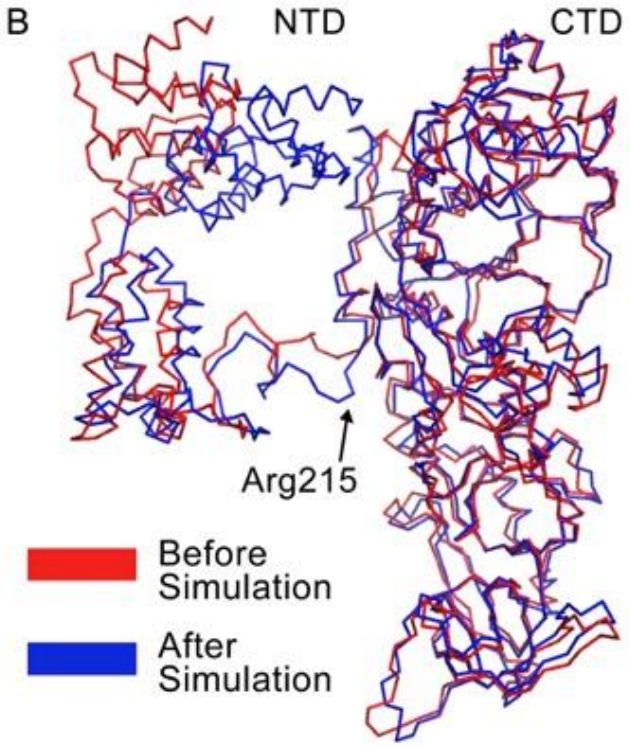

Molecular dynamics simulations indicates closure and stabilization

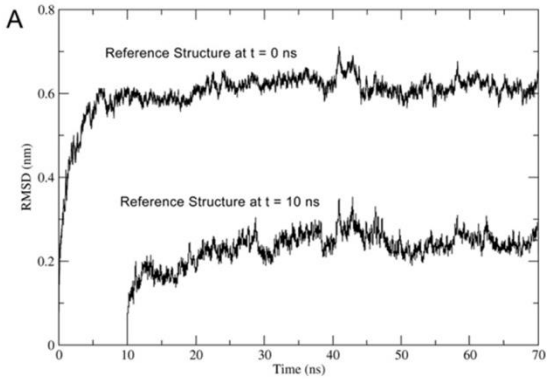

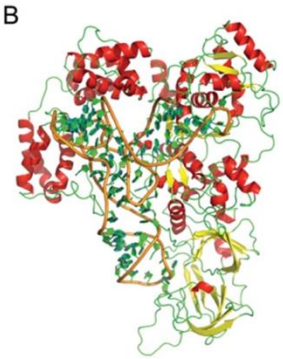

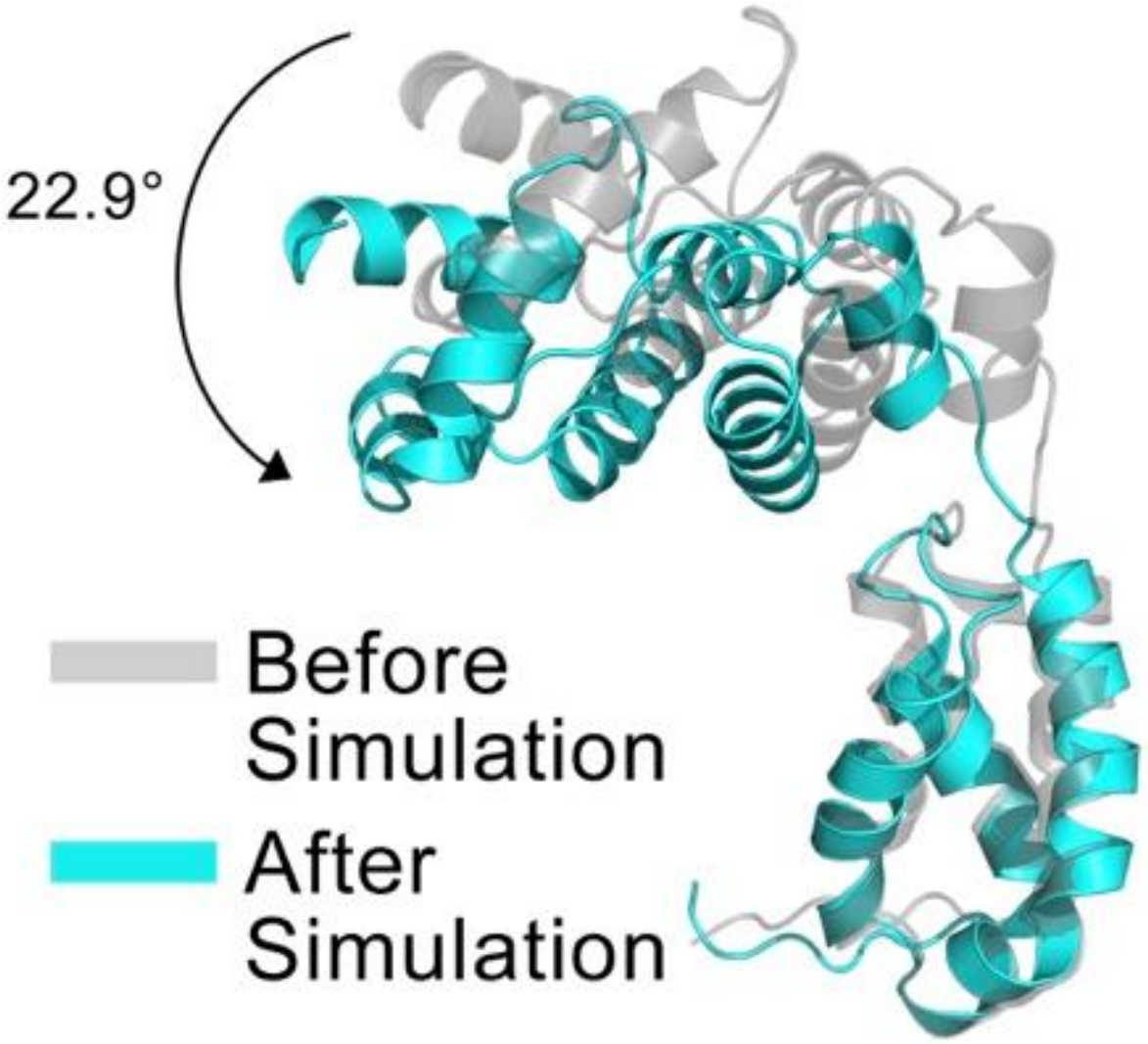
22.9°
Before Simulation
After Simulation

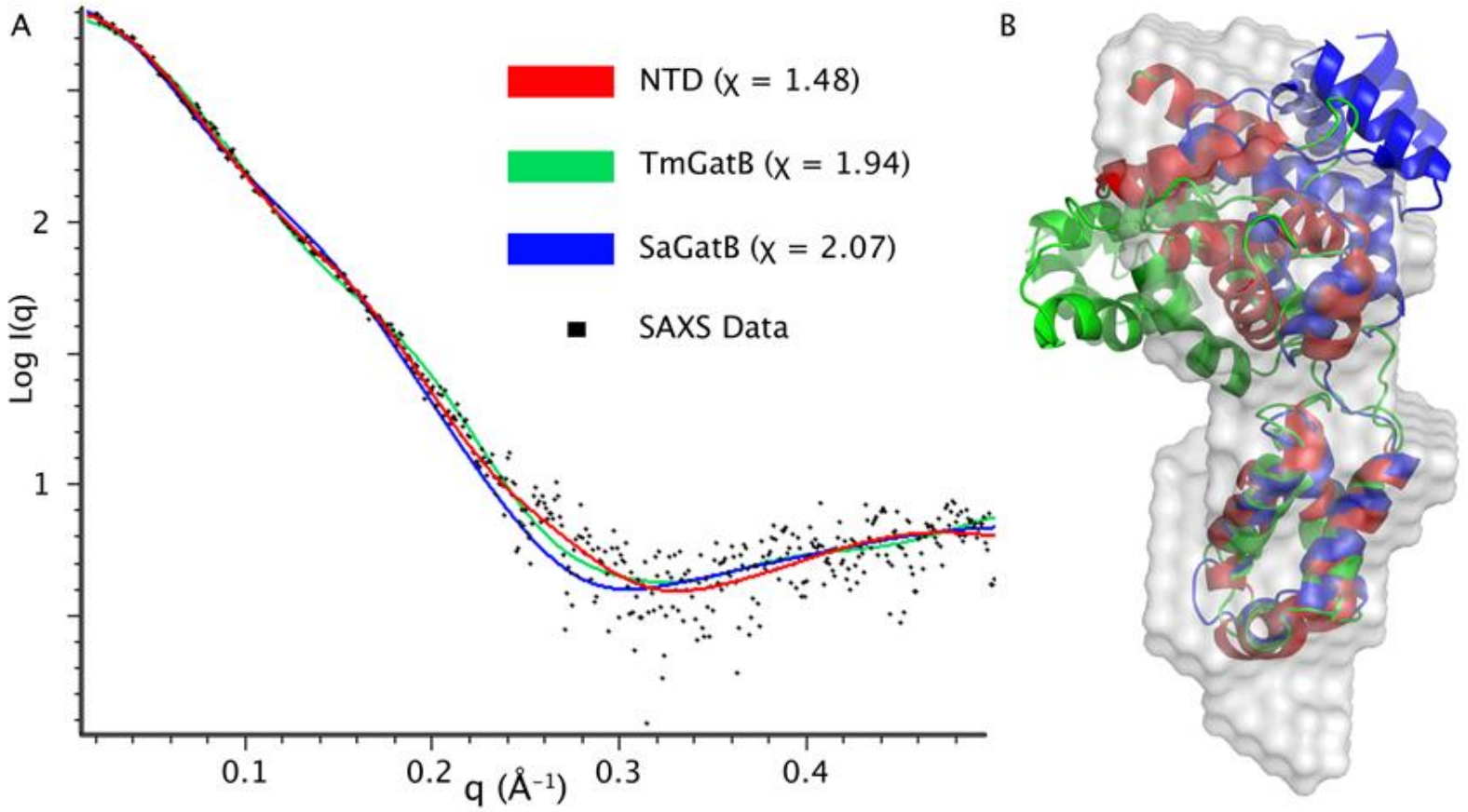

SAXS data shows that the NTD crystal structure is similar to that found in solution. A. Simulated scattering profiles calculated by CRYSOL for the Gln4 NTD (red), TmGatB (green), and SaGatB (blue) are shown overlaid on top of experimental SAXS data from the Gln4 NTD in solution. Goodness of fit values (χ) are given in parentheses. B. The ab initio envelope reconstructed from the experimental scattering profile of the Gln4 NTD is shown superimposed onto the crystal structures of the Gln4 NTD (red), TmGatB (green), and SaGatB (blue).

Homology model is not in agreement with solution envelope

Significance of solution envelope and homology model

- The full-length ScGlnRS bound to $tRNA^{Gln}$ shows a significant change in the NTD position when compared to the $tRNA^{Gln}$-free, SAXS-derived conformation .
- The model shows a ~160° rotation and a ~40 Å translation of the NTD with respect to the solution conformation.
- Fitting the simulated scattering of the protein portion of the protein-tRNA complex to the experimental SAXS data resulted in a poor fit, yielding a $\chi 2 = 12.25$ compared to 1.82 for the rigid body model . The limited flexibility of the NTD, coupled with the poor fit of the simulated scattering of the protein portion of the model bound to $tRNA^{Gln}$, suggests that without tRNA bound, this conformation does not exist in solution.
- Analysis with OLIGOMER showed that only the rigid body model exists in solution, while the homology model does not.
- Taken together, these observations suggest that **CTD binding of $tRNA^{Gln}$ induces substantial conformational reorientation of the NTD required for interactions with $tRNA^{Gln}$.**

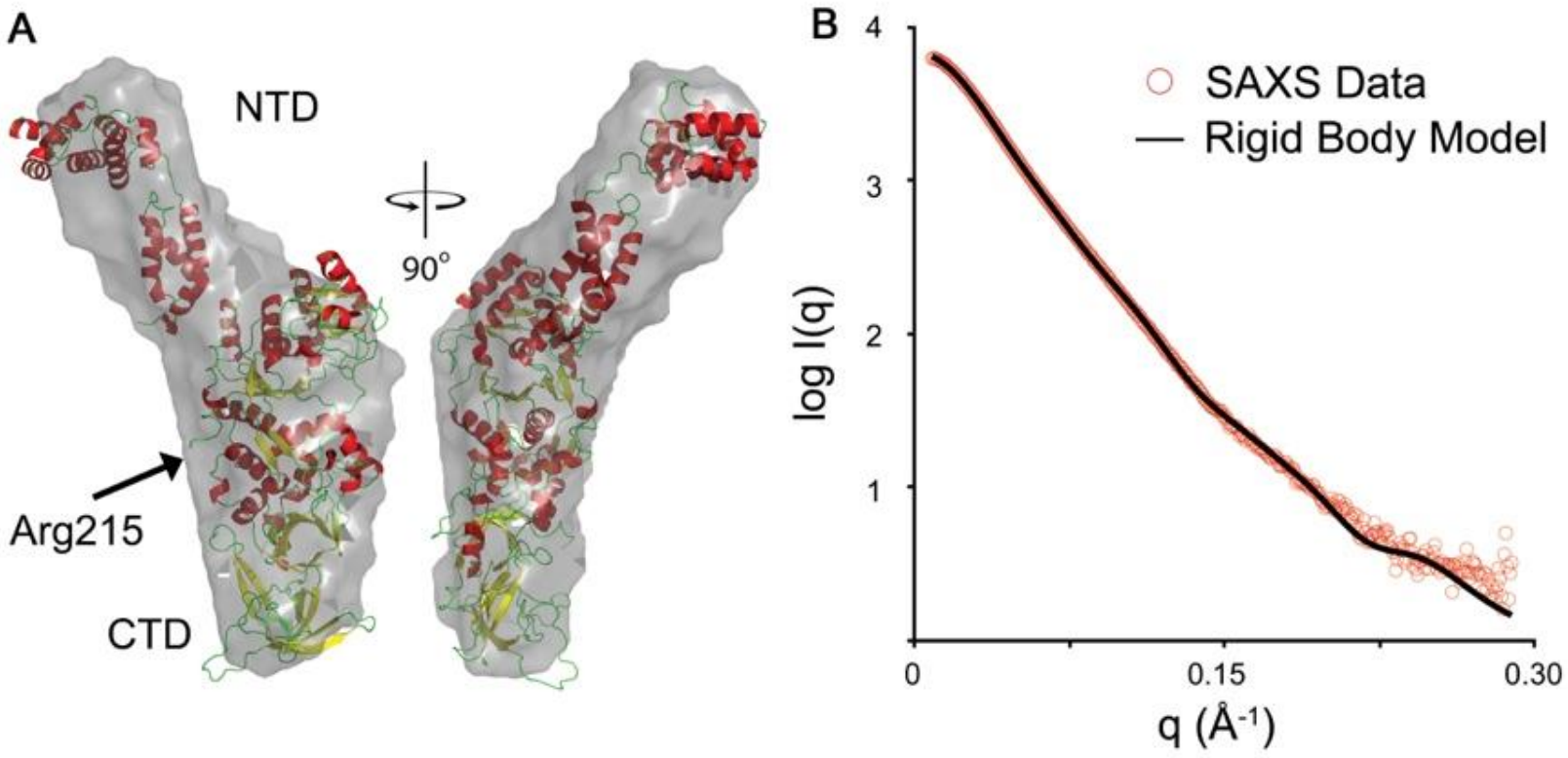

Ab. initio envelope of full length protein (no crystallographic information used)

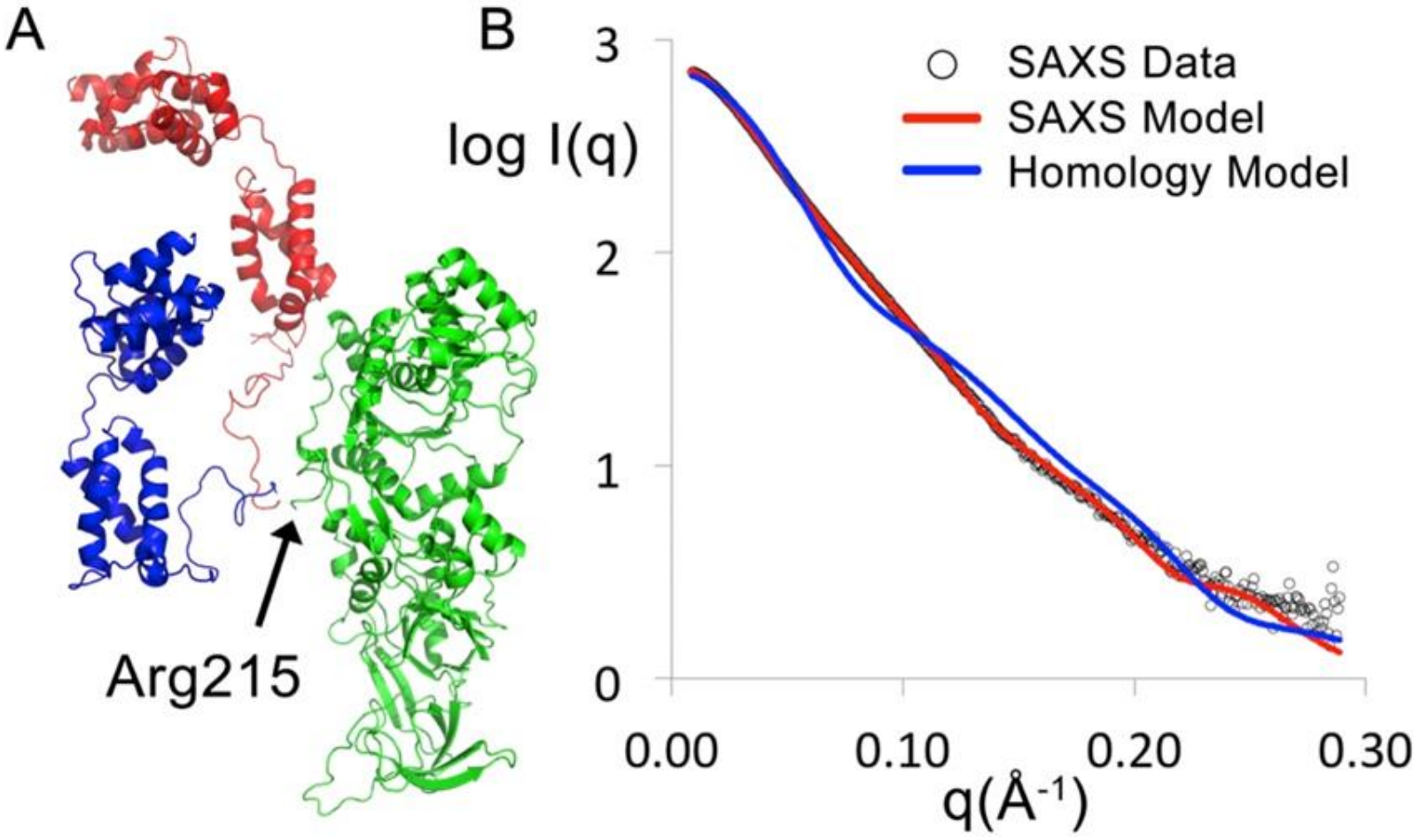

Without tRNA solution model shows an open conformation, tRNA binding induces a ‘closing’

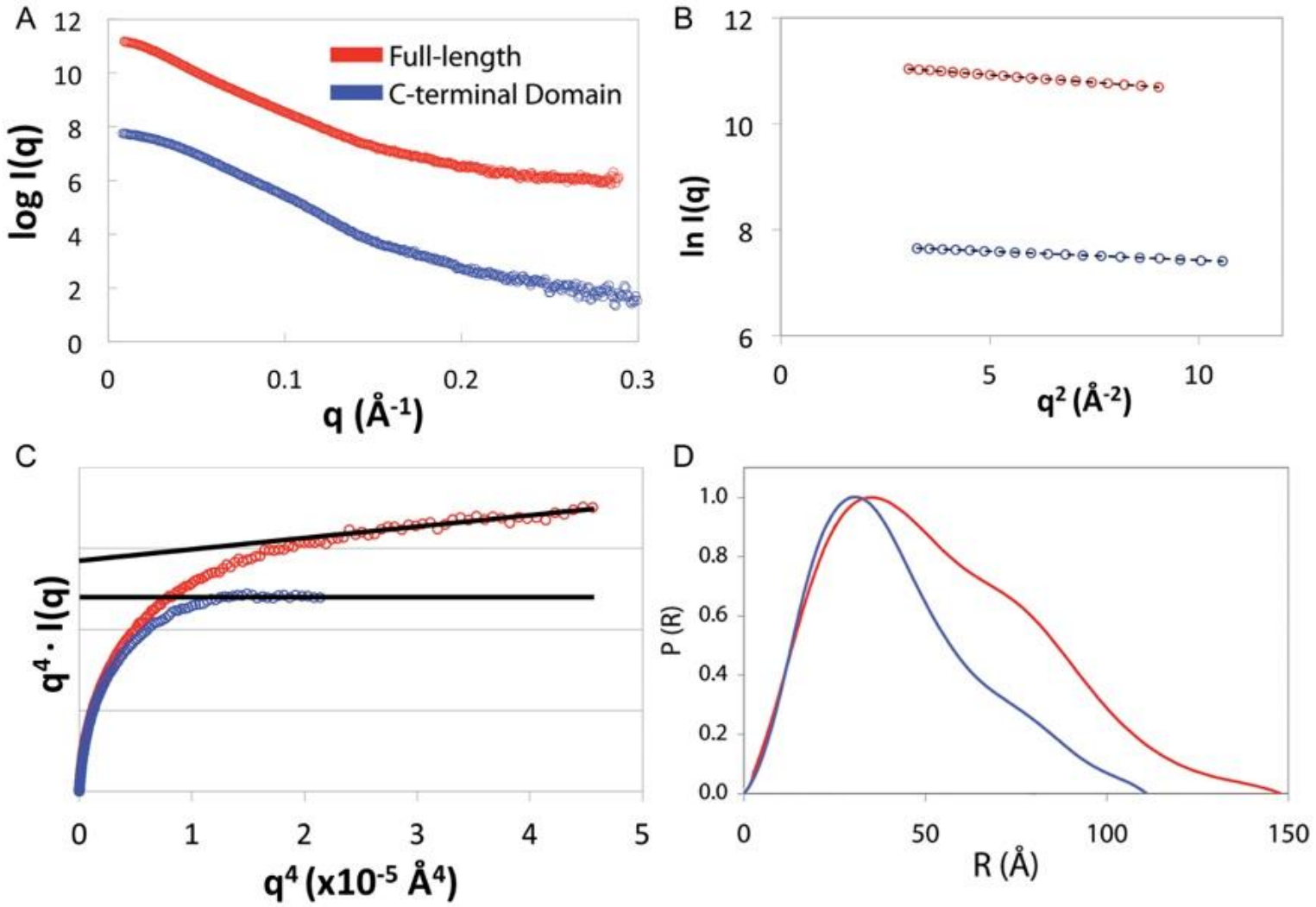

More flexibility indicated from SAXS data of full length protein than C-terminal domain

A combination of molecular biology, SAXS, crystallography and molecular dynamics

Gln4 a Eukaryotic
Glutaminyl-tRNA Synthetase

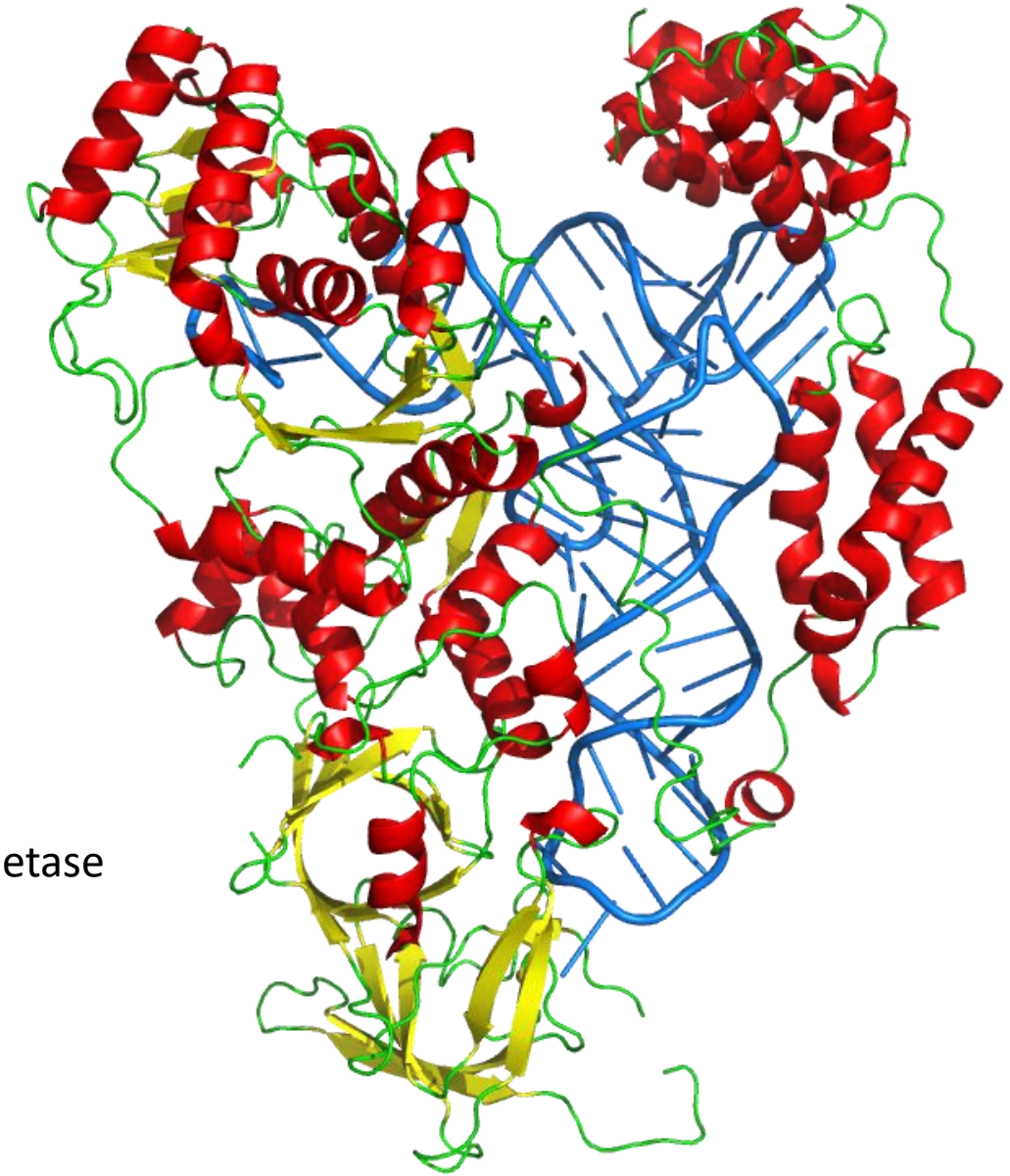

Summary

- The 187 amino acid Gln4 NTD consists of two subdomains, each exhibiting an extraordinary structural resemblance to adjacent tRNA specificity-determining domains in the GatB subunit of the GatCAB amidotransferase, which forms Gln-tRNA^{Gln}.
- These subdomains are connected by an apparent hinge comprised of conserved residues.
- Mutation of these amino acids produces Gln4 variants with reduced affinity for tRNA^{Gln}, consistent with a hinge-closing mechanism proposed for GatB recognition of tRNA.
- Our results suggest a possible origin and function of the NTD that would link the phylogenetically diverse mechanisms of Gln-tRNA^{Gln} synthesis.
- CTD binding of tRNAgln induces substantial conformational reorientation of the NTD required for interactions with tRNAgln

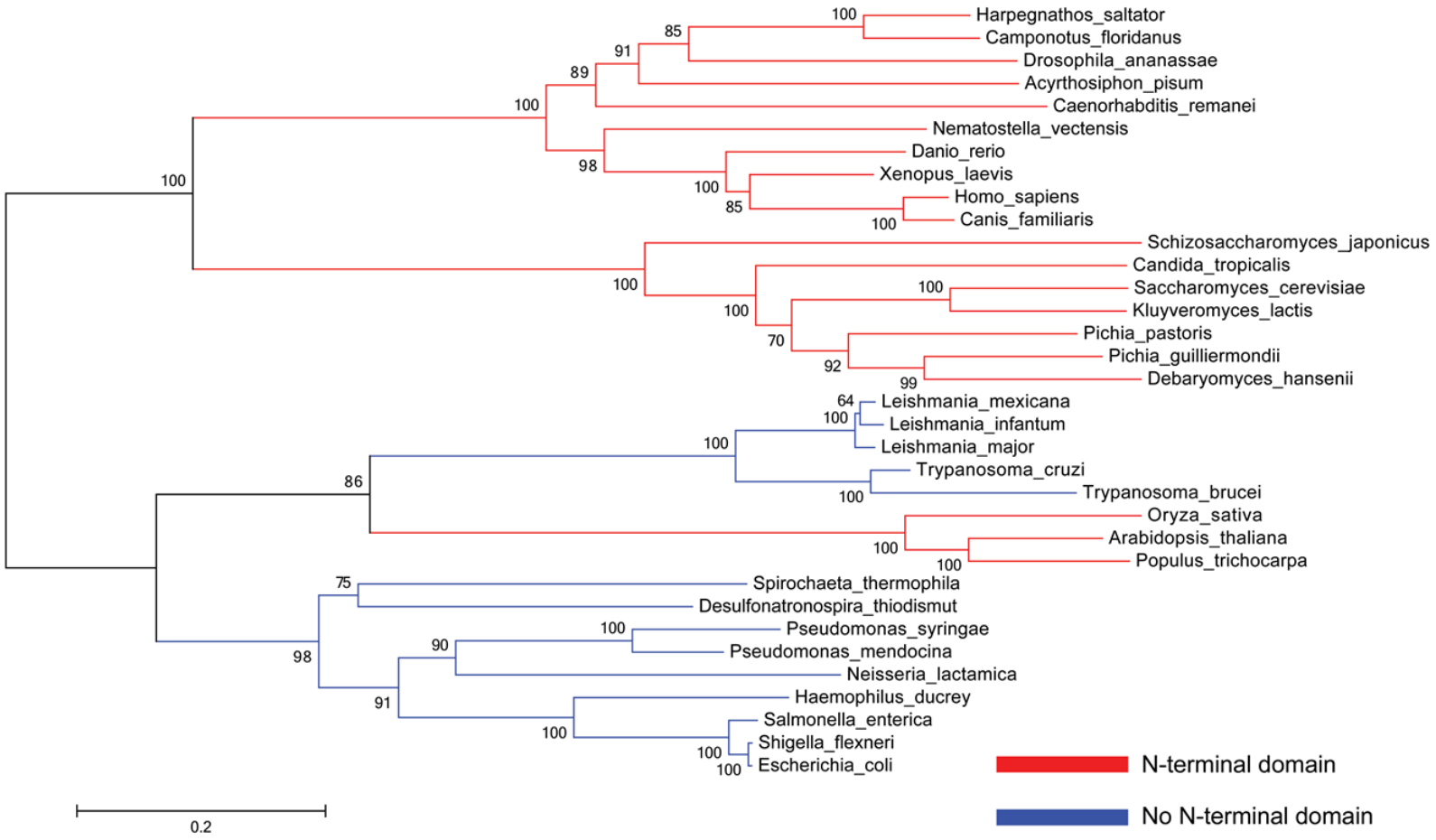

Phylogenetic distribution of GlnRSs with and without N-terminal appended domains. Eukaryotic and bacterial GlnRS sequences were aligned using ClustalW and a phylogenetic tree was constructed using MEGA5, with 200 bootstraps carried out to test statistical relevance. In addition to bacteria, a set of Euglenozoa protists lacks the appended domain.

Summary

- CTD binding to tRNA results in a large conformational reorientation of the NTD allowing for interactions between the NTD and the tRNA.
- Activity measurements (not discussed) suggest that the NTD plays a direct role in tRNA binding.
- Molecular dynamics imply that the helical and tail subdomains of the NTD undergo a hinge motion after binding to tRNA, allowing for tighter binding between the NTD and tRNA.
- NTD communicates with the CTD through Insertion 1, which is found in all eukaryotes.
- The absence of such an interaction may explain the loss of the NTD in bacterial GlnRS evolution.
- Since the NTD and the active site of ScGlnRS are too distant to interact directly, and since deletion of the NTD also increases KM for glutamine and ATP, it seems plausible that the effects on glutamine and ATP are due to the concerted conformational changes in ScGlnRS that occur upon tRNA binding (observed in E. coli).

SAXS is a complementary and powerful technique

Acknowledgements

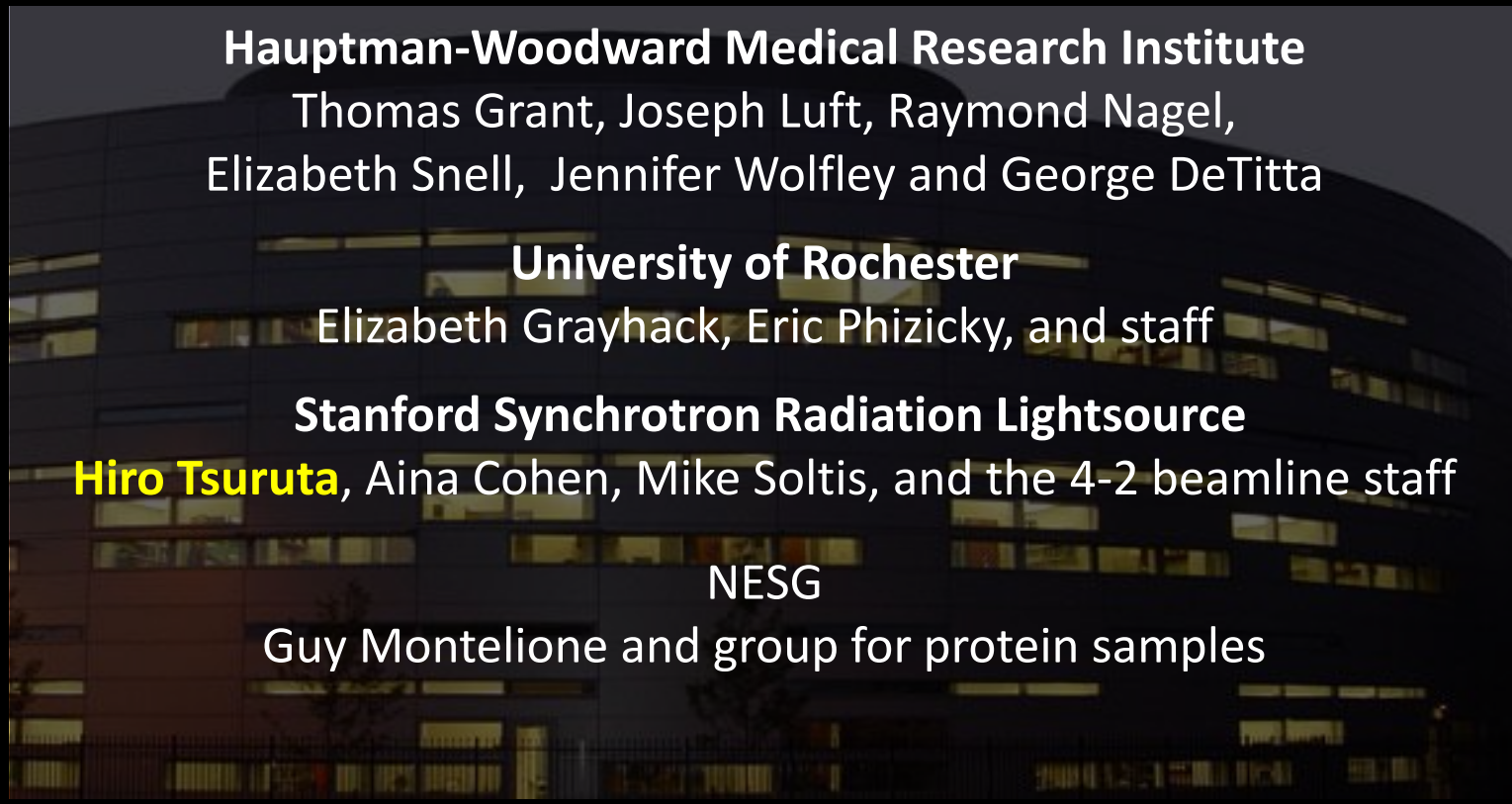

Hauptman-Woodward Medical Research Institute

Thomas Grant, Joseph Luft, Raymond Nagel, Elizabeth Snell, Jennifer Wolfley and George DeTitta

University of Rochester

Elizabeth Grayhack, Eric Phizicky, and staff

Stanford Synchrotron Radiation Lightsource

Hiro Tsuruta, Aina Cohen, Mike Soltis, and the 4-2 beamline staff

NESG

Guy Montelione and group for protein samples

Support and Funding

NIH, NSF and DoD support to Edward Snell

Thank you and questions?

esnell@hwi.buffalo.edu